



THE UNIVERSITY *of* EDINBURGH

This thesis has been submitted in fulfilment of the requirements for a postgraduate degree (e.g. PhD, MPhil, DClinPsychol) at the University of Edinburgh. Please note the following terms and conditions of use:

This work is protected by copyright and other intellectual property rights, which are retained by the thesis author, unless otherwise stated.

A copy can be downloaded for personal non-commercial research or study, without prior permission or charge.

This thesis cannot be reproduced or quoted extensively from without first obtaining permission in writing from the author.

The content must not be changed in any way or sold commercially in any format or medium without the formal permission of the author.

When referring to this work, full bibliographic details including the author, title, awarding institution and date of the thesis must be given.

Decision-making Techniques for Smart Grid Energy Management

Yuchang Wang



A thesis submitted for the degree of Doctor of Philosophy.
The University of Edinburgh.
August 2017

Abstract

This thesis has contributed to the design of suitable decision-making techniques for energy management in the smart grid with emphasis on energy efficiency and uncertainty analysis in two smart grid applications. First, an energy trading model among distributed microgrids (MG) is investigated, aiming to improve energy efficiency by forming coalitions to allow local power transfer within each coalition. Then, a more specific scenario is considered that is how to optimally schedule Electric Vehicles (EV) charging in a MG-like charging station, aiming to match as many as EV charging requirements with the uncertain solar energy generation. The solutions proposed in this thesis can give optimal coalition formation patterns for reduced power losses and achieve optimal performance for the charging station.

First, several algorithms based on game theory are investigated for the coalition formation of distributed MGs to alleviate the power losses dissipated on the cables due to power transfer. The seller and buyer MGs can make distributed decisions whether to form a coalition with others for energy trading. The simulation results show that game theory based methods that enable cooperation yield a better performance in terms of lower power losses than a non-cooperative approach. This is because by forming local coalitions, power is transferred within a shorter distance and at a lower voltage. Thus, the power losses dissipated on the transmission lines and caused by power conversion at the transformer are both reduced. However, the merge-and-split based cooperative games have an inherent high computational complexity for a large number of players.

Then, an efficient framework is established for the power loss minimization problem as a college admissions game that has a much lower computational complexity than the merge-and-split based cooperative games. The seller and buyer MGs take the role of colleges and students in turn and apply for a place in the opposite set following their preference lists and the college MGs' energy quotas. The simulation results show that the proposed framework demonstrates a comparable power losses reduction to the merge-and-split based algorithms, but runs 700 and 18000 times faster for a network of 10 MGs and 20 MGs, respectively.

Finally, the problem of EV charging using various energy sources is studied along with their impact on the charging station's performance. A multiplier k is introduced to measure the effect

of solar prediction uncertainty on the decision-making process of the station. A composite performance index (the Figure of Merit, FoM) is also developed to measure the charging station's utility, EV users charging requirements and the penalties for turning away new arrivals and for missing charging deadlines. A two-stage admission and scheduling mechanism is further proposed to find the optimal trade-off between accepting EVs and missing charging deadlines by determining the best value of the parameter k under various energy supply scenarios. The numerical evaluations give the solution to the optimization problem and show that some of the key factors such as shorter and longer deadline urgencies of EVs charging requirements, stronger uncertainty of the prediction error, storage capacity and its initial state will not affect significantly the optimal value of the parameter k .

Lay summary

Most of today's power generation is still heavily produced by fossil or coal-fired fuels that have a negative effect on the environment. The smart grid is introduced to bring more control to the existing power systems by enabling bi-directional information and power flow, renewable energy integration and distributed operation. However, the increased flexibility also brings more uncertainty to the energy management in terms of matching the energy supply with the demand across all timescales. This thesis identifies and designs suitable decision-making techniques to tackle the uncertainty issues in the energy management based on two smart grid applications.

The first application is based on an energy trading model among distributed microgrids (MG). The potential of these MGs to form coalitions and cooperate with one another is investigated. Since the uncertainty arising in renewable energy generation and consumers' behaviour brings difficulty in keeping the energy supply and demand balanced within a MG during a certain period of time, there is a need for MGs to trade energy with external sources. By forming coalitions, the power losses dissipated on the cables among nearby MGs due to the power transfer is likely to be less than that between the MGs and the main power grid. Novel algorithms are proposed based on game theory that can show how the coalitions are formed, so that the power losses are minimized with reasonable computational complexity.

In the second application, we specifically model an electric vehicles (EV) charging station as an MG that consists of controllable charging demand, renewable energy, and battery storage units. The aim is to match as many EV requirements as possible with the uncertain renewable energy sources, so that the utility of the charging station and the EV drivers are both satisfied. This is analogous to that of matching MGs in the first application in order to minimize the power losses. As the charging station usually has a limited charging capacity due to its physical constraints, it cannot accommodate all the arriving EVs. Thus, a decision has to be made whether an arriving EV can be admitted. This is not only based on EVs' charging requirements but also on how certain the charging station is towards its on-site renewable energy resources. The station should not be too optimistic towards its solar prediction as that will lead to over admission of vehicles and missing many charging deadlines, nor too pessimistic which will lead to charging less cars than the station's capacity and losing revenues. Thus, a two-stage scheduling mechanism is proposed to find the optimal trade-off between accepting EVs and

missing their charging deadlines by determining the best strategy for solar prediction.

Declaration of originality

I hereby declare that this thesis has been composed solely by myself and that it has not been submitted, in whole or in part, in any previous application for a degree. Except where states otherwise by reference or acknowledgement, the work presented is entirely my own.

Yuchang WANG

August 2017

Acknowledgements

This thesis has officially marked the end of an era of me being a student. Now, it almost feels weird to not owning a valid student ID and referring to myself as Dr. This has been a truly wonderful yet tough journey, and I could not be able to survive without the support from my supervisor, colleagues, family and friends. I will always be grateful for every single help, smile, understanding, believing, company, and encouragement along the way and to everyone who has made this thesis possible.

First and foremost, I would like to express sincere gratitude and appreciation to my supervisor Professor John Thompson for his valuable guidance, patience, and encouragement, not only for the academic development but also for my personal growth. The Ph.D. and this thesis would have been impossible without his dedication and commitment, professionalism, knowledge, guidance and support.

I want to express my gratitude to both of my examiners, Dr. James Hopgood and Dr. Bamidele Adebisi. Their comments have been priceless to shape the final version of the thesis. My sincere thanks also goes to my internal advisor Dr. Aristides Kiprakis and my second supervisor Dr. Dave Laurenson for their invaluable comments and feedbacks during my annual reviews, which contributed and helped bring depth and breadth into this work. Many thanks to my amazing Smart Grid Journal Club colleagues: Alex Kleidas, Sara Lupo, Rentao Wu, Gautham Krishnadas, Mehdi Zeinali, Dr. Aristides Kiprakis and Dr. Valentin Robu for their assistance, dedicated involvement, and lively discussions.

I would like to express appreciation to Iraklis Giannakis for introducing me to Dr. Antonios Giannopoulos who offered me a Teaching Assistant job in the last three years for his course: Numeric Methods and Computing 2. It is a truly enjoyable experience to be able to work with him and his team: John Hartley and Hossain Zadhoush. Thank you for all the laughter, support, discussions, career advice and friendship we have shared!

I thank my colleagues and friends at IDCCom for the inspiring discussions, for the late nights working together before deadlines, lunch and coffee breaks, nights out, and trips together with Chunli Guo, Andrea Chighine, Paula Aquilina, Sudip Biswas, Danai Korre, Bogomil Shtarkalev, Dobroslav Tsonev, Stefan Videv, Chen Cheng, Sakis, Wenjun Fu, Shendi Wang,

Acknowledgements

Di Wu and for all the fun we shared in the last four years. A very special thanks to my sweetest “agb quokkas”: JP Morrissey, Francesc Levrero Florencio, Utibe Umoh, Erika Sales, Tim Najuch and Jiaming Xu. You are my rocks and I will always remember the days and evenings we spent together working, playing, and having amazing dinners as well as questioning life. Thank you for all the joys and tears we shared and everything in between. Also thanks to Dr. Salvatore Caporale who has been the life coach, salsa motivator, booze pusher, and music encyclopedia in the last two years. Many thanks to Joe Burchell, Natasa Utjesanovic and Mia Ismail for always being there for me through many ups and downs in the last three years. Greatest thanks to all of you who made this journey full and unforgettable.

I would also like to extend the thanks to the many people in many countries who have inspired and encouraged me, and so generously contributed to the work presented in this thesis. I am also very grateful for the people who once broke my heart and taught me a lesson. This thesis would have been accomplished sooner without them. I truly appreciate all the good or bad that lead me to where I am today.

Last but not least, my deepest gratitude goes to my parents for their everlasting unconditional love, inspiration, encouragement, understanding and support. Thank you for always believing in me and standing by my side.

Contents

Lay summary	iv
Declaration of originality	vi
Acknowledgements	vii
Contents	ix
List of figures	xii
List of tables	xiv
Acronyms and abbreviations	xv
Nomenclature	xvii
1 Introduction	1
1.1 Introduction and Motivation	1
1.2 Objectives and Contributions	3
1.2.1 Objectives	3
1.2.2 Key Contributions	3
1.3 Organization of the Thesis	4
2 Background	7
2.1 Power System Foundations	7
2.1.1 Active and Reactive Power	9
2.1.2 Frequency Control	11
2.1.3 Simulation Software	12
2.2 The Smart Grid and its Applications	13
2.2.1 Microgrid	14
2.2.2 EV Charging	18
2.3 Selected Decision-Making Techniques	23
2.3.1 Game Theory	23
2.3.2 Stable Marriage and the College Admissions Problem	29
2.3.3 Scheduling Algorithms	30
2.4 Summary	31
3 Coalition Formation for Energy Trading Among Distributed MGs	33
3.1 Introduction	33
3.2 Literature Review	35
3.2.1 MG Research	35
3.2.2 Game Theory in Energy Trading	37
3.3 System Model	39
3.3.1 System Description	40
3.3.2 Power Metric Calculation	41
3.4 Algorithms	43
3.4.1 Non-cooperative Setting	43
3.4.2 Cooperative Setting for Coalition Formation	44
3.5 Simulation Results	50

3.5.1	An MG Distribution Network	50
3.5.2	Power Loss Comparison	51
3.5.3	Coalition Size Comparison	52
3.5.4	Complexity Comparison	53
3.6	Summary	55
4	College Admissions for Energy Trading Among Distributed MGs	57
4.1	Introduction	57
4.2	Literature Review	59
4.2.1	Stable Marriage and College Admissions	60
4.2.2	Economics in Energy Trading	61
4.3	System Model	63
4.3.1	Power Metric Calculation	64
4.3.2	Benchmark: Coalition Formation Game	65
4.4	The Proposed College Admissions Framework	66
4.4.1	The College Admissions Problem	66
4.4.2	The Buyer-driven Model	67
4.4.3	The Seller-driven Model	68
4.5	Algorithm Analysis	69
4.5.1	Stability and Convergence Analysis	70
4.5.2	Complexity Analysis	72
4.6	Simulation Results	74
4.7	Three MGs Case Study	77
4.8	Summary	80
5	EVs Charging Using Renewable Energy	83
5.1	Introduction	83
5.2	Literature Review	86
5.2.1	Charging Location	86
5.2.2	Energy Sources	88
5.2.3	Discharging	88
5.3	System Model	89
5.3.1	EV Arrival Model	89
5.3.2	Energy Supply Model	92
5.3.3	The Figure of Merit (FoM)	95
5.3.4	Optimization Problem Formulation	96
5.4	Two-stage Admission and Scheduling Mechanism	98
5.4.1	Admission Control Algorithm (ACA)	98
5.4.2	Charging Scheduling Algorithm (CSA)	99
5.5	Numerical Evaluations	100
5.5.1	Energy from the Grid	101
5.5.2	Energy from the Solar Panels	102
5.5.3	Energy from the Storage	109
5.5.4	Discussion of the cost of various energy sources	113
5.6	Summary	114
6	Conclusions and Future Work	117

6.1	Conclusions	117
6.1.1	Coalition Formation for Energy Trading among Distributed Microgrids	117
6.1.2	Priority-based Energy Scheduling Mechanism for Electric Vehicles Charging	118
6.2	Future Work	119
6.2.1	Microgrid Energy Trading	119
6.2.2	Electric Vehicles Charging Scheduling	120
	References	121

List of figures

1.1	A conceptual model to show the interactions of roles in different smart grid domains through ICT [5].	2
2.1	A power system from generation, transmission and distribution of electricity [1].	8
2.2	The graph of power triangle to show the relation between active power (W), reactive power (VAR) and apparent power (VA).	11
2.3	Frequency data to a 15 second resolution over the last hour, last access at 17:20 27th July 2017 at [2].	12
2.4	An example of a microgrid infrastructrue.	15
2.5	Illustration of three classes of cooperative games, after [3].	27
3.1	A paradigm for the proposed system model [67].	39
3.2	An example of various coalitions formed among three MGs over n scheduling timeslots.	41
3.3	One iteration of the merge-and-split process.	46
3.4	Comparison of the procedure of the merge-and-split and the switch operation. .	48
3.5	The process of the brute force method.	49
3.6	A partition of a MG distribution network resulting from the coalition formation algorithm with $N = 10$ MGs. The MGs are labelled 1 – 10, where buyer MG is denoted as B and seller MG is denoted as S	51
3.7	Average power loss per MG comparison versus number of MGs N	52
3.8	Average coalition size comparison versus the number of MGs N	54
3.9	Average operation numbers compared with utility function calls	55
4.1	A simplified illustration of the considered system model.	63
4.2	The process of q_c calculation in (a) BD-CAF and (b) SD-CAF, where c represents a seller and a buyer, respectively.	67
4.3	One iteration of BD-CAF process	69
4.4	Complexity comparison between merge-and-split and BD-CAF in terms of the frequency of utility calculations	73
4.5	Average power loss comparison.	75
4.6	Average coalition size comparison	76
4.7	Comparison of power loss per buyer, per seller and per MG when using BD-CAF and SD-CAF with the non-cooperative model as the baseline.	77
4.8	Aggregate power imbalance in a day with highlighted cooperation timeslots. . .	78
4.9	Four states of cooperation among the MGs and MS in a day, where MV = medium voltage 33 kV line and LV = low voltage 11 kV line, other simulation parameters following Table 4.1 and Figure 4.8.	81
5.1	System model.	90
5.2	A comparison of the Poisson probability density function (PDF) with parameter $\lambda = 5, 10, 12$	91

5.3	Examples of actual solar generation sample traces with low, medium and high generation profiles, extracted from [4].	93
5.4	Performance comparison between Admission Control and FIFO in terms of (a) Rejection probability (b) Service rate (c) Average delay per EV per timeslot (d) Average number of EVs in the system per timeslot.	102
5.5	EVs rejection probability over various arrival rate λ in (b) when using solar energy in (a).	103
5.6	Rejection probability when using the energy from the solar panels.	105
5.7	Figure of Merit (FoM) with shorter and longer deadline urgencies.	106
5.8	Performance comparison when the system has a stronger uncertainty.	107
5.9	Figure of Merit (FoM) when multiplier k is a function of time t	108
5.10	The set of lines in $k(t)$ with the highlighted optimal $k^*(t)$ and the optimal k^*	109
5.11	Comparison of FoM with (w/S) and without (w/o) storage facility under optimal k values from Table 5.4 and Table 5.3.	110
5.12	Figure of Merit (FoM) when multiplier k is a function of time t with sufficient storage capacity.	111
5.13	Figure of Merit (FoM) with various storage capacity under their corresponding optimal value of $k(t)$	112
5.14	The FoM comparison when the storage starts empty, 1/4 full, 1/2 full, and 3/4 full with the battery capacity $B = 193$ kWh.	114
5.15	Energy in the storage with various starting states for a 3B/4 size storage.	115
5.16	Financial cost paid by the station to cover various energy sources in one day.	116

List of tables

2.1	Specifications of EV charging levels.	21
2.2	Comparison of competing technologies to EVs.	22
3.1	Simulation parameters for Chapter 3	50
4.1	Simulation parameters for Chapter 4	79
4.2	Monetary saving before and after coalition formation	80
5.1	Simulation parameters for Chapter 5	101
5.2	Numbers for admission and scheduling process	104
5.3	Optimal value of k for solar only case.	104
5.4	Optimal value of k for solar with storage.	110

Acronyms and abbreviations

AC	alternating current
ACA, AD	admission control algorithm
AMI	advanced meter infrastructure
BD-CAF	buyer-driven college admissions framework
CAF	college admissions framework
CHP	combined heat and power
CSA	charging scheduling algorithm
D2D	device-to-device
DC	direct current
DG	distributed generation
DRR	deficit round robin
DSM	demand side management
EMS	energy management system
ES	energy storage
EV	electric vehicle
FIFO	first in, first out
FoM	figure of merit
GIS	geographical information system
HEV	hybrid electric vehicle
HVDC	high-voltage direct current
ICT	information and communication technologies
LST	least slack time
LTE	long term evolution
MG	microgrid
MILP	mixed integer linear programming
MIMO	multiple-input multiple-output
MS	macro station
OPF	optimal power flow
PCC	point of common coupling

PDF	probability density function
PHEV	plug-in hybrid electric vehicle
PMU	phasor measurement units
PSO	particle swarm optimization
QoS	quality of service
RES	renewable energy sources
RR	round robin
SD-CAF	seller-driven college admissions framework
TU	transferable utility
UPS	uninterruptible power supply
V2G	vehicle-to-grid
WFQ	weighted fair queuing
WRR	weighted round robin

Nomenclature

a_i^m	EV i 's maximum charging rate
$a_i(t)$	charging rate variable
a_n	an applicant or a student n
b	buyer MG
c_m	a college m
$e(t)$	solar energy prediction error
j	imaginary unit
$k, k(t)$	optimization variable
$k^*, k^*(t), FOM^*$	optimal value
p_b	cost of per unit energy usage from the storage
p_g	cost of per unit energy bought from the grid
p_s	cost of per unit energy usage from the solar panels
q_{c_m}	quota of college c_m
$r_{a_n}^m$	applicant a_n 's ranking of college c_m
$r_{c_m}^n$	college c_m 's ranking of applicant a_n
s	seller MG
$s_i \in \mathcal{S}_i$	one possible strategy in player i 's strategy set \mathcal{S}_i
\mathbf{s}_{-i}	vector of strategies taken by the other players in set $\mathcal{N} / \{i\}$
t	current timeslot
t_i	scheduling timeslot
t_i^a	arrival time of EV i
t_i^d	charging deadline urgency of EV i
$(u_i)_{i \in \mathcal{N}}$	set of utility functions of player $i \in \mathcal{N}$
$u_i(s_i, \mathbf{s}_{-i})$	utility function of player i when i chooses strategy s_i and the others choose \mathbf{s}_{-i}
\mathcal{A}	set of applicants
$A_w(t)$	admission window
B	storage capacity
$B(t)$	energy status of the storage at t
B_0	storage starting state

\mathcal{C}	set of colleges
$\mathcal{D} = \{i, j\}$	represents a coalition that consists of players i, j
E_b	energy left in the storage at the end of the day
E_i	charging energy requirement of EV i
FoM	figure of merit
$\mathcal{H} = \{\mathcal{D}_i, \mathcal{D}_j\}$	represents a partition that consists of coalitions $\mathcal{D}_i, \mathcal{D}_j$
$\mathcal{H}_i \triangleright \mathcal{H}_j$	the structure of partition \mathcal{H}_i is preferred over \mathcal{H}_j by the Pareto Order
$\mathcal{H}_i \succeq \mathcal{H}_j$	the structure of partition \mathcal{H}_i is preferred over \mathcal{H}_j by the relaxed Pareto Order
I	current
I^*	conjugate of current
M	number of chargers
\mathcal{N}	set of players
N	number of players in a set
$\mathcal{N}_{ad}(t)$	admission set
N_{ad}	number of admitted EVs
N_{ar}	number of new arriving EVs
$\mathcal{N}_c(t)$	charging set
$\mathcal{N}_{ex}(t)$	set of previously admitted EVs who are still waiting for service at t
N_{ms}	number of EVs who miss their charging deadlines
$\mathcal{N}(t)$	set of cars at the charging station
$\mathcal{O}(\cdot)$	big-O notation
P	active power
P_d	probability of rejecting cars upon arrival
P_{ij}	amount of active power exchanged between microgrid i and j
P_{ij}^{loss}	active power losses due to power transfer P_{ij} between i and j
Q	reactive power
\mathcal{R}	set of both colleges' and applicants' preference lists
R	resistance
$R_i(t)$	remaining energy requirement of EV i at t
R_s	ratio of missing charging deadlines
S	complex power
$S(t)$	energy generated from solar panels
$\hat{S}(t)$	prediction of $S(t)$

$SAT_i(t)$	satisfaction level
$(\mathcal{S}_i)_{i \in \mathcal{N}}$	set of strategies for player $i \in \mathcal{N}$
S_{lb}	lower bound of solar energy prediction interval
S_r	cumulative excess solar energy
S_{tot}	total solar energy generation
T	total timeslots in a day
U	utilization of the energy supply
U_o	medium voltage on the distribution line between MS and MG
U_1	local low voltage over the cable
$U_{coop}(\mathcal{N})$	utility of players in set \mathcal{N} in the cooperative fashion
$U_{non}(\mathcal{N})$	utility of players in set \mathcal{N} in the non-cooperative fashion
V	voltage
V^*	conjugate of voltage
X	reactance
Z	system impedance
α	fraction of the power losses at the transformer due to power conversion
γ	penalty factor
ζ_i	weight factor to represent the extra benefits each MG i gains by forming coalitions
λ	average arrival rate of Poisson distribution
σ	standard deviation of $e(t)$
τ	duration of one timeslot
$v_i(\mathcal{N})$	utility gain of player $i \in \mathcal{N}$
ϕ	angle of difference between current and voltage
ω_1	price of per unit of energy transferred between MS and MGs
ω_2	price of per unit of energy transferred among MGs
ω_{dn}	price of per unit energy paid by buyer MGs to buy energy from MS
$\omega_i(t)$	priority factor
ω_m	price of per unit energy paid or gained among MGs
ω_{up}	price of per unit energy gained by seller MGs to sell energy to MS
$\sim U(\cdot, \cdot)$	uniform distribution
$ \cdot $	number of elements in a set

Chapter 1

Introduction

This thesis has contributed to the design of suitable decision-making techniques for energy resource management in the smart grid. Two smart grid application scenarios are investigated with the emphasis on energy efficiency and uncertainty analysis. In the first scenario, distributed microgrids (MG) who act as agents are allowed to seek to form coalitions to trade energy so that the power losses dissipated on the cables might be reduced. In the second scenario, we look inside one MG and specifically model this as a charging station for Electric Vehicles (EV). The MG-like charging station aims to pair as many EVs as possible with the on-site solar energy generation so as to achieve an optimal utility. In this introductory chapter, Section 1.1 introduces the motivation of this research work. Then the objectives and key contributions of this thesis are summarized in Section 1.2. Finally, Section 1.3 presents an overview of the remaining chapters.

1.1 Introduction and Motivation

The electrical power grid has been powering the society for over a century and plays a major role in every aspect of the modern society. The conventional power grid is operated in a centralized fashion and only supports unidirectional power flow from the generation stepping down to transmission and distribution networks. This structure has become limited in balancing the generation with the demand efficiently at all times. In addition, longer transmission distance will cause significant power losses over the cables and overheating on the components in the system. In this regard, the concept of a “smart grid” is envisioned aiming to make the best use of the available energy, to reduce power losses, to gain more control throughout the power generation, transmission to distribution, as well as to alleviate global warming and carbon emission levels. The smart grid incorporates modern computer systems, information and communication technologies (ICT), control theory, and artificial intelligence to support two-way energy and information flows so that energy efficiency, real-time operations, and systems reliability and sustainability are improved. A conceptual model of smart grid from the National Institute of

Standards and Technology (NIST) [5] is shown in Figure 1.1. It introduces distributed intelligent elements to the existing power grid infrastructure and interoperates with high-speed, robust and reliable communication networks.

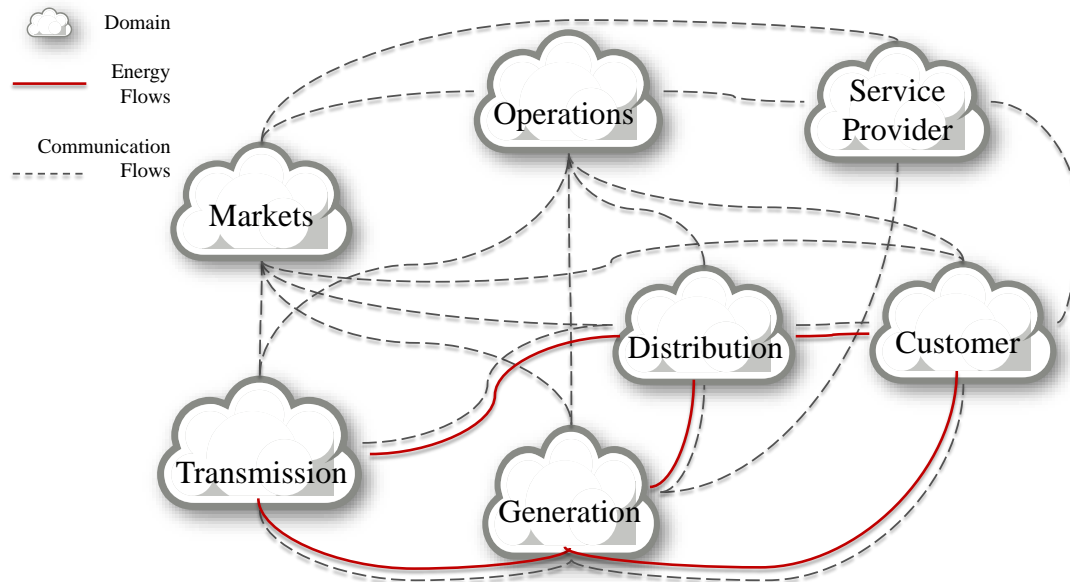


Figure 1.1: A conceptual model to show the interactions of roles in different smart grid domains through ICT [5].

Further, a MG is defined as a networked group of distributed energy generators and controllable loads serving a local area like a small-scale smart power grid [6, 7]. The operation and construction of a MG is flexible and can be considered as a good example to study the many features in a large-scale smart grid. Traditionally, a MG either operates in the grid-connected or islanded mode and is able to switch between these two modes when needed. However, less attention has been paid to encouraging distributed MGs to cooperate to save energy. In fact, the time-varying nature of renewable generation and demand within a MG makes it challenging to match the power supply with the demand consistently. This requires a MG to seek power from external sources. By forming coalitions, the power losses are anticipated to be reduced due to a shorter distance between nearby MGs when the energy is transmitted.

Another important component under the concept of the smart grid is EV. As an alternative to the traditional internal combustion engine vehicles, EVs are widely perceived as a green solution to improve energy efficiency and reduce carbon emissions [8–10]. However, if the charging energy for an EV is entirely from traditional coal-fired power plants, the CO₂ produced is generally more than for a standard fuel-driven vehicle [11]. One promising solution is to integrate

renewable energy in coordination with EV charging scheduling. A charging station that consists of renewable energy generators and controllable charging demand such as the EVs can be generally perceived as a MG. The stochastic and unpredictable characteristics of renewable generation and individual EV's charging requirement makes the charging scheduling at the MG-like charging station more challenging than using the energy directly from the main power grid.

Motivated by the above scenarios, the use of decision-making techniques from the field of game theory is investigated to study the coalition formation problem among distributed MGs for energy trading. Advanced scheduling approaches and stochastic optimization are utilized to analyse the uncertainty issues in EVs charging scenarios.

1.2 Objectives and Contributions

1.2.1 Objectives

The objective of the work conducted in this thesis is to study the performance of energy management techniques for MG energy trading and EV charging within the smart grid. It aims to develop game theoretic algorithms to guide distributed MGs to form coalitions so as to minimize the power losses during energy trading. The next part of the work is to investigate the computational complexity of the algorithms and to propose new frameworks that are more efficient in forming MG coalitions. Finally, this work also aims to design advanced scheduling approaches to a stochastic optimization problem in EV charging scenarios so that both the EV drivers and the charging station can achieve their best outcomes.

1.2.2 Key Contributions

The key contributions of this thesis are summarized as follows:

- A coalition formation game based on merge-and-split is implemented for energy trading among distributed MGs based on their geographical locations and power losses dissipated on the cables.
- Three alternative approaches to the state-of-the-art method are proposed to improve the performance of coalition formations. A modified weak-merge-weak-split method, a

switch operation and a set partition algorithm are designed and compared in terms of power loss, coalition size and algorithms' computational complexity. These results have been published in the 15th Annual PostGraduate Symposium on the Convergence of Telecommunications, Networking and Broadcasting [12].

- A low complexity two-sided matching framework for the power loss minimization problem as a college admissions game is designed. The computational complexity of the college admissions based algorithm only grows at a quadratic rate. Thus, the algorithm is more efficient for a network with a large number of distributed MGs. These findings have published in IEEE International Energy Conference [13] and in IEEE International Conference on Smart Grid and Clean Energy Technologies [14].
- Further, the problem that a MG-like charging station needs to decide how to optimally schedule the randomly arriving EVs under uncertain renewable energy generation is studied. A stochastic solar generation model, a performance index to measure the charging station's utility and a two-stage priority-based scheduling mechanism are proposed to solve this utility maximization problem. The material has been published in IEEE International Conference on Communications Workshops [15]. A detailed extension of the work [16] has been submitted to IEEE Transactions on Smart Grid and is under the first round revision.

1.3 Organization of the Thesis

The remainder of the thesis is organized as follows:

Chapter 2 This chapter presents the general principle background knowledge related to the topic of the research work conducted in this thesis. It starts with an introduction to power system foundations including the concept of active and reactive power, frequency control and selected simulation software for power systems. Then, smart grid and its applications in MG and EVs are introduced. A review of selected decision-making techniques including game theory, two-sided matching and scheduling algorithms is given in the end.

Chapter 3 This chapter first gives a comprehensive literature review on some of the key research findings in recent years that are related to the development of the research work in this

chapter. This includes MG research in the areas of system control, communication techniques, decision making and MG cooperation. Game theory related ideas in energy trading such as non-cooperative games, cooperative games and behaviour games are also discussed. Then, it specifies the system model of distributed MGs that are allowed to trade energy with each other. A comparison of the state-of-the-art coalition formation game theoretic approach with three alternative approaches and a non-cooperative baseline game is investigated. Finally, the performance of the proposed algorithms is analysed in terms of computational complexity, power loss, and coalition size through Monte Carlo simulations.

Chapter 4 This chapter extends the study of the power loss minimization problem for distributed MG energy trading, as it has low complexity and good performance in terms of power losses and coalition size. This efficient framework is formulated as a college admissions game with variable energy quotas and its complexity to grow at a quadratic rate with the number of MGs. A review of recent research works in stable marriage and college admissions problem and economics in energy trading is given first in this chapter. Then, the considered system model, a detailed description of the proposed framework, a mathematical proof of the properties of the proposed framework and a case study are given subsequently.

Chapter 5 This chapter studies the case that EVs are scheduled and charged at a MG-like charging station using on-site solar energy. We look inside the MG, i.e. the charging station, in this chapter, where the problem of pairing EVs with solar energy is analogous to that of pairing of MGs in Chapter 3 and Chapter 4. Some of the key on-going research works are first reviewed in terms of charging location, charging energy source and discharging service. Then, the system model of the charging station is illustrated in terms of the EV arrival model, the energy supply model, the charging station's utility metric and the formulation of the optimization problem. Next, the proposed two-stage priority-based scheduling mechanism is described. Finally, a comprehensive numerical evaluations of the proposed mechanism applied to the EV charging scenario is conducted through Monte Carlo simulations.

Chapter 6 This chapter gives conclusion of this thesis and summarizes some of the key research findings and possible directions to future work.

Chapter 2

Background

In this chapter, we introduce the general background knowledge related to the topic of this thesis. First, the basics of power systems including the concept of active and reactive power, frequency control and selected simulation software for power systems are presented. Then, the introduction to the smart grid and its applications in MG and EVs is given. Finally, selected decision-making techniques such as non-cooperative and cooperative game theory, two-sided matching, and scheduling algorithms is introduced.

2.1 Power System Foundations

The electric power system is a network of electrical components deployed to transfer electricity generated to customer load. The network can be widely divided into different sections: generators, transmission (high voltage) and distribution (medium and low voltage). An overview of conventional electrical grid power system from generation, transmission and distribution of electricity is shown in Figure 2.1. It is shown that electricity is generated at power stations and the voltage is stepped-up to 400 kV or 275 kV for national wide transmission since a higher voltage can reduce power losses and allow for a longer distance. Then the voltage is stepped-down to 132 kV and electricity is distributed by regional electricity companies. The voltage is further stepped-down to 11 kV and 33 kV to serve different customers such as small and large industrial users. For residential users, a second transformer is used to step the voltage down to the low voltage level 240 V for local use.

However, the centralized power grid who mainly offers unidirectional power flow is less capable of providing a dynamic power match between the supply and the demand with the constantly increased demand, limited available resources and climate change concerns. Nor is this structure robust enough to guarantee a highly reliable power supply under emergency or fault situations [64]. Thus, it is of many interests to transform the current electrical power system to a more efficient one with the aid of distributed control and ICT, aiming to make the best

use of energy, reduce power losses caused on the cable, and to reduce carbon emission levels [29, 46, 65, 66]. This motive brings many challenges to the conventional power grid, such as the integration of renewable energy, supply and demand variation, transport electrification (e.g. EVs), and financial reflections.

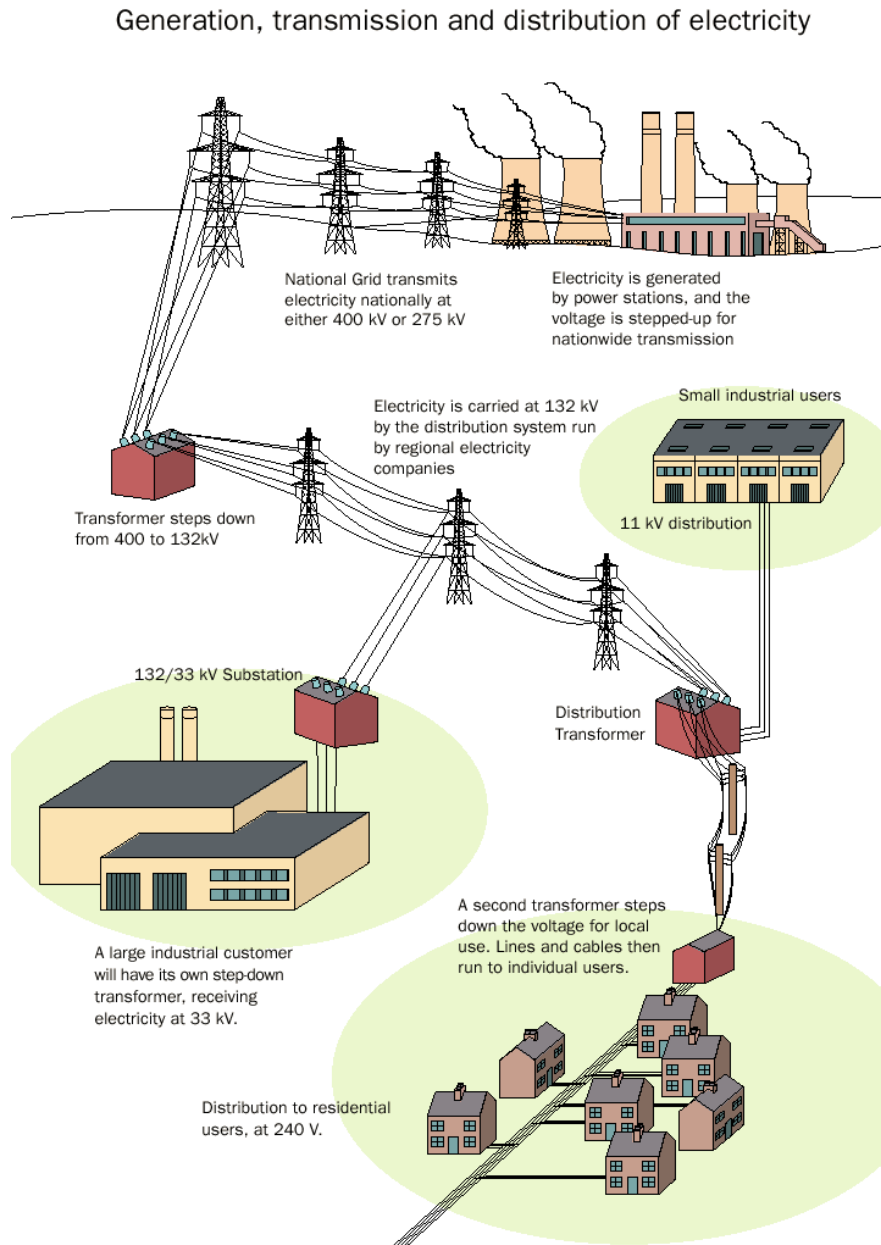


Figure 2.1: A power system from generation, transmission and distribution of electricity [1].

Next, we will introduce three fundamental aspects so as to have a brief idea of how the ex-

isting electrical power system works before implementing advanced techniques for the next generation grid - the smart grid.

2.1.1 Active and Reactive Power

The concept of active, reactive and apparent power plays an important role in understanding how energy is transmitted [17, 18]. Power is the rate of flow of energy being transmitted through electric power systems. In alternating current (AC) circuits, components such as inductors and capacitors may result in reverse direction of energy flow that returns to the source in each cycle of the AC waveform. This portion of power is known as reactive power. Another portion of power resulted in non-inductive purely resistive components such as heaters and irons is known as active power or real power.

A simplified circuit diagram shows the generation of active power P and reactive power Q in Figure 2.2 (a), where the system impedance Z consists of resistance R and reactance X . The relation of P and Q can also be represented in the power triangle, as shown in Figure 2.2 (b), where ϕ is the angle of difference between current and voltage, S is the complex power being the product of the sinusoidal voltage and current, and the length of S is the apparent power. If the load in an AC circuit is purely reactive, the phase of the voltage and current has 90 degrees of difference (i.e. $\phi = 90^\circ$). The product of voltage and current is positive for half of each cycle and negative for the other half of the cycle. This indicates that on average, the amount of energy flows toward the load flows back. Thus, there is no net energy transferred to the load. Since the same amount of energy keeps flowing alternately from the source to the load and back from the load to the source, reactive power does no actual work on the load. Thus, reactive power is also called imaginary power and usually represented as the imaginary axis in the vector diagram. Active power, also called real power, is represented as the real axis. The mathematical relationship among them can be also represented in the form of complex numbers as:

$$S = P + jQ, \quad (2.1)$$

where j is the imaginary unit. For a purely resistive load, active power can be simplified as:

$$P = \frac{|V|^2}{R}, \quad (2.2)$$

where R denotes resistance of the load, units in ohms Ω . For a purely reactive load, reactive

power can be simplified as:

$$Q = \frac{|V|^2}{X}, \quad (2.3)$$

where X denotes reactance of the load, units in ohms Ω .

When power flows through the circuits, system will generate heating losses. This may be expressed in terms of the complex power flow in the network as

$$Loss = II^*R = \frac{(P + jQ)(P - jQ)}{VV^*}R = \frac{P^2 + Q^2}{V^2}R, \quad (2.4)$$

This shows that the power losses for a certain load R are proportional to the sum of the squares of active power P and reactive power Q , and inversely proportional to the square of voltage V . Reducing reactive power reduces losses and CO2. So it is only natural to want to reduce reactive power so as to improve the energy efficiency of the electrical network. The energy efficiency is generally defined as the power factor, which is the ratio between the active power (W) and the apparent power in (VA). The value of the power factor is required between the limits of 0.85 (lagging) and 0.9 (leading) in the United Kingdom. However, the disadvantage of having insufficient reactive power is that it will lead to lowered voltage levels and cause severe damage to the electric power system. Since if voltage is not high enough, active power cannot be supplied. Thus, the control of reactive power is often associated with voltage regulation in power systems.

Some major objectives to ensure a normal operation of a generation, transmission and distribution network can be further summarized as follows:

1. The amount of real power generated and consumed must maintain balanced at all times:

$$P_{gen} = P_{demand} + P_{losses} \quad (2.5)$$

2. The system frequency has to be controlled within a limit. This will be discussed later in Section 2.1.2.
3. The amount of reactive power generated and flew back (stored) must maintain balance at all times:

$$Q_{gen} = Q_{stored(load)} + Q_{stored(network)} \quad (2.6)$$

4. Voltage profile has to be maintained in range. Reactive power provides the important

function of regulating the voltage. The conventional voltage control approach is by injecting or consuming reactive power through inserting capacitive or inductive components in the circuits. The details of voltage control and reactive power compensation techniques can be found in research papers such as [17, 19, 20].

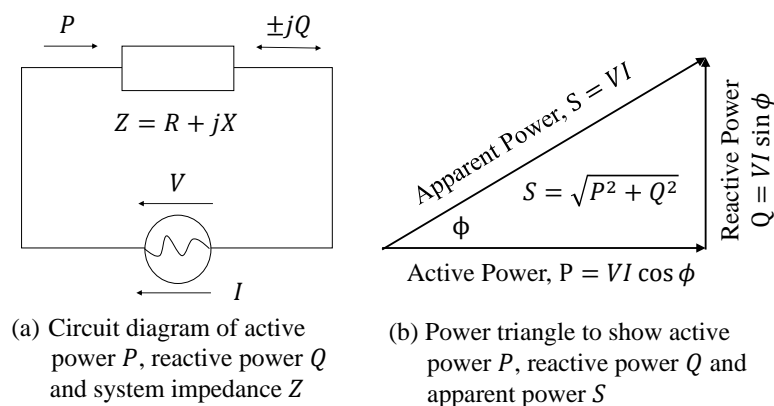


Figure 2.2: The graph of power triangle to show the relation between active power (W), reactive power (VAR) and apparent power (VA).

2.1.2 Frequency Control

The frequency in power system is the nominal frequency of the oscillations of alternating current (AC) that is transmitted from generation to end-users. The trend in system frequency is a measure of mismatch between power generation and demand, and is one of the fundamental principles for the grid operation. It is a continuously changing variable on a second-by-second basis and has to be controlled balance between the generation and the demand. Since appliances are designed to operate efficiently and safely on a certain frequency. In the majority parts of the world the frequency is 50 Hz, except for Americas and parts of Asia (e.g. Japan) it is typically 60 Hz.

If the generation is greater than the demand, the frequency goes up; while if the demand is greater than the generation, the frequency falls. This is because with the increased demand, the power generator engine would also need to supply more power to the axle of the alternator. But the alternator cannot ramp up immediately, so the rotation speed of the alternator drops causing a drop in frequency for a short period. Since the power supply is catching up, there will be more

current flowing to the load through the long wire, thus the voltage at the electrical load end will go lower as well. Therefore, the grid operator has an obligation to control the frequency within a certain limit, i.e. at 50 ± 0.5 Hz, as shown in Figure 2.3. It is an example taken from [2] and shows that the system frequency is fluctuating around the nominal value 50 Hz.



Figure 2.3: Frequency data to a 15 second resolution over the last hour, last access at 17:20 27th July 2017 at [2].

The frequency response is a control mechanism to ensure the system frequency within the right range. The control of frequency can be done from both the generation side and the demand side. For instance, on windy days, there might be more wind energy injected to the grid, thus some wind turbines might need to be turned off to maintain the balance of the total generation and the total demand. On the other hand, frequency control can be done by demand management through interruption of customers' demand. If the total load is greater, some electricity demand can be automatically interrupted for up to 30 minutes duration. This usually happens, for example, when there is the loss of a significantly large generation.

2.1.3 Simulation Software

In this thesis, implementation of the proposed algorithms, simulations and experiments are conducted using MATLAB software. However, there are a few other available software for power systems simulation that might be of interest to the readers of this thesis. Some well-

known simulation software are summarized as below.

PowerWorld PowerWorld Corporation that was founded in 1996 provides a wide range of products and tools needed for transmission planners, power marketers, system operators and trainers, educators to analyse power system information in a user-friendly manner. The software offers a set of interactive power system packages to simulate power system operation on a time frame that can be ranging from several minutes to several days. In addition, the power flow analysis package is capable of large power networks modelling and can efficiently solve systems of up to 250,000 buses. More details about the simulator can be found on its website [21].

MatPower MatPower is a set of open-source MATLAB-based power system simulation packages presented in [22]. It provides tools for optimal power flow (OPF) analysis. The OPF architecture is designed to be extensible and easy to add customized variables, costs, and constraints to the standard OPF problem. A detailed example of a large-scale network modelling and an extensible OPF problem formulation by MatPower can be found in [22].

MATLAB Simulink MATLAB software and Simulink platform can be used to simulate, model and assess power system performance from power generation, integration of power plants to the electric grid, and system parameter estimation. Some of the examples and manuals can be found in [23].

2.2 The Smart Grid and its Applications

The existing electrical grid was built up over more than 100 years. It is now one of the most important infrastructures on which the modern society depends to run effectively. The power grid delivers electrical energy to almost all sectors of the society such as industry, commercial and residential consumers to meet their increasing demands. While most of today's generation capacity still heavily rely on fossil or coal-fired fuels, this will contribute to a significant increase of carbon dioxide with a negative effect on the global climate and environment. To satisfy the ever-growing demand for power and the need to reduce carbon emissions, the concept of the smart grid is introduced to provide a more reliable, sustainable, scalable and economical

control of the electricity supply. It is realized by integrating bi-directional information flow along with the electrical cables, which can provide more effective and better controlled power generation and demand [24]. This two-way information flow enables active components in the smart grid to coordinate and keep the generation and the demand in balance.

In the traditional power grid, energy is generated at the high-voltage transmission network usually from a relatively small number of large power stations, then dispatched to the distribution networks which can be viewed as cables delivering electricity to the end-users. Unlike the way how the existing power grid works, the benefits of having more flexibility in the smart grid brings more uncertainty (such as the prediction of renewable energy generation, the scheduling of the widespread EVs, and the transition of the role of consumers to prosumers¹) to the whole system. At the transmission level, new types of renewable energy sources such as the offshore wind farms and photovoltaic panels will be connected to the conventional power stations and contribute to the generation capacity. This type of energy is sustainable and has many benefits to the environment, but it relies entirely on the weather such as when the sun shines or the wind blows and cannot be controlled like a conventional generator [25]. At the distribution level, customers would have the option to connect with new loads such as EVs and install small distributed energy generators such as solar photovoltaic panels. This has changed the role of end-users from energy consumers to energy producers. The result of the widespread implementation of these new components in the smart grid motivates the adoption of advanced techniques for information exchange and control at different levels. Next, two emerging applications: MG and EVs under the concept of the smart grid is introduced.

2.2.1 Microgrid

MGs can be viewed as a novel distribution network architecture within the smart grids concept. A MG is a localized power system serving a small geographical area, that consists of controllable loads and distributed energy resources, such as distributed generators and storage devices. It can operate in a controlled and coordinated way either connected to the grid or islanded, if required, can also switch between these two modes [6, 7, 26–28].

An example of a MG infrastructure from the generation, distribution to the consumption of energy is shown in Figure 2.4. The MG in Figure 2.4 is connected to the utility grid at a

¹A prosumer not only consumes energy but also produces energy, such as from its roof-top solar panels.

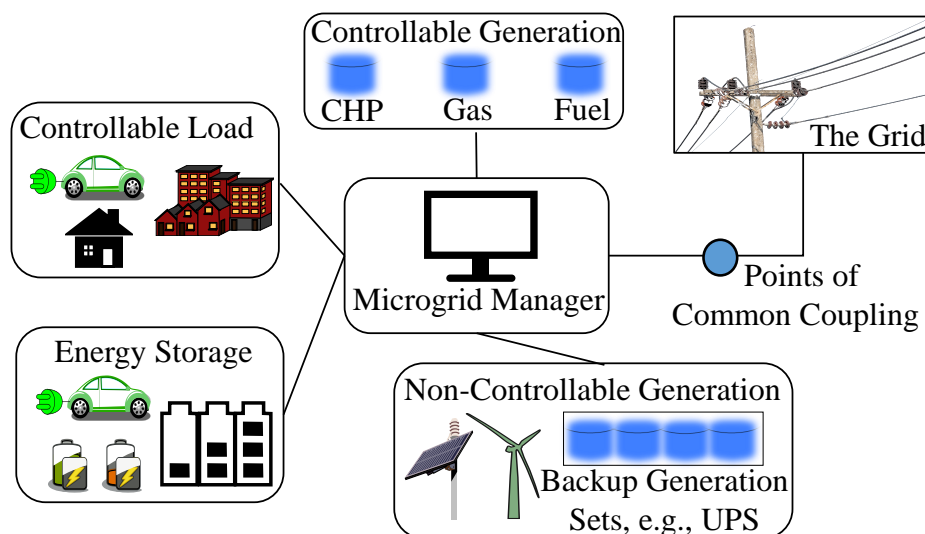


Figure 2.4: An example of a microgrid infrastructure.

Point of Common Coupling (PCC) that can maintain voltage at the same level as the main grid [7]. A switch can separate the MG from the main grid either automatically or manually to enable it to function as an island. This may be required when part of the main grid needs to be repaired under emergency situations such as storms and power outages. The MG then can disconnect from the main grid and operate on its own using local distributed energy generation. The MG manager, also seen as an aggregator, is responsible for the coordination of both the information exchange and power flow dispatch within the MG. A MG can be powered by both controllable generation (such as natural gas fired small-scale combined heat and power (CHP) and fuel cells) and non-controllable generation (such as solar photovoltaic panels) that can be stored in the uninterruptible power supply (UPS) units and used as backup generation when the main power fails. The energy consumptions such as in buildings and EVs might be also controllable by applying various Demand Side Management (DSM) techniques [29]. Consumers are normally encouraged and rewarded to time-shift some of their energy demand to reduce the energy demand peak-to-average ratio. Naturally in small power systems, the load variability and generation fluctuation will be more severe than in the main power networks [6]. Storage devices are often introduced as energy buffer and play an important role in the MG. This includes all sorts of electrical, pressure, flywheel, gravitational and heat storage technologies.

The heterogeneous nature of MGs enables an improved management of energy so as to con-

control and ensure an efficient, smooth and reliable operation in both islanded and grid-connected modes. Generators and loads might be controlled by a local energy management system (EMS) to optimize the power flow within the MG network. The objective of the EMS depends on the mode of MGs operation. Some of the key challenges for MGs operation [30] can be summarized as :

- Economical dispatch of the distributed generation (DG) units.
- Satisfactory operation of renewable energy sources (RES).
- Stability and control of the MG.

These concerns have been addressed in both the autonomous and grid-connected manners, as well as a combined mode in recent studies.

Autonomous MG Operation. The main target of the energy management in MGs islanded mode is to stabilize the system through frequency and voltage controls [30]. One way to realize this aim is by introducing economic incentives to the MG. Various optimization approaches, such as stochastic optimization, multi-objective optimization, and hybrid optimization have been proposed to minimize the operational cost and environmental impact, to maximize generation so as to export to the main power grid and to maximize the utilization of renewable generations. More specifically, various approaches have been proposed to address the uncertainty issues of renewable generation, such as direct load control [31], resource scheduling [32] and optimal power flow methods [33]. Energy storage (ES) devices are often employed to enhance the reliability of MGs with a high renewable energy penetration. However, the use of ES devices introduces extra cost for battery installation and maintenance. Thus, apart from the power balance issues between the generation and consumption, battery management system must also be taken account of. On the other hand, a holistic view that considers both the MG operator and consumers have also been studied. The work in [30] has proposed an integrated framework that not only guarantees an economical and stable MG operation but also provides the opportunity for the consumers to minimize their energy bills.

Grid-connected MG Operation. The main objectives of the MG energy management in the grid-connected mode are to minimize the costs of importing energy at the PCC, to improve power quality and to minimize the voltage fluctuation within the MG [33]. Energy management in MGs can be usually viewed as a three-level control system. The first control level is

often called the autonomous control and consists of a number of local distributed controllers that can make decisions independently. The secondary control level employs communication technologies and is responsible for the frequency and amplitude information exchange within the MG. The tertiary control level is related to the control of active and reactive power flow and often utilizes an optimal power flow (OPF) solver. However, the interaction with the main power grid in the grid-connected mode requires the OPF solver to be able to represent the unique aspects of MGs, such as distributed energy sources, storage devices, and pricing methods. The studies of OPF can be categorized into three directions [33]. The first one focuses on the allocation of renewable generation such as solar and wind; the second one addresses the economic aspects and often aims to maximize the overall profit of energy generation; and the third category is to optimize the power dispatch considering energy storage devices. The work in [33] further proposed an advanced OPF solver that not only considers the limitation of storage devices but also takes account of the constraints of the network regarding voltages, currents and power levels.

Case Study: Bornholm Island, Denmark. In this paragraph, a practical MG implementation as a case study is introduced, aiming to show one example of how a MG works in real life. Bornholm is a Danish island that represents approximately 1% of Denmark's population (around 28,000 customers) and electricity load (around 63 MW peak load and an annual electricity consumption of 262 GWh in 2007). The island is powered by 14 diesel generators (34 MW), 1 oil-fired steam turbine (25 MW), 1 mixed-fired steam turbine (37 MW), 35 wind turbines (29 MW, accounted for 30% generation in 2007) and 2 biogas turbines (2 MW), as well as a high-voltage direct current (HVDC) interconnector to Sweden. The distribution network consists of a 60 kV network and a 10 kV network. The island is one of the field test sites for an European Framework 7 project named EU-EcoGrid. Due to its ability to go planned islanded mode, it is also used for demonstration of new challenges such as how to achieve a 50% penetration of wind power during islanded operation. The project also combines market, commercial and technical solutions to guide households' energy consumption based on the real-time market energy price to alleviate the congestion on the local network. The local electricity company, OSTKRAFT, incorporates two systems for the real-time MG operation. The first system takes measurements as 10 second instantaneous values, 1 minute and 1 hour average values; while the second system is used for controllable wind turbines and takes measures as 10 minute average values. The company also established a smart platform to demonstrate the impact of everyday life of a typical household, so as to encourage more participants from politi-

cians, industry, academia, research institutes and local community groups joining the project [6, 25]. However, a MG can come in a variety of sizes and designs in practice as there is no specific definition for a MG so far, as long as it is able to work as a self-contained localized energy system. Particularly, in Chapters 3 and 4, we look at the behaviours of energy trading on the MG's level but neglect the detailed modelling of each MG. While in Chapter 5, we look inside a MG and specifically model this as an EV charging station equipped with solar panels and battery storage. The link behind the rationale is rather obvious since pairing of MGs can be seen as similar as to pairing of EVs with solar panels.

2.2.2 EV Charging

For decades, pressures such as the environment, economics, and security have been motivating inventors, manufacturers and consumers with the idea of electrified transportation. However, the global transportation nowadays still remains fossil fuel based and accounts for nearly 72 percent of the global oil demand [34]. The adoption of EV is believed to fundamentally change the transformation of electrifying transportation sector. It is also expected that more electric cars will be on the road in the UK, according to a draft report [35] that Britain is to ban all petrol and diesel cars from 2040. The term EV² often indicates several different vehicle technologies including hybrid-EVs (HEV), pure-EVs and plug-in hybrid EVs (PHEV). The definition of them is listed below [36].

- HEVs run on gasoline-powered motor and use batteries to improve fuel efficiency. But external electricity is not used.
- Pure-EVs run on battery-powered electric motor. The battery can be recharged by plugging in the vehicle.
- PHEVs can be not only recharged with electricity like EVs but can also run like HEVs. This combination offers extended driving range, potential sufficient fuel, reduced costs and carbon emissions.

Impact on the Power Grid. If a large fleet of EVs are connected to the grid without effective coordination, the impacts on the distribution networks are likely to be significant since EVs usually have a high energy demand. Instead, customers can be given rewards to charge their

²In this thesis, the term "EV" is used to mainly refer to the purely battery-powered vehicles.

vehicles during off-peak hours to flatten the peak load on the grid. Enabled by the smart grid and battery technologies, EVs are able to adapt to various grid conditions. Short-term (< 5 minutes) interrupting charging can help with the grid regulation and renewable integration. Longer term (30 minutes) interrupting charging can benefit the grid by reducing the electricity generation by taking advantage of the batteries in EVs [37]. Since the energy stored in EVs' batteries can be discharged and provide the power back to the utility grid during peak hours. In this context, the charging of EVs can be controlled in three ways [34]:

- Demand response: such as in response to pricing signals so as to influence EVs charging time.
- Demand side management: to prevent overloading on the grid by actively managing the overall electricity demand.
- Vehicle-to-grid (V2G) service: to allow the battery to be discharged and supply the energy back to the grid.

As the vehicles are only used for a limited period each day and the charging urgencies are often flexible, the benefits offered by the aforementioned control approaches can be very promising to the utility grid.

Charging Station. The limitations of the charging rate of both the EV's battery and charging outlets will result a relatively longer time for an EV to be fully charged than a conventional internal combustion engine vehicle with the same driving range. If the required charging energy is entirely produced by coal-fired power plants, the charging process will still cause a considerable amount of carbon dioxide emissions [38]. One possible solution is to integrate renewable energy as the source of energy for charging EVs. The rate of charging can also be viewed as a trade-off between the costs and charging times. For instance, a 40-mile-range EV might take six hours to charge at 120 V or three hours at 240 V. A higher charging rate requires the utility and household to upgrade their charging infrastructures that will lead to extra costs. Some people suggest the idea of swapping batteries at charging stations to eliminate the delay involved in waiting for the vehicle's battery to charge [39]. The range of the vehicles will also have a major impact on the charging facilities since the required charging rate will have to increase proportionally with the increased vehicle range so as to ensure a reasonable charging time. In addition, the availability of public charging facilities such as at work, at shopping areas and

roadsides plays an important role in extending EVs driving range and reducing drivers' range anxiety.

A charging station is designed to provide electric power for recharging EVs so as to extend their travel range. It often consists of three main components: energy supply, power cords, and connectors [40].

- **Energy supply** component is used to supply electric power and provide system protection. It can also integrate information systems to measure the amount of charging energy to the EVs.
- **Power cords** are the cables that connect the power supply device with the connectors of the on-board charging outlets. They can either carry alternating current (AC) or direct current (DC) as well as communication signals to transmit the electrical currents.
- **Connectors** are the plugs on the power cords that connect the energy supply to charging outlets on EVs.

Charging stations at residential homes and public areas may have different charging specifications and provide different services. The charging rates are normally divided into three levels [36, 40].

- Level 1 AC charging is widely available at homes and businesses with standard outlet and voltage level. It can take 8-14 hours to fully charge an EV, thus it may not be the preferred charging method.
- Level 2 AC charging is faster than Level 1 but will often require an upgrade to the existing infrastructure. It can take less than half of the time required in Level 1 to fully charge an EV.
- Level 3 DC charging is often available at fast charging stations. It can take 20-30 minutes to fully charge an EV. Since the capacity of the power required in this level is beyond most residential capacity, it is often expected to be implemented for public charging stations.

The specifications of these three charging levels are summarized below [36].

Level	Voltage and current	Usage	Charging rate (kW)	Time to fully charge
1	110 V, 15 A	Opportunity	1.4	18 hours
2	220 V, 15 A	Home	3.3	8 hours
	220 V, 30 A	Home/Public	6.6	4 hours
3	480 V, 167 A	Public/Private	50-70	20-50 minutes

Table 2.1: Specifications of EV charging levels.

The business model of EV charging also differs under various circumstances. Depending on how the utility will support EVs, how actively EVs want to participate in the market, which technology infrastructure is available and whether the market is regulated or deregulated, there are three possible approaches for the residential charging scenario [34] as listed below.

- Utility owned charging station is metered, managed and secured as part of a smart grid. The utility is to determine when the charging occurs and how much the charging rates are.
- Utility subsidized charging station is owned by the consumers or a third party. In exchange to provide incentives to the charging station, the utility would still have some rights to control the charging.
- Charging station as an appliance is owned and managed by the consumers.

The deployment and operation of EV charging stations also rely on some related technologies, such as smart grid communication, renewable integration and battery swapping. Recharging even a low level of EV battery pack might present a significant impact on the electrical grid. Smart grid technology can help the grid to manage this impact through scheduled and controlled smarter charging. By providing communication capability to the grid, utilities can better manage EVs charging. For instance, in a V2G scenario, additional communication might be required among the electrical grid, the charging station and the EV drivers so as to decide when and how much of the energy to be supplied back to the grid. Charging stations are usually supplied by the main electrical grid, which often indicates that the electricity originates mainly from fossil-fuel or nuclear power stations. Recent research and demonstrations have investigated the integration of renewable energy to the charging station, such as solar-powered (e.g.

SolarCity [41]) and wind-powered (e.g. the Sanya SkyPump [42]) charging stations. A battery swapping service can be also provided at EV charging stations. Depleted batteries can be immediately swapped for a fully charged one so as to reduce the delay involved in waiting and charging the batteries [39].

Consumer’s Point of View. Despite the many environmental benefits of electrified transportation, the number of EVs in use is still insignificant so far. One possible reason behind the low adoption of EVs is the consumers’ perception of EVs. A review [43] has given a comprehensive overview on consumer EV adoption from both theoretical and empirical research perspectives. The authors identified five main themes on consumer EV adoption behaviour, that is behaviour influenced by rational choice, environmental attitudes, symbolic and lifestyle behaviour, innovation adoption behaviour, and consumers’ emotional behaviour. These factors can be taken into account of future charging infrastructures design and provide insights in future research directions.

Comparison of Competing Technologies. The review given in [36] has summarized the current competing technologies to EVs. The pros and cons of gasoline-, natural gas-, diesel-, and hydrogen-powered vehicle technologies are listed below altogether with the EV technology in Table 2.2.

Technologies	Pros	Cons
Gasoline	- Well-known technology	- Limited sources in the long term
Natural gas	- High energy density and quick refuel - Domestically available	- Safety concerns - Volatile price - Lack of roadside infrastructure
Diesel	- More efficient than gasoline - Well-known technology - Availability of infrastructure	- Relies on foreign fuel sources - Noise and smell concerns
Hydrogen	- High efficiency - No local emissions	- Lack of infrastructure - Difficulty of storage - High cost
EV	- No tailpipe carbon emissions - High efficiency - Availability of electricity, inexpensive, flexible	- High battery cost - Long charging times - Require extra infrastructure, such as fast charging stations

Table 2.2: Comparison of competing technologies to EVs.

2.3 Selected Decision-Making Techniques

In this section, we introduce some of the selected decision-making techniques that are related to the development of this thesis. First, game theory including non-cooperative games and cooperative games is discussed; then, two-sided matching algorithms including stable marriage and the college admissions problem are given; scheduling algorithms are given in the end.

2.3.1 Game Theory

Game theory can be viewed as a set of mathematical formulations to model the conflict and cooperation between intelligent and rational decision makers. The notion “game” often refers to an event when people interact with each other. Based on the interactive situations where whether conflicts or cooperation exist among the decision makers, the games can be distinguished into two categories: non-cooperative game theory and cooperative game theory. Both theories have been widely used in applications such as economics, politics, military, evolutionary biology and engineering. In recent years, game theory has attracted a growing interest from researchers and been utilized to model and analyse the interactive relations among intelligent components under the smart grid context, especially for energy management [44–46].

Early work published in 1941 by John von Neumann and Oskar Morgenstern has first paved the way of modern game theory by providing mathematical formulations regarding strategic behaviour in conflict situations. They further identified the different research focus on non-cooperative games and cooperative games. In the former game, each involved decision maker has chosen its best strategy depending on the strategy of others. While in the latter game, the patterns of coalition formation among rational decision makers are more important. Following work published in 1950 by John Nash has contributed substantially to the non-cooperative game theory by developing a general formulation of the equilibrium idea, known as the Nash Equilibrium. It is a combination of strategies where no decision maker could achieve a better payoff by unilaterally deviating from its original strategy. Meanwhile in the field of cooperative game theory, Gillies (1959) and Shapley (1953) have introduced important concepts called the Core and the Shapley value to analyse the fairness allocation for cooperative n-person games [47]. Game theory can be also viewed and distinguished from various perspectives. Some famous classifications include zero-sum and non-zero-sum games, symmetric and asymmetric games, simultaneous and sequential games, perfect information and imperfect information games, and

so on [48]. The focus of this thesis is to investigate the interactive relations among intelligent decision makers under the smart grid context, thus it is natural to adopt the classification of non-cooperative and cooperative game theory. Some basics in these two categories and some related techniques are introduced below.

2.3.1.1 Non-cooperative Games

Non-cooperative game theory focuses on the study of competitive decision making involving a number of players who have totally or partially conflicting interests. In a non-cooperative game, each player makes its decision independently given the possible actions of the other players and their effects on the player's utility. It is worth noting that the term "non-cooperative" does not necessarily mean that the players do not cooperate, it indicates that any cooperation that might be formed must be self-enforcing without negotiation of strategic choices among other players. For instance, in the smart grid, a customer who has the access to the real-time electricity price via smart meters can make a decision on whether to use the washing machine or not at a certain time without consulting the "neighbours" [19].

Static and Dynamic Games. Non-cooperative games can be further divided into two groups: static games and dynamic games, based on whether time or information will affect the decision making process. In a static setting, the players take their actions in one-shot independently of each other without any notion of time. The decision has been made without any knowledge of the other players. Thus, such a game can be generalized as a process that the decisions are made simultaneously. In contrast, a dynamic game is one in which the players have some information about the others' choices and can act more than once. Thus, time has played a central role in the decision making process [3, 46].

- **Static Games.** For static non-cooperative games, one of the most popular representations is given as in a strategic (or normal) form. Such a game in a strategic (or normal) form has three components: the set of players \mathcal{N} , the set of their strategies $(\mathcal{S}_i)_{i \in \mathcal{N}}$ and their utility functions $(u_i)_{i \in \mathcal{N}}$. Each player i wants to choose a strategy $s_i \in \mathcal{S}_i$ so as to optimize its utility function $u_i(s_i, \mathbf{s}_{-i})$. The utility function $u_i(s_i, \mathbf{s}_{-i})$ is not only determined by player i 's strategy choice s_i but also by the vector of strategies taken by the other players in set $\mathcal{N} / \{i\}$, denoted as \mathbf{s}_{-i} . In static games, a strategy that is made regardless of any other information coincides with the concept of an action. Thus, the notions of a strategy

and an action are interchangeable for static games.

- **Dynamic Games.** Unlike the static games where the concepts of a strategy and an action are identical, they have different meanings in dynamic games. An action is often taken based on the strategy that maps the information acquired by the player to his action. For instance, if a person is to decide what to do for the evening with the possible options of either going camping or staying at home, then one strategy would be like “If the weather is dry, I will go camping; otherwise, I will stay at home.”. By knowing the weather condition (i.e. the available information to the decision maker), an action is taken (i.e. to go camping or to stay at home) [3]. In this thesis, the terms action and strategy will be used interchangeably unless explicitly distinguished when necessary.

Nash Equilibrium. Solving non-cooperative games is not always easy in practice. One of the most widely accepted solution concepts for game theory and in particular, non-cooperative games is that of a Nash equilibrium [49]. Generally speaking, a Nash equilibrium represents a state in a non-cooperative game where no player has the incentive to unilaterally change its strategy to another one, if other players’ strategies are fixed. For a static non-cooperative game in a pure strategic form, the Nash equilibrium can be defined as below.

Definition 1. The solution strategy vector $\mathbf{s}^* \in \mathcal{S}$, where \mathcal{S} is the set of all possible strategies, is a Nash equilibrium of the non-cooperative game $G = (\mathcal{N}, (\mathcal{S}_i)_{i \in \mathcal{N}}, (u_i)_{i \in \mathcal{N}})$ such that $\forall i \in \mathcal{N}$, the following holds:

$$u_i(s_i^*, \mathbf{s}_{-i}^*) \geq u_i(s_i, \mathbf{s}_{-i}^*), \forall s_i \in \mathcal{S}_i \quad (2.7)$$

In a game, if $u_i(s_i^*, \mathbf{s}_{-i}^*) > u_i(s_i, \mathbf{s}_{-i}^*), \forall s_i \in \mathcal{S}_i, s_i \neq s_i^*, \forall i \in \mathcal{N}$, the Nash equilibrium is said to be strict [3, 46, 50]. In practice, the Nash Equilibrium can be found by calculating the payoff of each player under different strategies. The state that satisfies **Definition 1** can be called a Nash Equilibrium.

Pure and Mixed Strategies. For a game that is represented in strategic form, each player i chooses a strategy $s_i \in \mathcal{S}_i$ so as to optimize its utility function. If i selects a strategy s_i in a deterministic manner with probability 1, then this strategy is known as a pure strategy and the corresponding solution to the game in terms of Nash equilibrium is known as a pure Nash equilibrium. Instead, if a player i selects each pure strategy with a certain probability, then this strategy is known as a mixed strategy. It consists of several possible moves and a probability distribution that corresponds to the frequency of each move chosen by player i .

2.3.1.2 Cooperative Games

Unlike the non-cooperative game theory that studies the interactive behaviour among competing players, cooperative game theory provides a framework to study the cooperative behaviour of rational decision makers when they are allowed to communicate and receive shared utilities within a group. In this respect, the players in a cooperative game are allowed to form agreements among themselves to act together as one entity so as to strengthen their positions (e.g. improved utility) in a group. For instance, in politics, the formation of a coalition government can improve the chance of each participated party in obtaining a share of the power. Cooperative games can be divided into two main branches: Nash bargaining and coalitional games. The former deals with situations where a set of players need to agree on the terms of cooperation, while the latter focuses on the formation of cooperative groups, known as coalitions [3]. The theory of cooperative games provides a set of mathematical tools to investigate with whom the players to cooperate and under which terms such as incentives and fairness rules [3, 46–50].

Nash Bargaining Games. This branch of cooperative games deals with a number of players who are interested in achieving an agreement over the sharing of a resource but have a conflict of interests on the terms of the agreement. In this situation, two or more players can mutually benefit from a certain agreement but have conflicting interests on the terms [3, 50]. It is also worth noting that each player must mutually agree on the division of the resource and make its decision with consensus. One simple example in economics is a trade between a seller and a buyer. They must agree on a price so as to complete the transaction, but at the same time they have a conflict of interest regarding the price. A bargaining game can be further divided into two stages: the bargaining process and the bargaining outcome. The bargaining process is the procedure that players follow to reach an agreement, while the latter is the result of the former. John Nash has identified four axioms to represent the properties that a bargaining solution must satisfy: Pareto efficiency, symmetry, invariance to equivalent utility representation, and independence of irrelevant alternatives. A detailed discussion of Nash bargaining games can be found in [3].

Coalitional Games. The main branch of cooperative games is to investigate the formation of cooperative players, known as coalitions, aiming to improve each player's utility in the coalition. Hence, it becomes a powerful analytical framework for designing fair, robust, practical and efficient cooperative strategies in numerous research areas such as economics, political science and engineering. A coalition represents a set of players who have decided to cooperate

and act together as a single entity. Further, coalitional games can be divided into three classes: canonical games, coalition formation games, and coalitional graph games. Before diving into the details of these games, it is essential to understand two important concepts first.

- **Characteristic form:** is the most common form of a coalitional game and implies that the value of a coalition depends on the members in that coalition solely with no dependence on how these players in the coalition are structured.
- **Transferable utility (TU):** is a property of those coalitional games whose total utility of a coalition can be divided in any manner between the members of that coalition.

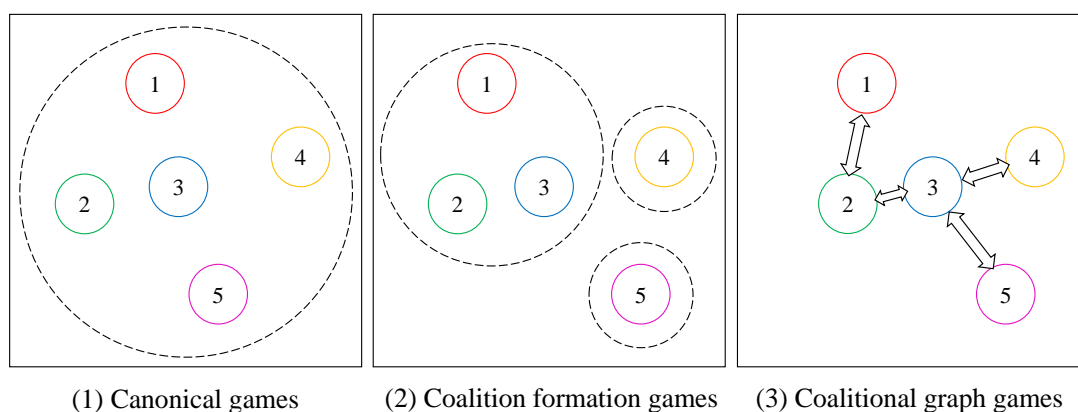


Figure 2.5: *Illustration of three classes of cooperative games, after [3].*

1. **Canonical Games.** This type of games is in characteristic form and can be with or without transferable utility. The main property in canonical games is that the formation of a single grand coalition, which is a coalition that includes all members, is seen as the optimal solution, as illustrated in Figure 2.5 (1). It shows that the five members choose to cooperate as a single entity since no one can do worse by joining the grand coalition than by acting non-cooperatively. The main question for canonical games is under which circumstances a stable and fair grand coalition can be formed [50]. Some common solution concepts have also been presented in the literature, such as the concept of the core, the

Shapley value and the Nucleolus. The details of their definitions, differences, properties and existence can be found in [49].

2. **Coalition Formation Games.** Unlike the canonical games, the network structure and the cost for cooperation play a central role in forming coalitions. This category of game theory is mainly exploited in this thesis since its resemblance to grouping local MGs. The formation of different coalition groups among five players is shown in Figure 2.5 (2). Some of the main characteristics in a coalition formation game are as follows:

- The gains by forming a coalition is not the only factor that matters to its members, the cost for such a network structure is also considered. Thus, forming a grand coalition is not always the optimal solution. Especially, if the size of the grand coalition is relatively large, the cost for a central control and operation might increase. To this regard, the optimal coalition size is one of the essential questions to be answered so as to solve a coalition formation game.
- Another important aspect is that coalition formation games are able to adapt to the changes of the game. For instance, if one or more players leave the game, the coalitions can be dynamically reformed according to some criteria such as physical restrictions of the problem, total social welfare and so on.

These characteristics have made the coalition formation game framework a promising candidate to model various practical engineering problems. However, if a centralized approach is used to find the optimal partition over a number of players, the computation is complex and impractical due to the exponentially search over all the possible partitions. Thus, it is natural to investigate distributed algorithms that have low computational complexity for forming coalitions [3, 46, 48, 49]. In this respect, the main question is to design the rules that allow the players to autonomously decide with whom to form a coalition so as to maximize their utility. The details of a merge-and-split [12] rule can be found in Chapter 3 and a two-sided matching (i.e. the college admissions framework [13, 14]) rule can be found in Section 2.3.2 and Chapter 4.

3. **Coalitional Graph Games.** From the previous discussions, we know that both the canonical games and the coalition formation games are in characteristic form. However, in some scenarios, the underlying structures between the players can have a significant impact on the total utility of the coalition. This type of games is named as coalitional graph game and can be represented in graph form. The formation of the coalitional graph

games among five players is illustrated in Figure 2.5 (3). The main issues in solving a coalitional graph game is to investigate the interconnection between the players within each coalition as well as to design low complexity distributed algorithms [49].

2.3.2 Stable Marriage and the College Admissions Problem

The stable marriage problem is the problem of finding a stable matching between two equally-sized sets of men and women, given their preferences for a marriage partner from the opposite set. In 1962, David Gale and Lloyd Shapley proposed an algorithm, known as the Gale-Shapley algorithm, that is proved to always solve the stable marriage problem for any equal number of men and women [51]. The algorithm involves a number of iterations.

For instance, in the man-proposing algorithm, at first, each woman and each man ranks each member from the opposite set, each man proposes to the woman he prefers most. Some women may receive several proposals, but she only accepts the man who ranks highest on her preference list and puts him on her waiting list and rejects the rest. In the second iteration, the men who were rejected in the first round propose to their second choice. This process continues until everyone is engaged. Since after each round, each woman accepts her best possible proposal and rejects the others, the matching is stable and optimal. Some of the key theorems of the algorithm can be also summarized as follows [51–53]:

- The algorithm always terminates and everyone gets married.
- The algorithm finds stable marriages.
- There may be different ways to solve the problem that lead to multiple stable marriages. The Gale-Shapley algorithm assigns every man his best possible wife. This means the solution to the stable marriage problem that is found by this algorithm is simultaneously optimal for all the men. Thus, the stable marriage found by this algorithm is optimal.
- The algorithm assigns every woman her worst possible husband. Thus, this algorithm favours one (i.e. the proposer) than the other (i.e. the one being proposed to).

The stable marriage problem (i.e., one-to-one matching) can be seen as a special case of the college admissions (i.e., many-to-one matching), in which the number of applicants and colleges are the same and the quota of each party is unity. The stability and optimality of the algorithm

still holds to solve a college admissions problem. The details of the stable matchings for the stable marriage and college admissions problems and their variants can be found in [51–57].

Practical Implications. The Gale-Shapley algorithm for finding solutions to the stable marriage and college admissions problems have many applications in various real-world situations. The best known of these applications is the assignment of matching medical graduates to residents. In the 1950s, the medical board in the US face a problem that the graduating medical students have to be matched to a residents program for further training, called the National Intern Matching Program. All the medical graduates submit their preferences to a central office who interviewed these students and made preference lists for residents. A computer runs this algorithm to assign graduating students to residents [53]. In fact, matching seller MGs with buyer MGs closely resembles with the problem of assigning applicants to colleges. In Chapter 4, we exploited this idea and designed a college admissions framework that is able to match MGs in a energy context.

2.3.3 Scheduling Algorithms

In computing, scheduling is the method to assign resources to tasks. The tasks maybe virtual computational elements such as data flows, threads or processes which are scheduled often on limited resources such as processors, or frequency bandwidth. For instance, in wireless networks, packet scheduling is a decision process used to select which packets should be transmitted at each time slot. The decision will often be based on a variety of network characteristics, such as frequency bandwidth, packet arrival rate, the size of the packet, deadline of packet, importance of packet, and security to meet the requirements of various network quality of service (QoS) [58]. These dynamics are also of interest to many smart grid applications, such as the scheduling scenarios where EVs are charged within their deadlines but subject to limited energy resources and charging outlets. Some of the most well-known scheduling algorithms are introduced as follows.

First in, First out (FIFO) Also known as first come, first serve, FIFO is the simplest scheduling algorithm that serves customers one at a time in the order of their arrivals. The drawback is that customers might have to wait for a longer time to be served. The lack of prioritization will sometimes cause congestions, thus the system might have troubles in meeting many deadlines.

Round-robin Scheduling (RR) The algorithm assigns each task a time slot in equal portions and interrupts the task if it is not completed by the end of the current time slot [59]. In the following time slot, the next task is processed. The tasks are processed in circular orders, in which the task is resumed in the next round when a time slot is allocated to it. Similar to FIFO, the tasks are processed without priority but following the order of their arrival time. The algorithm is simple and easy to implement but has extensive overhead especially with a small time slot. If differentiated quality of service is required, some variants of RR scheduling algorithms can be considered, such as weighted round-robin (WRR), deficit round-robin (DRR) and weighted fair queuing (WFQ) [60].

Least Slack Time Scheduling (LST) This algorithm assigns priority to the tasks based on the slack time. Slack time is defined as the amount of flexible time for a task to finish (if it has started) from the current time slot to its deadline, denoted as

$$t_s = (t_d - t) - t_c, \quad (2.8)$$

where t_d is the task's deadline, t is the current time slot, t_c is the amount of time left to complete the task. This scheduling algorithm is often used before accepting an aperiodic task with a hard deadline since the system might have no prior knowledge of when the task will arrive. This dynamics fits into the EVs charging scenario quite well [15, 16, 61]. Since vehicles are usually arriving aperiodically to the charging station with a deadline to satisfy their charging requirements. Based on the individual vehicle's charging requirement and the amount of time left before its deadline, the vehicles can be charged in the order of priority that is related to the slack time in eq. (2.8).

However, the main drawback of LST scheduling algorithm is that it does not look ahead but makes the acceptance decision only based on the current system state. Thus, the solution found by LST might be suboptimal under certain network conditions such as overload of the system. The details of the least slack time scheduling algorithm and its variants can be found in [62, 63].

2.4 Summary

In this section, the related background knowledge to the conduct of this thesis is presented. Specifically, foundations of power system in terms of active and reactive power, frequency con-

trol, and some well-known power system simulation software are summarized first in Section 2.1. Then, the smart grid and its applications in MG and EVs are discussed in Section 2.2. Last, game theory including non-cooperative games and cooperative games and its related techniques including stable marriage problems and scheduling algorithms are introduced in Section 2.3.

In the next chapter, we introduce the energy trading model among distributed MGs in a cooperative game.

Chapter 3

Coalition Formation for Energy Trading Among Distributed MGs

In this chapter, we study the energy trading problem among the MG sellers and buyers in a distribution network under a cooperative game theoretic framework, and compare it with two baseline cases: a non-cooperative game and a brute force method. The cooperative option would allow MGs to form coalitions among themselves to trade energy with each other as well as with the main power grid; while the non-cooperative game would only allow MGs to trade energy with the main power grid.

3.1 Introduction

A MG is a networked group of distributed energy sources that cooperate through energy management in small-scale geographical areas and provides energy to local groups of consumers [67]. MGs can either work in conjunction with the main power grid or work in an islanded manner separated from the main grid. When a MG is in island mode, it can help ease the load on the main power grid by incorporating distributed renewable generations, such as solar or wind farms. MGs will also support the widespread deployment of EVs that can be treated as both controllable load and supply by taking advantage of their batteries to provide various vehicle-to-grid services [68–71]. Many existing research works in MG have mainly focused on the system control and communication technologies inside a MG. It is lack of exploitation in the deployment of MGs in a distribution network. By making cooperative decisions, MGs can help reduce the load on the main power grid so that the overall energy efficiency can be improved.

In this chapter, we take advantage of game theory methodologies to explore the possibilities of cooperation among distributed MGs. To achieve this aim, novel coalition formation algorithms are exploited to group MGs by forming coalitions. Based on MGs' locations and the corresponding power losses on the cable due to power transfer, the power imbalance of each MG

can be traded with MGs from the same coalition so that the power losses associated with using power from the grid might be reduced. Thus, we propose a set of algorithms based on the coalition formation game [46,49] to minimize the power losses caused by energy trading among distributed MGs. First, the state-of-the-art algorithm from [67] that performs a merge-and-split process is implemented. It follows the Pareto optimal rule, where no individual is better off under the current assignment, in the coalition formation. Then, we propose three alternative approaches to this method as follows:

- Firstly, by relaxing the constraints of the Pareto Order, a modified weak-merge-weak-split method has been proposed, which only compares the overall utility of each potential coalition rather than the individual utility improvement of each MG in the coalition. This approach can reduce the power losses relative to merge-and-split that follows the strict Pareto optimal rule.
- Secondly, a switch operation has been proposed and utilized in the coalition formation process, which allows each MG to make an individual decision whether to leave its current coalition and join another one instead of merging two coalitions. The processing complexity of this method is reduced compared to merge-and-split.
- Thirdly, a set partition algorithm [72] that acts as a brute force method has been proposed. It finds all possible partitions for a specific number of MGs and provides a view of the “best” utility of each possible scenario.

The main contributions of this chapter can be summarized as follows:

- Implement the state-of-the-art coalition formation game, and propose three alternative methods to study the energy trading among distributed MGs;
- Evaluate the performance of the considered algorithms, in terms of 1) average power loss per MG, 2) average coalition size, 3) average number of operations and utility calculations per MG. Compare the performance of game-theory-based algorithms with two baseline cases: a non-cooperative game and a brute-force method, respectively. Simulation results have shown that game theory methods always yield a better performance than the baselines.
- The complexity of the proposed algorithms is analysed and verified by simulations using MATLAB.

The rest of this chapter is organized as follows. Section 3.2 first gives a comprehensive literature review on the recent research in MG and game theory ideas in energy trading. Then, the system model, the proposed algorithms and the simulation results are presented in Section 3.3, 3.4, and 3.5. Finally, a summary of this chapter is given in Section 3.6.

3.2 Literature Review

3.2.1 MG Research

In this section, some of the on-going research in MGs have been introduced in terms of system control, communication techniques and decision making strategies. These methods focus on enabling MGs to work autonomously and to be able to adapt to environmental changes. While some other works have studied the cooperative behaviour among MGs.

3.2.1.1 System Control

A number of research papers primarily focus on the system control of a MG. The work in [73] discussed the major issues and challenges in MG control and reviewed the main control strategies and trends such as droop control, model predictive control and multi-agent systems. Further, the work in [28] discussed control strategies specifically designed to coordinate distributed energy storage systems in a MG. The range of services that distributed energy storage systems can provide and the corresponding control challenges are also reviewed in this paper. In [74], a MG containing renewable energy resources is considered. Since the inherent variability of such resources further complicates the operation of the MG, the authors formulated it as a stochastic energy scheduling problem that not only minimizes the expected operational cost of the MG but also accommodates intermittent renewable energy resources. In [75], decentralized multi-agent MG controllers and Java based platforms are implemented in practical MG power networks.

3.2.1.2 Communication Techniques

Another direction for research in smart MGs is to exploit various communication techniques to support the operation of MGs. The work in [65, 76–78] has given a comprehensive review on a variety of communication technologies, challenges, solutions, standardizations and require-

ments for potential smart grid applications. Specifically, references [79–81] have focused on the communication technologies applied in MG scenarios. Reference [79] proposed an IEC 61850 based communication architecture and provided a platform to model and evaluate it for MG automation. The work in [82] analyses the latency and bandwidth aspects of LTE (Long Term Evolution) communication technology when applied to a smart grid scenario. Specifically, the latency and bandwidth requirements for a hypothetical smart MG consisting of distributed generation, phasor measurement units (PMU) and the advanced meter infrastructure (AMI) are studied. It has been proven that with low latency and large bandwidth, an LTE network is a promising solution to interconnecting smart objects in a smart MG. Reference [83] instead exploited machine-to-machine communication technology that is used to support the information exchange among smart meters and electrical appliances in smart grid scenarios. The work in [84, 85] analysed how wireless sensor networks can be applied to improve the safety and reliability in various smart grid scenarios, such as monitoring early warnings for the system, fault location detection for power systems, smart metering and smart homes, and so on.

3.2.1.3 Decision Making

As autonomous power systems, MGs often require robust real-time energy management, thus various control decisions has to be made to provide reliable services. References [27, 86–88] utilized multi-agent systems to tackle decision-making challenges for real-time MG energy management. In [27], the authors proposed a decentralized agent-based control architecture for MG energy management that utilized agent cooperation through negotiation to achieve the desired energy management objectives. While [86] proposed a novel distributed multi-agent based load restoration algorithm to restore the out-of-service loads in a timely manner so that each agent makes a synchronized load restoration decision according to the available MG status information. The research in [89, 90] applied multistage stochastic dynamic programming to tackle decision-making challenges from both real-time energy imbalance management and economic factors.

3.2.1.4 MG Cooperation

On the other hand, the uncertainty of renewable energy generation in a MG and the unpredictability of consumers' behaviour brings difficulty in balancing the demand with the supply within small to medium size MGs in a timely fashion. Instead, there is a need to identify both

buyer MGs who have insufficient power generation and seller MGs who have excess power generation to trade energy with each and the main power grid. The power losses among nearby MGs due to power transfer is believed to be less than for long distance cables between the MGs and the main power grid. To alleviate this power loss and enhance energy efficiency, recent research has drawn attention on the potential of the cooperation among distributed MGs. Reference [91] studied a case where two islanded MGs exchange energy with each other. The authors proposed generic cost functions and applied the method of Lagrange multipliers to minimize the total cost of the energy generation and transportation. However, this work did not consider the case that there might be other available MGs nearby to cooperate with. In addition, one MG might not always have the incentive to trade energy with a second MG which might have a lower energy generation available or a higher price for energy trading. In a dynamic manner, a MG should have the flexibility and autonomy to choose which of the available MGs to cooperate with in order to achieve its goals. Further, references [12, 46, 67, 92, 93] consider the possibility of forming coalitions among islanded MGs, and give a comprehensive view of how game theory can be applied to solve such a problem.

3.2.2 Game Theory in Energy Trading

The smart grid allows energy to flow back from customers into the grid. Customers can sell their excess energy back to the grid or to other customers. This is usually referred as energy trading. Game theory is a set of mathematical models to study conflict and cooperation between intelligent decision-makers. Recent work on game theory has given insights on strategic energy trading model designs. In this section, we summarize some related works in the field of game theory that are of relevance to energy trading in MGs. The work in [46] has given a comprehensive review on the potential and challenges of applying game theoretic methods for various energy trading problems in smart grid. The authors discussed both non-cooperative games and cooperative games that are used in this area including MG systems, demand side management, communication requirements and so on.

3.2.2.1 Non-cooperative Games

Reference [44] proposed a non-cooperative double auction game to study the interactions and energy trading decisions among a number of distributed storage units. In this scenario, the storage units' owners compete to sell as much as of their stored energy to a local market to

maximize their tradeoff between gaining revenue from the energy trading and reducing the accompanying costs. The proposed auction game can not only determine the quantity and the price of the energy that each storage unit trades with the market, but can also guarantee to reach at least one stable Nash equilibrium operating point. In [45], a non-cooperative game was proposed among multiple utility companies who have the incentive to maximize their profits, where the energy price of each utility company would have some effect on the energy consumption of each household. The existence of a Nash equilibrium operating point was proved, thus the optimal energy price for each utility company was determined. The work in [94] studied the problem that the consumers who own energy storage units can decide the amount of energy to produce or store to minimize their monetary expenditure on the energy from the main grid. The authors further formulated this problem as both a non-cooperative game and a cooperative game. The former game focused on a user-oriented model where each consumer competes to optimize their individual monetary expense while the latter game focused on a holistic-based model that allows cooperation among the consumers.

3.2.2.2 Cooperative Games

Reference [67] investigated coalition formation games among distributed MGs for energy trading. A coalition can be formed among MGs who have an excess of energy to sell and MGs who acquire additional energy to meet their demand that each MG's utility can be maximized. Similarly, references [12–14, 92, 93, 95] have discussed the alternative games and variations of the coalition formation games for distributed MGs energy trading. In [96], a coalition formation game is formulated to analyse cooperation between small-scale electricity suppliers and end-users in direct electricity trading without going through retailers. An optimal electricity pricing scheme is derived by using the asymptotic Shapley value so that a fair division of revenue can be achieved between the small-scale suppliers and the end-users. While in [97], the authors proposed a price discrimination game for energy-users to trade energy with a shared facility controller. In this game, the participating energy-users are able to decide the price per unit of energy that guarantees a fair energy trading market. All the aforementioned works have given a solid demonstration of how cooperation can be utilized to optimize distributed energy trading, while [98] has taken a different step to study cooperation games by taking the advantage of visualization techniques. The authors used the Geographical Information System (GIS) to demonstrate real-time data on a geographical map and its role in a cooperative game optimization problem.

3.2.2.3 Behaviour Games

References [18, 99, 100] have studied the realistic behaviour of consumers and their biased perceptions towards decision-making. In practice, this can deviate from the conventional norm set by game theory that all users can make decisions rationally and objectively for energy trading. A static non-cooperative game is formulated in [100] to solve the problem of optimally charging (buying energy from the grid) or discharging (selling energy to the grid) customer-owned storage units. Unlike traditional game-theoretic models, the proposed behavioural game allows the customers to make decisions by subjectively evaluating their real-world consideration of payoffs.

3.3 System Model

A MG comes in a variety of sizes and designs. In practice, the size of a MG can vary from a smart home, a community up to an island (e.g., serving around 28,000 residents in Bornholm island, Denmark, see Section 2.2.1 and References [6, 7]).

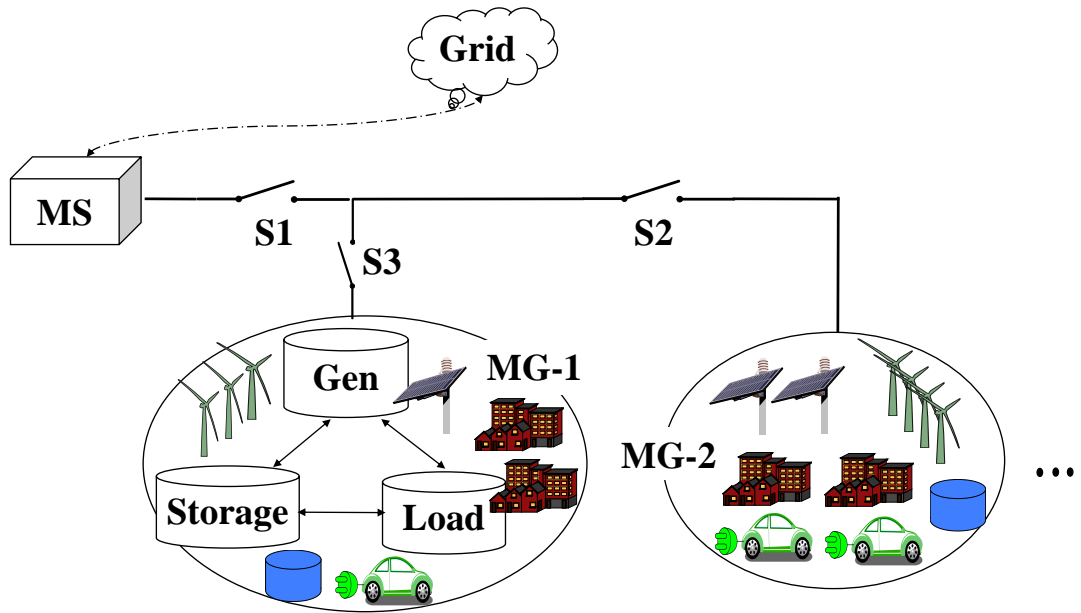


Figure 3.1: A paradigm for the proposed system model [67].

In this section, we consider a distribution network which consists of one substation termed as macro station (MS) which is connected to the main power grid and a set of community-level MGs $\mathcal{N} = \{1, \dots, m\}$ which are allowed to trade energy with each other in a small geographical

area. As shown in Figure 3.1, closing and opening switches S1, S2 or S3 allows MG 1 and 2 to operate in a cooperative and an islanded mode, respectively. Similar to the system model described in [67], the “MG” considered here consists of several households or offices powered by small-scale renewable generators such as solar photovoltaic panels and micro wind turbines, as well as energy storage units at the MG control centre. The control centre is in charge of the power allocation using advanced optimal power flow approaches within the MG. Therefore each MG can be seen as an intelligent agent that can make independent decision in terms of when and with whom to trade energy.

3.3.1 System Description

We first divide the system time \mathcal{T} into n scheduling intervals, where $\mathcal{T} = \{t_1, \dots, t_n\}$. During interval t_i , we consider an aggregate power imbalance $P_j(t_i)$ of MG j to be $(G_j(t_i) - D_j(t_i))$ (i.e. the generation – the demand) and define those MGs who have a power surplus ($P(t_i) > 0$) as sellers and those who have a power demand ($P(t_i) < 0$) as buyers. Those who have a zero power imbalance ($P(t_i) = 0$) during interval t_i will be excluded from the current scheduling process. The set of MGs \mathcal{N} can be further divided into two subsets \mathcal{S}_b and \mathcal{S}_s , which represent the set of buyers and the set of sellers respectively, written as buyer $b \in \mathcal{S}_b$ and seller $s \in \mathcal{S}_s$. An example is illustrated in Figure 3.2 to show that different coalitions may exist among three MGs during n timeslots.

We assume that the aggregate power imbalance of each MG is known either through prediction based on historical data or through being measured at the beginning of each interval [91]. Hence the power imbalance P_j is a time-varying variable and can be seen as a random number with a certain observed distribution determined by the composition of different types of loads (e.g., residential, commercial, industrial, etc.) and the power sources of MG j ; this also differs from urban to rural areas. In practice, this schedule can also be operated on a day-ahead basis which encourages those MGs who have the incentives to form coalitions to trade energy with each other during the next day. For simplicity, the following analysis is based on one time interval t_i .

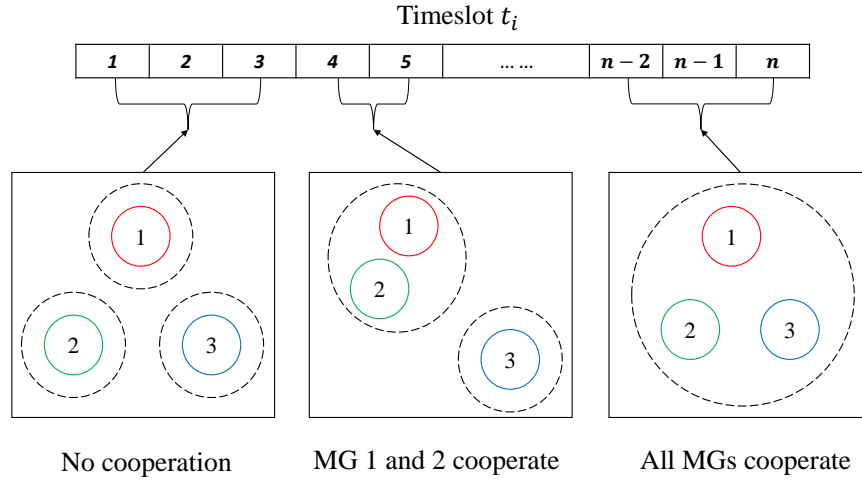


Figure 3.2: An example of various coalitions formed among three MGs over n scheduling timeslots.

3.3.2 Power Metric Calculation

Before we define the utility function of a coalition, consider the case where each MG operates in the conventional grid-connected mode and only exchanges power with the MS while no cooperation exists among the MGs. Hence the active power loss¹ due to the power exchange between MG i and the MS can be written in a simplified form as

$$P_{io}^{\text{loss}} = \frac{P_{io}^2 R_{io}}{U_o^2} + \alpha P_{io} \quad (3.1)$$

where the first term on the right hand side of eq. (3.1) is the power loss over the distribution line due to power transfer, R_{io} is the corresponding resistance on the distribution line, U_o is the medium voltage on the distribution line between the MS and MG i and α is the fraction of the power loss at the transformer due to power conversion at the MS. The value $|P_{io}|$ is the constant power flow on the distribution line. Further if MG i is a buyer, an extra amount of power is needed to compensate for the power loss due to the power transfer, so that the power deficit of buyer MG i can be fully met. Hence the actual amount of power flow $|P_{io}|$ sent to MG i from

¹Active power loss could be one dominant measurement to evaluate the utility function defined in the proposed model. More sophisticated metrics (such as pricing, quality of service, environmental impacts, etc.) can also be considered when modelling a more realistic utility function in MG implementations.

the MS can be obtained by solving the following quadratic equation:

$$\begin{aligned} P_{io} &= P_{loss}^{extra} + |P_i| \\ &= \frac{P_{io}^2 R_{io}}{U_o^2} + \alpha P_{io} + |P_i| \end{aligned} \quad (3.2)$$

where $|P_i|$ is the required power for MG i . If MG i is a seller it simply sends its power surplus P_i to the MS thus $P_{io} = P_i$. Depending on the values of other parameters from eq. (3.2), the solution P_{io} of the quadratic eq. (3.2) can either admit real roots or complex roots. We consider the value of the power flow P_{io} that buyer MG i needs to meet its power deficit to be the minimum between the real part of eq. (3.2)'s two roots. More discussion of this issue can be found in [67].

Here each MG can be seen as a coalition that only consists of one member, thus the utility of each coalition can be represented as the total power loss of each MG due to the power transfer to the MS. The utility function of the considered distribution network can be written as:

$$U_{\text{non}}(\mathcal{N}) = \sum_{i \in \mathcal{N}} \omega_1 P_{io}^{\text{loss}} \quad (3.3)$$

where ω_1 is the price of per unit of power transferred between the MS and the MGs.

It is worth noting that when forming coalitions, the local power loss due to the power transfer among buyer MG i and seller MG j within the same coalition, denoted as P_{ij}^{loss} , will yield no power loss at the macro station transformer, thus the power loss between MG i and j can be written as:

$$P_{ij}^{\text{loss}} = \frac{P_{ij}^2 R_{ij}}{U_1^2} \quad (3.4)$$

where R_{ij} is the resistance between buyer MG i and seller MG j within the coalition, U_1 is the local low voltage over the cable, while P_{ij} is the actual amount of power that buyer MG i needs and is given by eq. (3.2).

In the cooperative case, some MGs might prefer to form coalitions with other fellow MGs via

local power transfer in order to reduce the power loss caused on the cable as defined in eq. (3.4). By forming coalitions, the cooperative utility can now be expressed as:

$$U_{\text{coop}}(\mathcal{N}) = \sum_{i,j \in \mathcal{D}_h} (\omega_1 P_{io}^{\text{loss}} + \omega_1 P_{jo}^{\text{loss}} + \omega_2 P_{ij}^{\text{loss}}) \quad (3.5)$$

where P_{ij}^{loss} is the power loss between buyer MG i and seller MG j as defined in eq. (3.4). The scalar ω_2 is the price of per unit of power transferred among the buyer MGs and the seller MGs. After forming coalitions, the set \mathcal{N} can be expressed as one of the possible partitions formed, i.e. \mathcal{D}_h , where h represents the index of the possible coalition formed over a set \mathcal{N} . For instance, if $\mathcal{N} = \{a, b, c\}$, the maximum number of coalitions is 5 and the possible combinations are $\mathcal{D}_1 = \{\{a, b, c\}\}$, $\mathcal{D}_2 = \{\{a\}, b, c\}$, $\mathcal{D}_3 = \{\{b\}, a, c\}$, $\mathcal{D}_4 = \{\{c\}, a, b\}$, $\mathcal{D}_5 = \{\{a\}, \{b\}, \{c\}\}$.

Now the considered problem can be seen as an active power loss minimization problem in the network of the MS and MGs. In the next section, we show how the coalitions can be formed following various principles.

3.4 Algorithms

To study the cooperative behaviour of rational MG buyers and MG sellers in the considered system, we first proposed a non-cooperative setting as the baseline in order to compare with the cooperative case. Then we discuss how coalitions can be formed based on cooperative game theory algorithms.

3.4.1 Non-cooperative Setting

This is the case where no cooperation exists among the MGs, and each MG (either a buyer or a seller) trades energy directly with the macro station. This method is used as a benchmark to evaluate the power loss reduction if coalitions are formed when using the cooperative game theory approaches. The total non-cooperative utility of a set of MGs, \mathcal{N} , can be calculated following eq. (3.1), (3.2), (3.3).

3.4.2 Cooperative Setting for Coalition Formation

The state-of-the-art coalition formation game [67] and its modified algorithms for energy trading based on MGs' location and power losses are implemented. Suppose that the algorithms follow a buyer-driven and a location-oriented order where a buyer MG always initiates the negotiation with the nearest seller MG in a pairwise manner.

We first introduce the merge-and-split rule that follows the Pareto Order. Then we relax the constraints in the Pareto Order for merge and split, followed by an alternative Switch Operation rule. In the end, a brute-force method is implemented to compare the utility gain with the proposed game theory approaches.

3.4.2.1 Merge and Split Algorithm

Before we introduce the process of merge-and-split for the coalition formation, the definition of the Pareto Order (**Definition 1**) is first given as follows:

Definition 1. (Pareto Order) [101] - Let $\mathcal{N} = \{1, \dots, N\}$ be the set of players. Consider two partitions \mathcal{H}_a and \mathcal{H}_b of set \mathcal{N} . If and only if the utility of every player i in \mathcal{H}_a given by eq. (3.6), denoted as $v_i(\mathcal{H}_a)$, is improved over its utility value in set \mathcal{H}_b , denoted as $v_i(\mathcal{H}_b)$, i.e. $v_i(\mathcal{H}_a) \geq v_i(\mathcal{H}_b)$, then the structure of partition \mathcal{H}_a is preferred over the structure of partition \mathcal{H}_b by the Pareto Order, i.e. $\mathcal{H}_a \triangleright \mathcal{H}_b$. Hence, $\mathcal{H}_a \triangleright \mathcal{H}_b \Leftrightarrow \{v_i(\mathcal{H}_a) \geq v_i(\mathcal{H}_b), \forall i \in \mathcal{H}_a, \mathcal{H}_b\}$. Further, there should be at least one MG player for whom strict inequality holds, i.e. $v_i(\mathcal{H}_a) > v_i(\mathcal{H}_b)$.

Definition 2. (Merge and Split) [46, 67, 101] - A **merge** action is executed if and only if this satisfies the **Pareto Order**, i.e. for two coalitions \mathcal{D}_a and \mathcal{D}_b , where $\forall i \in \mathcal{D}_a$ and $\forall j \in \mathcal{D}_b$, \mathcal{D}_a and \mathcal{D}_b will merge into a new coalition \mathcal{D}_c , where $\mathcal{D}_c = \{\mathcal{D}_a + \mathcal{D}_b\}$, $\forall g \in \mathcal{D}_c$, if and only if the relation in **Definition 1** holds. Further, a subsequent split will be investigated by computing all possible set partitions when there are more than 3 MGs in one single coalition; a **split** action will be conducted if breaking up one larger coalition into two or more smaller coalitions satisfies the **Pareto Order**. Thus, the **merge** and the **split** action can be summarized as:

Merge - Given a set of coalitions $\{\mathcal{D}_1, \dots, \mathcal{D}_m\}$, merge if and only if every player $i \in \mathcal{D}_j$ satisfies the **Pareto Order**, i.e. $\{\bigcup_{j=1}^m \mathcal{D}_j\} \triangleright \{\mathcal{D}_1, \dots, \mathcal{D}_m\}$.

Split - Given any coalition $\{\bigcup_{j=1}^m \mathcal{D}_i\}$, split if and only if every player $j \in \mathcal{D}_i$ satisfies the **Pareto Order**, i.e. $\{\mathcal{D}_1, \dots, \mathcal{D}_m\} \triangleright \{\bigcup_{i=1}^m \mathcal{D}_i\}$.

where \triangleright represents that the left hand side is preferred.

The total cooperative utility within a set of MGs, \mathcal{N} , by forming coalitions can be calculated as a sum of the power losses on the cable and at the transformer following eq. (3.1), (3.2), (3.4), (3.5). Since the cooperative utility of each coalition solely depends on the members of MGs in that coalition and has no dependence on how they are structured, it can be considered as a TU (transferable utility) game [102]. Therefore the overall utility of a coalition calculated by eq. (3.5) can be divided up using different fairness criteria [49]. We use a proportional fair division scheme to compute the individual utility among MGs within one coalition, according to their individual power loss contribution in the non-cooperative setting in eq. (3.1). A weight factor ζ_i is further defined to represent the extra benefits each MG i gains by forming coalitions. Hence, for MG i in a coalition \mathcal{D} , its utility gain can be calculated as follows:

$$\begin{aligned} v_i(\mathcal{D}) &= \zeta_i \cdot (U_{\text{coop}}(\mathcal{D}) - U_{\text{non}}(\mathcal{D})) + U_{\text{non}}(\{i\}) \\ &= \frac{U_{\text{non}}(\{i\})}{U_{\text{non}}(\mathcal{D})} \cdot (U_{\text{coop}}(\mathcal{D}) - U_{\text{non}}(\mathcal{D})) + U_{\text{non}}(\{i\}) \end{aligned} \quad (3.6)$$

where $i \in \mathcal{D}$, and $\{i\}$ denotes the i th MG in coalition \mathcal{D} .

The process of the algorithm is shown in Figure 3.3. Given a partition $\mathcal{H} = \{\mathcal{D}_1, \dots, \mathcal{D}_M\}$ of the buyers' set \mathcal{S}_b . For each round of the negotiation, a buyer MG $i \in \mathcal{D}_m$, $m \in \{1, \dots, M\}$ attempts to pair up with a seller MG $j \in \mathcal{S}_s$ in turn in a distance ascending order, where \mathcal{S}_s is the sellers' set. After calculating the corresponding utilities, if it satisfies the Pareto Order then buyer i and seller j will merge into a coalition, denoted as $\tilde{\mathcal{D}} = \{i, j\}$. If buyer i still has a power deficit to satisfy, it will continue searching for the next nearest seller $w \in \mathcal{S}_s$ until buyer i 's power demand is met. If this satisfies the Pareto Order then seller w (or the coalition \mathcal{G} where seller w is currently in) will merge with coalition $\tilde{\mathcal{D}}$ into a larger coalition $\tilde{\tilde{\mathcal{D}}}$.

Likewise a coalition including buyer i and seller j can decide to split into smaller coalitions if the individual utility of each MG from this coalition is improved when compared to that in the old coalition according to the Pareto Order. Whenever the number of MGs within a single coalition is equal or greater than 3 MGs, a split action is investigated by generating all the

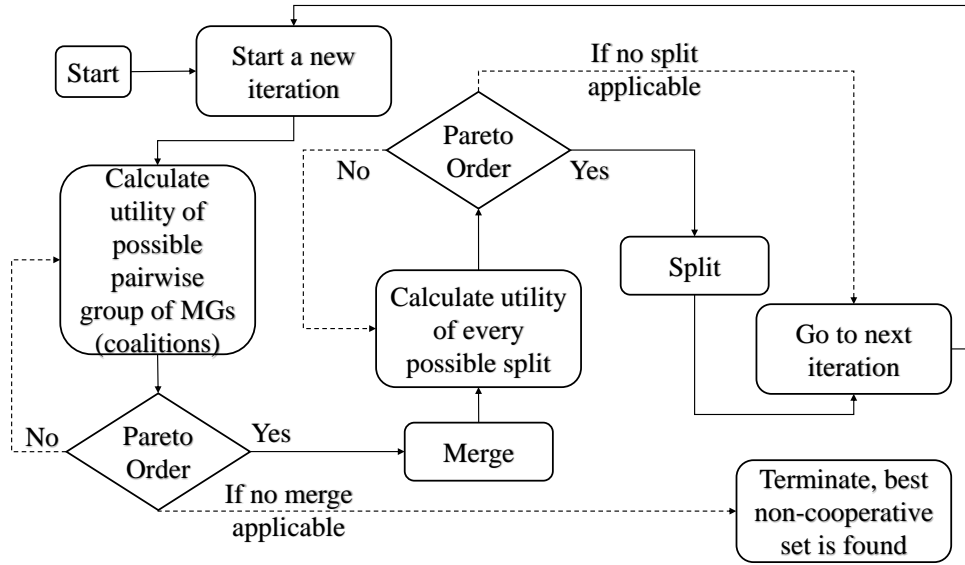


Figure 3.3: One iteration of the merge-and-split process.

possible set partitions of the merged coalition. If this is preferred by the Pareto Order, a split action is conducted. A multiple iterations of the merge-and-split process might be needed until the network of MGs reaches a stable state where there is no incentive for each MG to leave the current coalition and join another one [12, 67, 92, 93].

3.4.2.2 Relaxed Pareto Order

Further, we relax the constraints of the Pareto Order aiming to reduce the computational complexity and propose a weak-merge-and-weak-split algorithm for the coalition formation. The algorithm only compares the overall utility of each potential coalition rather than the individual utility of each seller MG and buyer MG. From Section 3.4.2.1, the procedure of a weak-merge-and-weak-split algorithm is given as follows:

A Weak Merge and Weak Split scheme only compares the overall utility of each potential coalition given by eq. (3.5) rather than looking into the individual utility of each MG in that coalition given by eq. (3.6). This means that the algorithm does not enforce improvement of every entity within the same coalition but the overall utility of the coalition. Compared to the process in Section 3.4.2.1, it only weakens the constraints of the Pareto Order. Hence, the definition of the modified Pareto Order after relaxation is given as follows:

Definition 3. (Relaxed Pareto Order) - Let $\mathcal{N} = \{1, \dots, N\}$ be the set of players. Consider two partitions \mathcal{H}_a and \mathcal{H}_b of set \mathcal{N} . If and only if the overall utility of \mathcal{H}_a where player i currently is, given by eq. (3.5), denoted as $U_{\text{coop}}(\mathcal{H}_a)$ is improved when compared to that in set \mathcal{H}_b , denoted as $U_{\text{coop}}(\mathcal{H}_b)$, i.e. $U_{\text{coop}}(\mathcal{H}_a) \geq U_{\text{coop}}(\mathcal{H}_b)$, so the structure of partition \mathcal{H}_a is preferred over \mathcal{H}_b by the relaxed Pareto Order, i.e. $\mathcal{H}_a \succeq \mathcal{H}_b$. Hence, $\mathcal{H}_a \succeq \mathcal{H}_b \Leftrightarrow \{U_{\text{coop}}(\mathcal{H}_a) \geq U_{\text{coop}}(\mathcal{H}_b), \forall i \in \mathcal{H}_a, \mathcal{H}_b\}$.

3.4.2.3 The Switch Operation

We investigate an alternative rule for the coalition formation to the merge-and-split family as the Switch Operation [103], where each buyer MG $i \in \mathcal{S}_b$ will make an autonomous decision whether to leave (or to break the cooperation with) the current coalition. It is different to the **merge and split** rule discussed in Section 3.4.2.1 that is based on coalitions merging and splitting. The difference between a merge-and-split process and a switch operation is further explained in an example in Figure 3.4. Instead of merging the coalition $\{C, D\}$ with the coalition $\{A, B\}$, player C leaves the coalition $\{C, D\}$ to join the coalition $\{A, B\}$ in the switch operation. In this way, a large coalition is less likely to be formed than that in the merge-and-split process. In average, the probability of investigating a split action is lower than the merge-and-split. Thus, the computation is less demanding. The procedure of the switch operation is similar to that of the merge-and-split as shown in Figure 3.3, except the ‘‘Merge’’ action is replaced by the ‘‘Switch’’ action.

The definition of a Switch Operation is given as follows:

Definition 4. (Switch Operation) [104] - Given a partition $\mathcal{H} = \{\mathcal{D}_1, \dots, \mathcal{D}_M\}$ of the MGs’ set \mathcal{N} , a buyer i decides to leave its current coalition $\mathcal{D}_m \in \mathcal{H}$ to join a coalition \mathcal{D}_k , where \mathcal{D}_k is either an existing coalition in \mathcal{H} or $\mathcal{D}_k = \emptyset$. Hence a new partition \mathcal{H}' is formed and written as $\mathcal{H}' = \{\mathcal{H} \setminus \{\mathcal{D}_m, \mathcal{D}_k\}\} \cup \{\mathcal{D}_m \setminus \{i\}, \mathcal{D}_k \cup \{i\}\}$, if and only if **Definition 1** holds, i.e. $\mathcal{D}_k \succ \mathcal{D}_m$.

3.4.2.4 The Brute-force Method

A set partition algorithm [72] that performs as a brute force method has been proposed. The algorithm can generate all possible partition sets on a set of MGs, \mathcal{N} . The partition who minimizes the overall power losses is chosen, as shown in Figure 3.5. Subject to the membership of

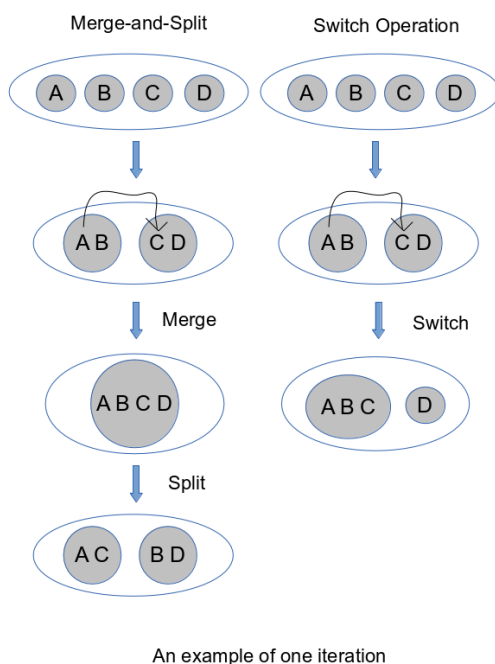


Figure 3.4: Comparison of the procedure of the merge-and-split and the switch operation.

each coalition and the feasibility constraint. This constraint is in two parts:

1. For any coalition \mathcal{D} which has two or more members, it must have at least one buyer MG and one seller MG;
2. For each MG $i \in \mathcal{D}$, it must participate the local energy exchange and make an actual contribution (in terms of reducing the power losses) within the same coalition.

Together with the previous methods that are illustrated in Sections 3.4.1, 3.4.2.1, 3.4.2.2 and 3.4.2.3, the results and runtime of the brute force method is compared and analysed to show how much extra effort is required to achieve the “best” results.

In the next section, we show via simulations the performance comparison of the proposed game theory methods: weak-merge-weak-split in Section 3.4.2.2 and switch operation in Section 3.4.2.3 with two proposed benchmark cases: non-cooperative game in Section 3.4.1 and the

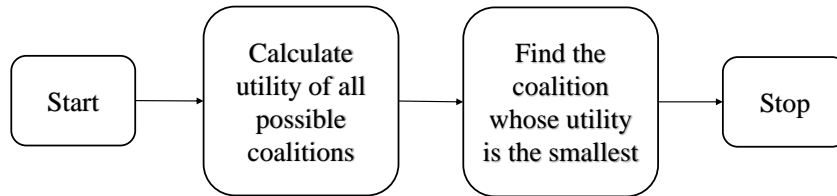


Figure 3.5: *The process of the brute force method.*

brute force method in Section 3.4.2.4 as well as the state-of-the-art algorithm: merge-and-split in Section 3.4.2.1. Among these algorithms, the ones who have showed performance advantage in higher power loss reduction are generally more computationally demanding. For instance, the brute force method can give the highest power loss reduction but it is the most complex one to compute due to the exhaustive search that grows factorially with the number of agents in the network. While the non-cooperative game being the simplest one to compute results the highest power loss since the arrangements of how MGs would trade energy is fixed, the algorithm performs a fixed number of calculations regardless the number of agents in the network that requires constant time. The power loss reduction resulted from merge-and-split, weak-merge-weak-split, and switch operation fall in between the non-cooperative game and the brute force method, this is because by applying game theory ideas, some of the “least favourable” combinations from the brute force search would be filtered out. This helps significantly reduce the computing requirements but leads to suboptimal solutions due to some of the “best” cases from the brute force might be missed out. The degree of optimality compared to the best solution found by the brute force depends on which set of game theory rules are employed. The trade-off between performance improvement and computational complexity becomes a critical measurement when designing algorithms to solve different problems. For instance, for a small problem set, if the performance improvement is favourable, brute force might become a viable option.

3.5 Simulation Results

A coalition formation game for energy trading based on MG location and power loss is implemented. This set of algorithms implemented are the merge-and-split algorithm, the weak-merge-and-weak-split algorithm, and the switch operation, respectively. A set partition algorithm and a non-cooperative algorithm have been implemented as well as the lower and upper benchmarks, respectively. The set partition algorithm performs the brute force method and gives all possible partitions for a specific number of elements, and gives the “best” possible results for the coalition formation, while the non-cooperative setting gives the “worst” results in terms of power losses.

We consider a distribution network that consists of up to 30 MGs. The simulation parameters are given in Table 3.1, where ω is the electricity price paid per MG for one unit of power transferred. Each MG, denoted as $i \in \mathcal{N}$, is assumed to be uniformly distributed over the considered area, the value of parameters R , α , U_0 and U_1 is chosen following [67]. The quantity of power imbalance P_i for each MG i is generated as a Gaussian random variable with a zero mean and a variance which is uniformly distributed in a range from 100 to 100,000 (MW^2).

Parameter	Settings
Price of power (ω)	1 unit/MW
Simulated area (S)	10 km \times 10 km
Cable resistance (R)	0.2 Ω/km
Fraction of transformer loss (α)	0.02
Medium voltage (U_0)	50 kV
Low voltage (U_1)	22 kV

Table 3.1: Simulation parameters for Chapter 3

3.5.1 An MG Distribution Network

A partition of a typical MG distribution network resulting from the coalition formation algorithm (e.g. merge-and-split process in Section 3.4.2.1) with $N = 10$ MGs is shown in Figure 3.6. We can see a couple of examples of the non-cooperative clusters, such as the cluster of MG 1, and the cluster of MG 6; one group of two MGs, such as the group of MG 2 and 7; and two groups of three MGs, such as the group of MG 3, 4 and 10 and the group of MG 5, 8 and 9.

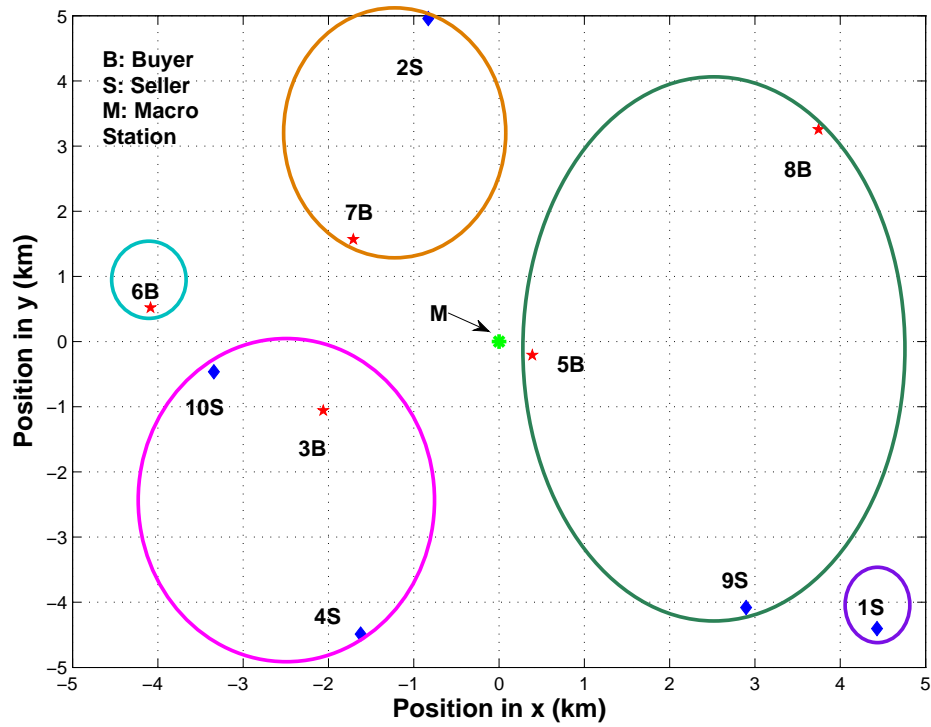


Figure 3.6: A partition of a MG distribution network resulting from the coalition formation algorithm with $N = 10$ MGs. The MGs are labelled 1 – 10, where buyer MG is denoted as B and seller MG is denoted as S.

3.5.2 Power Loss Comparison

The performance comparison in terms of the average power loss per MG resulting from the proposed algorithms (over 10,000 different scenarios via Monte Carlo simulations) is shown in Figure 3.7. As the number of MGs increases, the power losses per MG resulting from the cooperative game theory methods are significantly reduced when compared to the non-cooperative setting where the average power loss remains at a higher constant value regardless of the number of MGs in the network. This is because the arrangements of how the MGs would trade energy with the macro station is fixed. More MGs joining the network would not affect the way how other MGs trade energy, thus the average power loss per MG does not vary with the number of MGs in the network. It is also seen that the brute force method gives the “best” solution in terms of power loss reduction when compared to the other three game theory methods (i.e., merge-and-split, weak-merge-and-weak-split, switch operation). In practice, investigating all the possible set partitions is not always the most practical way to

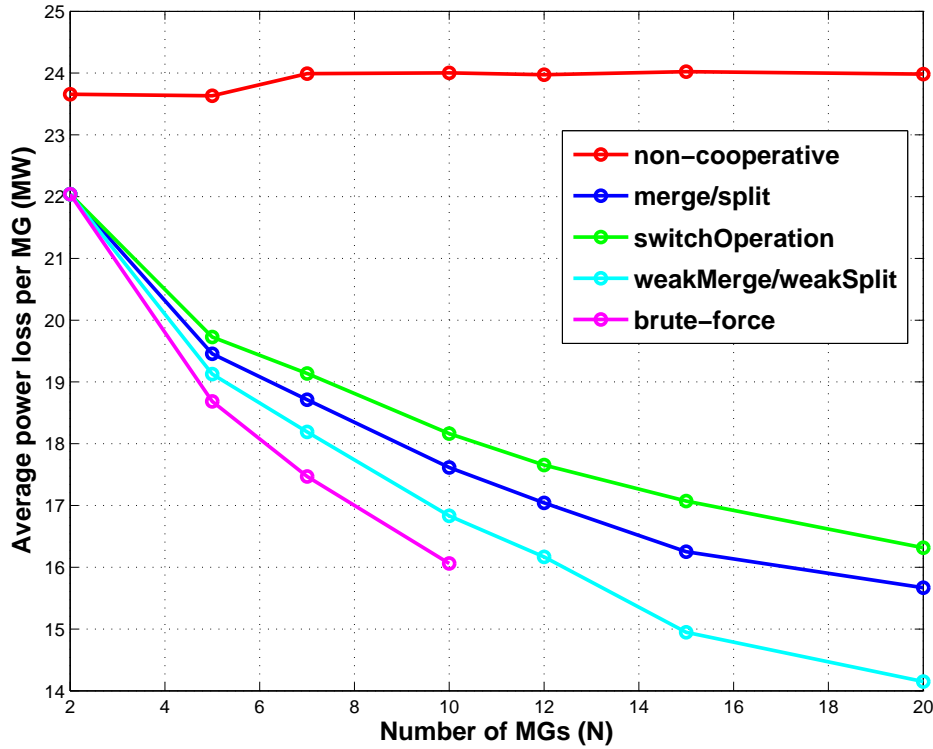


Figure 3.7: Average power loss per MG comparison versus number of MGs N .

find the “best” solution when forming coalitions since this requires a very high calculation complexity. In Figure 3.7, we can also see that the weak-merge-and-weak-split method yields a lower average power loss (i.e., a better utility) than the merge-and-split method. This is because, by relaxing the Pareto Order, MG i is more likely to make merge and split decisions which will lead to more chance of cooperation, so does a further reduced average power loss. Compared to the merge-and-split and weak-merge-and-weak-split methods, the switch operation algorithm gives a higher average power loss. This is due to the fact that the switch operation (defined in **Definition 4**) leads to forming partitions with smaller size coalitions on average as shown in the example in Figure 3.4. This might lead to less chance for MGs in the same coalition to exchange energy among themselves, thus yield a higher average power loss.

3.5.3 Coalition Size Comparison

The performance comparison in terms of the average coalition size from the Monte Carlo simulations is shown in Figure 3.8. As the number of MGs N increases from 2 to 20, we observe that

the average coalition size increases gradually from 1.3 to 1.9, 2.3 and 2.5 MGs per coalition under the switch operation, the merge-and-split, and the weak-merge-and-weak-split, respectively. In a coalition formation game, a larger coalition indicates that there will be more chance for the local cooperation among the members within the same coalition. In the proposed MGs distribution network, a larger coalition will always provide more chance for the MGs within the same coalition to exchange energy locally rather than with the macro station. This will not only mitigate the power losses over the distribution lines but also avoid the power conversion losses at the macro station transformer. Hence, we can see forming larger coalitions will help to reduce the power loss in the power network. In addition, this is in line with the results shown in Figure 3.7 where the weak-merge-and-weak-split algorithm that leads to the largest coalition sizes gives the best power loss reduction when compared to the merge-and-split and the switch operation. It is worth noting that the downside of the weak-merge-and-weak-split algorithm is that sometimes a MG may increase its individual power losses when forming a coalition due to the relaxed Pareto optimality. The same pattern can be also seen under the switch operation algorithm that leads to the smallest average coalition sizes but shows the worst average power loss when compared to the merge-and-split and the weak-merge-and-weak-split.

3.5.4 Complexity Comparison

Figures 3.9 (a) and (c) show the performance comparison in terms of the average number of the operations per MG under the merge-and-split process and the switch operation, with the number of MGs in the distribution network chosen as $N = 7$ and $N = 15$. Similarly, Figures 3.9 (b) and (d) show the average number of the overall utility calculations under the merge-and-split process and the switch operation. To show these results, the x-axis of Figure 3.9 indicates the number of times that the power imbalance of the MGs in the distribution network changes in 24 hours [12]. In Figure 3.9, we can see that both the number of operations per MG and the number of overall utility calculations under the merge-and-split and switch operation increase with the number of power imbalance changes in a day. In the distribution network of $N = 7$ MGs and $N = 15$ MGs scenarios, the number of the switch operations increases more steeply than that of the merge-and-split process. However, for the number of the overall utility calculations which gives a better impression of the computational complexity, it can be seen in (b) and (d) that the result from the merge-and-split is higher than that from the switch operation. We also observe that a larger network (e.g. $N = 15$) always has a higher computational complexity than a smaller one (e.g. $N = 7$). We also note that part (d) shows a highly variable number of

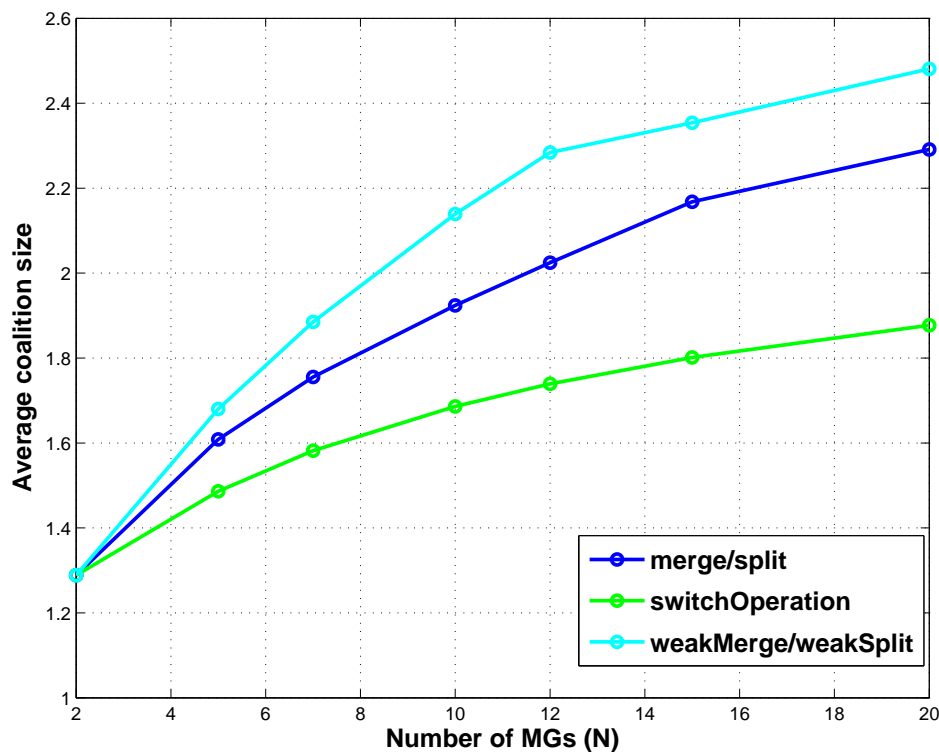


Figure 3.8: Average coalition size comparison versus the number of MGs N .

the overall utility calculations for the merge-and-split process, the reasons for this might be in the following three points:

1. The dataset used is uniformly distributed (random);
2. $N = 15$ MGs could be considered as a “big” case when applying the merge-and-split process that will always lead to larger potential coalitions, thus there will be more chance for MGs to be tested to see if they should split into multiple groups of smaller coalitions. This tends to be very computationally intensive to evaluate.
3. The number of the overall utility calculations is relatively high since very few merge-and-split operations would be successful when compared to the large number of the actual overall utility calculations.

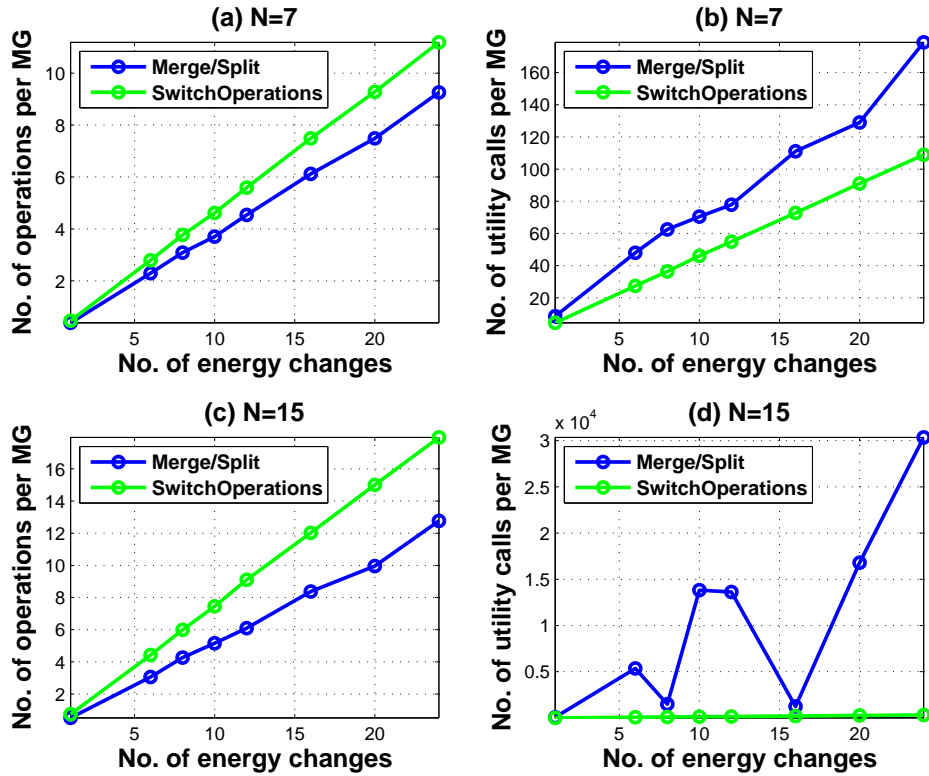


Figure 3.9: Average operation numbers compared with utility function calls

3.6 Summary

In this chapter, we have investigated a coalition formation game for the energy trading among neighbouring MG in a distribution network, based on the MGs' location and the power losses due to the power transfer. The state-of-the-art algorithm for coalition formation [67] performs as a merge-and-split process, and follows the Pareto Order. Further, we have developed three alternative approaches to this method [12] to improve and better evaluate the network's performance. Due to the strict constraint of the Pareto Order, the merge or the split operation is limited by the size of the coalitions it can form. Thus, by relaxing the Pareto Order, a weak-merge-and-weak-split algorithm is first proposed. In addition, by replacing the merge-and-split procedure with the Switch Operation, a modified coalition formation game using the switch rule is formulated that allows each MG to make an individual decision whether to switch to another coalition. Finally, a brute force method based on a set partition algorithm is implemented to serve as the lower bound benchmark of the "best" solution that the network can achieve, while the upper bound benchmark of the "worst" solution is implemented as a non-cooperative set-

ting.

We have simulated not only the system power loss but analysed the system performance from multiple perspectives, such as the average coalition size, the average number of the actual operations and the average number of the overall utility calculations. The simulation results have shown that the game theory based methods always yield a better overall performance than the non-cooperative setting and the brute force method. Furthermore, we can see from the simulation results that the weak-merge-and-weak-split method yields a better performance in terms of smaller power loss and larger coalition size than both of the merge-and-split and switch operation methods.

However, the weak-merge-and-weak-split method that follows the relaxed Pareto Order cannot guarantee the fairness among all MGs in the same coalition. It means some MGs may have to accept higher power losses in order to achieve reduced overall power losses within the their coalition. Thus, the fairness division of a coalition needs to be further investigated when considering a practical power system. Another limitation of our work in this chapter is the assumption of having a perfect communication and physical connection among the MGs and the macro station. In practice, one should consider various communication requirements from case to case for different smart grid applications. Especially, in some rural areas or under extreme cases, there might be a lack of contiguous coverage of the communication signals. This will affect the process of the coalition formation and will reduce the network's utility due to a lack of information being exchanged. Regardless of the aforementioned practical issues when implementing the proposed algorithms, it is worth noting that the merge-split based algorithms will always yield a high computational complexity. This is because the split process will have to look up all the possible combinations among the MGs within a coalition, whose computational complexity grows in a factorial order in the worst case scenario.

In the next chapter, we establish an efficient framework for the power loss minimization problem, whose computational complexity only grows at a quadratic rate with the number of MGs in the network.

Chapter 4

College Admissions for Energy Trading Among Distributed MGs

In Chapter 3, we have shown that the merge-and-split based coalition formation games can yield significant power loss reduction compared to a non-cooperative game. However, the growth of the computational complexity of such games follows a factorial order with the number of MGs in the network. In this chapter, we establish an efficient framework for the power loss minimization problem as a college admissions game with variable energy quotas, whose computational complexity only grows at a quadratic rate. The college admissions based algorithm becomes a good candidate for a network with a large number of distributed MGs.

4.1 Introduction

It is expected that MGs will use various renewable energy sources (RES) as the main power supplies considering both the environmental and financial benefits [6, 7]. On the other hand, the uncertainty of renewable energy generation and consumers' behaviour brings difficulty in matching the demand with the supply within the MG during a certain period.

Instead, there is a need for buyer MGs and seller MGs to trade energy with the main power grid. However, the power loss between the MGs and the main power grid is likely to be higher than that between nearby MGs due to the power transfer. To alleviate this power loss and enhance energy efficiency, recent research has drawn attention to the potential of cooperation among buyer MGs and seller MGs. In [12, 67, 92, 93], a cooperative game theoretic framework is proposed to study the energy trading problem among seller and buyer MGs, where the MGs can make distributed decisions whether to form a coalition with others. Although the merge-and-split based coalition formation games can yield significant power loss reduction, they tend to be highly computationally demanding as the number of MGs increases. Thus, it is of interest to investigate an alternative approach for coalition formation among distributed MGs for energy trading that is efficient and minimizes complexity.

The college admissions problem was first proposed in [51] and used to assign residents to medical schools. As a many-to-one matching algorithm, it has shown the analogy in energy trading between buyer and seller MGs. From the analysis of the college admissions problem [52, 54, 56, 105, 106], it is proved that the entities take the role of applicants and propose coalitions first will get a better outcome or utility. A buyer-driven game indicates that buyers take the role of applicants and apply for admission to sellers who act as colleges. Each seller must decide which one from the buyer applicants to admit to achieve a better utility within its quota, whilst each buyer must apply for the most preferable seller whose cost might be lower. Since the matching process is based on both applicants' and colleges' preference lists, the algorithm guarantees the stability of the coalitions formed in the end. This also shows important trait in comparison with the merge-and-split based coalition formation game that can also guarantee a stable partition of the coalitions.

Therefore, a College Admissions Framework (CAF) algorithm that allows distributed MGs to form disjoint coalitions for energy trading is established in this chapter. MGs who have the incentive to cooperate can reduce power loss and increase revenues significantly compared to a non-cooperative game model where no cooperation among the MGs exists. In addition, Monte Carlo simulation and theoretic analysis have both shown that CAF runs much faster than the merge-and-split based coalition formation games proposed in Chapter 3. The aggregate power imbalance of each MG is used to classify MGs as buyers who have insufficient power generation and sellers who have excess power generation. From the theory of the original college admissions problem, who takes the role of applicants will result in different optimal solutions. Thus, two forms of the CAF (buyer-driven and seller-driven) are designed to accommodate practical market preferences. For instance, the buyer-driven model indicates that the market favours buyer MGs who apply to buy energy and form a coalition with a single seller. Thus, a coalition resulted from this model includes one seller and multiple buyers. In addition, the quota of a college is usually pre-determined in the original college admissions problem. While in the energy trading scenario, the quota of a college MG (being the number of applicant MGs that it can accommodate) is calculated based on each MG's aggregate power imbalance that varies with time. The proposed CAF with varied quotas is proved to be stable and to converge to a final solution. Further, the computational complexity of CAF is analysed and compared with the state-of-the-art coalition formation game that is based on merge-and-split. Unlike the non-cooperative model where the power loss is high and the state-of-the-art coalition formation game where the computational complexity is high, it is shown that the proposed CAF is much

less complex, especially when operating with a large number of MGs. The performance of the proposed CAF is shown through computer-based Monte Carlo simulations and followed by a case study.

The main contributions of this chapter can be summarized as follows:

- Develop a College Admissions Framework to study the coalition formation among distributed MGs for energy trading in order to minimize total active power loss.
- Define the quota of each college MGs and the preference lists of both college and applicant MGs based on power system constraints.
- Evaluate the performance gained from the College Admissions Framework with the merge-and-split based coalition formation game in terms of 1) average power loss per MG, 2) average coalition size, 3) computational complexity from Monte Carlo simulations and a case study.
- Prove the stability and the convergence of the proposed algorithm and analysed the computational complexity of the College Admissions Framework with the merge-and-split based coalition formation game.

The rest of this chapter is organized as follows. Section 4.2 gives a comprehensive literature review on research in college admissions games and MG energy trading. Section 4.3 presents the system model followed by the proposed algorithms in Section 4.4. The properties of the proposed algorithms in terms of stability, convergence and complexity are analysed in Section 4.5. The simulation results and a case study are shown in Section 4.6 and 4.7. Finally, the summary of this chapter is given in Section 4.8.

4.2 Literature Review

In this section, the Stable Marriage and College Admissions Problem applied in recent research is reviewed first. Recent research that involves economics in energy trading for smart grid is summarized and given next.

4.2.1 Stable Marriage and College Admissions

The college admissions problem, also known as the many-to-one game, was first introduced by Gale and Shapley in 1962 in their seminal paper [51], and has attracted interest in the areas of mathematics, computer science, economics and game theory. The later work developed by Alvin Roth and Looyd Shapley for the theory of stable allocations and the practice of market design has been awarded for the Nobel Prize in Economics Sciences in 2012.

This problem falls into the category in combinatorial theory of ordered sets in “pure” mathematics and has been applied to real-world situations such as to assign junior doctors to hospitals, job assignment for the labour market and so on. It is a general extension to the simpler problem of how to find a matching between a set of men and a set of women considering their preferences over the members of the opposite gender to form a stable marriage in time $\mathcal{O}(n^2)$. Unlike the stable marriage problem where both the man and the woman can only be matched with one person from the opposite gender, each college (that students wish to apply to) has a fixed quota given the upper bound on the number of students it can admit. The problem is then to assign students to colleges in a way that takes account of their respective preferences and the quota of each college. The matching is called the student-optimal stable matching. Likewise, if the role of students and colleges is exchanged, the resulting stable matching is college-optimal. Then the algorithm can be seen as a sequence of proposals from students to colleges and finds the final stable match that ensures that each student gets accepted by his or her best possible college among all stable matchings [56]. While by the nature of stable matching [52], the student-optimal stable matching is simultaneously the college-pessimal stable matching, that is, each college gets its worst possible students. Hence, it is natural to seek for a matching that is not only stable but also to satisfy, as much as possible, all preferences for both students and colleges.

Apart from the standard stable marriage problem and its extension to the college admissions games, reference [56] discussed some of the variant models with incomplete preference lists, preference lists with ties and incomplete preference lists with ties and how those conditions affect the algorithms’ stability and running time. The work in [107] further discussed a situation that the college has type-specific quotas to different types of students and how this constraint affects the truthfulness when students reveal their preferences. An algorithm was developed in [108] to find all the stable matchings in a situation if some applicants form couples. The work in [57, 109] takes a different path to investigate the various requirements of colleges quotas.

The algorithms' stability and complexity have been shown for the situations when the colleges have lower and upper bounded quotas as well as common quotas. The work in [57] further proved that the college admissions problems with the presence of lower and common quotas, and paired applications are NP-hard to solve.

In recent years, the framework of college admissions games and its variants have been used in applied problems to model the interactions between two sets of players seeking to cooperate. For instance, the work in [110] formulated a college admissions game for uplink user association in wireless small cell networks. In this game, small cell and macro-cell stations take the role of colleges that seek to recruit a number of students such as uplink users to optimize their utilities. The work in [111] modelled the interactions between single antenna devices such as mobile users and the relay stations in a virtual multiple-input multiple-output (MIMO) scenario as a stable marriage game with incomplete lists. In this game, coalitions of the single antenna devices are formed to minimize the circuit consumed power of each devices. The work in [112] modelled the assignment of transmitter-receiver links to frequency resources within a direct device-to-device (D2D) communication network as a stable many-to-many matching game. In this game, several links can share the same frequency resources and several resources can be consumed by a single link but restricted to matching quotas, aiming to optimize the utilization of the spectral resources.

Although the college admissions game has been studied thoroughly in the “pure” mathematics and been used in wireless resource allocation management applications, such as the work proposed in [111], where single antenna devices are allowed to cooperate and form virtual MIMO links to reduce the energy consumption in the network. To our best knowledge, the work in this chapter that is also published in [13, 14] is the first attempt to apply such a model in an energy trading context within the smart grid, inspired by the resemblance of assigning seller MGs with buyer MGs to that of allocating students to the colleges.

4.2.2 Economics in Energy Trading

The smart grid as the next generation electricity grid introduces revolutionary features to the existing power grid that allow end-users to not only to request the energy from the utility company but also to make use of distributed energy sources, energy storage and electric vehicles and be able to trade energy within the grid to make profit. There have been a numerous studies on how different smart grid components have the incentive to trade energy with each other.

The works in [44, 113–116] investigated energy trading between end-users who have energy storage facilities with the grid. A simple method was proposed in [113] to maximize the profit of end-users who equipped with renewable energy generators and battery storage. By leveraging the time-varying electricity price with the size of battery storage, users can trade energy with the grid and can achieve a near-optimal solution without requiring future energy information, such as demands, price and renewable energy generation. A special type of energy storage, electric vehicles, is considered in [114]. Their batteries can be utilized to store energy during off-peak hours when the grid electricity price is low and supply the extra energy back to the grid during peak hours when the price is generally high. Collaborative and non-collaborative approaches are proposed to maximize the social welfare of a power system with an aggregator and several EV users by taking account of the uncertain residential load scheduling. References [115, 116] further discussed the relationships of energy storage, market price and the customers using game theory analysis and multi-agent models.

On the other hand, the work in [26, 117, 118] addressed the impact of the uncertainty issues of renewable energy generation for the energy trading in the smart grid. The forecast errors of energy consumption and production can be reduced through the creation of groups of users. The relationship between the group size and the forecast accuracy is investigated in [117] by using Seasonal-Naive and Holt-Winters algorithms in an intra-day local energy trading market to minimize customers' costs. A stochastic model predictive control approach is proposed in [118] to optimize the energy dispatch from storage and renewable generators to minimize the system costs. A scenario-based decomposition and a temporal-based decomposition are formulated to give solutions to the cost minimization problem. An optimal bidding strategy in the day-ahead market is proposed in [26] to help a MG to coordinate its energy consumption and production in both the day-ahead and real-time market to minimize its operating costs. Hence, a hybrid stochastic optimization model is proposed and solved by mixed-integer linear programming.

The work in [119, 120] considered an energy market where multiple MGs can trade energy with each other. A multi-leader-multi-follower Stackelberg game is proposed in [119] for seller MGs to act as leaders to decide the amount of energy for sale. Then buyer MGs follow the sellers' actions by submitting bid to the sellers, aiming to maximize the payoff of both seller and buyer MGs. While in [120], the energy trading between interconnected MGs is formulated as a distributed convex optimization framework and solved by a subgradient-based cost minimization

algorithm.

Economic incentive plays an important role in motivating and enabling energy trading and can be used to influence consumers' participation in adopting various smart grid applications. In this chapter, we have further addressed the economic factor in energy trading within MG by introducing a price differentiation scheme, where the price per unit energy is different when buying or selling energy within the coalitions and with the main power grid, so that MGs might have higher incentives to form local coalitions.

4.3 System Model

We study a distribution network composed of one grid connection (termed as the macro station, MS) and several community-level MG over a small area. Similar to the system model described in Chapter 3, each MG considered here is assumed to consist of several households powered by small-scale renewable energy sources such as solar panels and micro wind turbines. The MG control centre is in charge of the power collection and allocation using advanced optimal power dispatching approaches within the MG. Thus, one MG can be seen as an aggregator that can make independent decisions of when and with whom to trade energy by switching on and off the MG-to-MG and MG-to-MS connections, as shown in Figure 4.1.

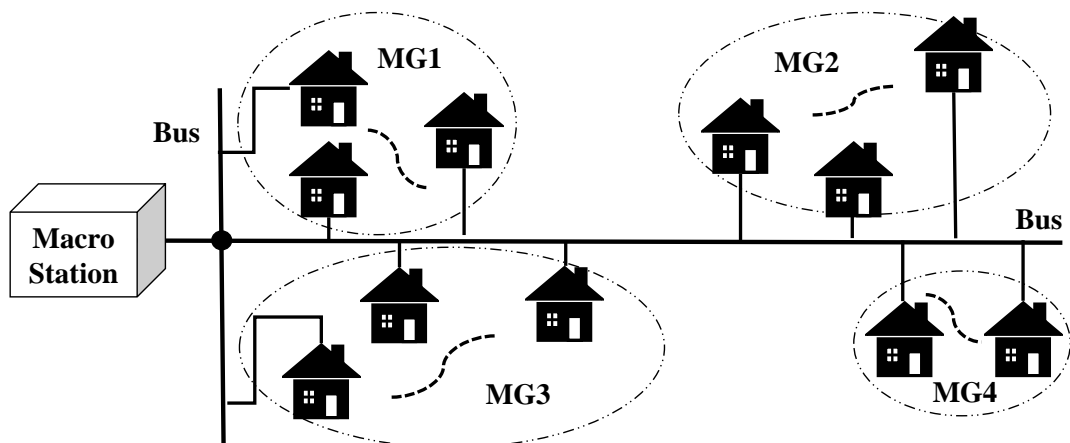


Figure 4.1: A simplified illustration of the considered system model.

4.3.1 Power Metric Calculation

From Chapter 3, the power loss due to the power transfer between MG-to-MG and MG-to-MS following a non-cooperative game and a cooperative game can be calculated as discussed in eq. (3.1), (3.2), (3.3), (3.4), (3.5) and (3.6). Further, a price differentiation scheme is introduced to the existing system model. Buyer MGs buy the energy from the MS at price ω_{dn} per unit energy, and seller MGs sell the energy to the MS at price ω_{up} per unit energy. The value of ω_{up} is determined by the main power grid and is likely to be the wholesale price which is reasonably supposed to be lower than the retail price ω_{dn} . If a seller MG i sells M_{io} power to the MS, the power loss due to the power transfer can be denoted as P_{io} . In the non-cooperative setting where MGs only trade energy with the MS, the total power loss over the power lines can be captured in a cost function with the price factor as

$$C_{\text{non}}(\mathcal{N}) = \sum_{i \in \mathcal{S}} \omega_{up} P_{io}^{\text{loss}} + \sum_{j \in \mathcal{B}} \omega_{dn} P_{jo}^{\text{loss}}, \quad (4.1)$$

where \mathcal{S} is the set of seller MGs and \mathcal{B} is the set of buyer MGs, i.e. $\mathcal{S} \cup \mathcal{B} = \mathcal{N}$. We further define a utility function that accounts for the power loss costs of MG i in the non-cooperative model as

$$U_{\text{non}}(\mathcal{N}) = -C_{\text{non}}(\mathcal{N}). \quad (4.2)$$

Alternatively, some MGs may have the incentive to trade power at price ω_m (which can be reasonably assumed to follow the order of $\omega_{up} < \omega_m < \omega_{dn}$, if $\omega_{up} = \omega_{dn}$, this would simplify to be equivalent to the model described in Chapter 3 eq. (3.5)) with neighbouring MGs by forming coalitions, while minimizing the power loss costs. Thus, in the cooperative model, the cost function can be written as

$$C_{\text{coop}}(\mathcal{D}_h) = \sum_{i,j \in \mathcal{D}_h} (\omega_{up} P_{io}^{\text{loss}} + \omega_{dn} P_{jo}^{\text{loss}} + \omega_m P_{ij}^{\text{loss}}), \quad (4.3)$$

where $i \in \mathcal{S}, j \in \mathcal{B}$, h is the number of all possible coalitions formed over a set \mathcal{N} and \mathcal{D}_h is the set of each coalition indexed by h . Similar to eq. (3.5), if the set \mathcal{N} has three elements, the maximum number of coalitions formed is 5. Further, the utility function of coalition \mathcal{D}_h in the cooperative model can be expressed as the opposite of the cost function:

$$U_{\text{coop}}(\mathcal{D}_h) = -C_{\text{coop}}(\mathcal{D}_h). \quad (4.4)$$

Thus, the cost minimization problem is transferred to be a utility maximization problem.

4.3.2 Benchmark: Coalition Formation Game

By forming coalitions with neighbouring MGs, the power loss due to the power transfer can be reduced, the problem can be formulated as an active power loss minimization problem.¹ The coalitions can be formed following the coalition formation game based on merge-and-split discussed in Chapter 3. It works in a way that, at each round of negotiation, buyer MG i attempts to pair up with seller MGs in turn following a distance ascending order. A pair of buyer MG i and seller MG j will merge into a coalition if this satisfies the Pareto Order. For instance, for two coalitions \mathcal{D}_a and \mathcal{D}_b , where $\forall i \in \mathcal{D}_a$ and $\forall j \in \mathcal{D}_b$, \mathcal{D}_a and \mathcal{D}_b will merge into a new coalition \mathcal{D}_c , where $\mathcal{D}_c = \{\mathcal{D}_a + \mathcal{D}_b\}$, $\forall g \in \mathcal{D}_c$, if and only if relation **Definition 1** holds. Likewise a coalition including buyer i and seller j can be further merged into a larger coalition with other available MGs if this satisfies **Definition 1**.

Definition 1. The **Pareto Order** guarantees that a structure of a set is preferred if and only if its utility is improved, i.e., structure $\{i, j\}$ is preferred over $\{\{i\}, \{j\}\}$, if and only if $U_{\text{coop}}(\{i, j\}) \geq U_{\text{non}}(\{i\}) + U_{\text{non}}(\{j\})$. For instance, for a player i , set \mathcal{H}_a is preferred over set \mathcal{H}_b by the Pareto Order if and only if the utility of i in \mathcal{H}_a is improved over its utility in \mathcal{H}_b , so $U_{i \in \mathcal{H}_a} \geq U_{i \in \mathcal{H}_b}$. There should be at least one player for whom holds strict inequality.

On the other hand, a split is investigated by computing all possible set partitions when there are more than 3 MGs in one single coalition and is executed if breaking up one coalition into two or more smaller coalitions improves each MG's utility compared to that in its old coalition according to the Pareto Order. The negotiation of merge and split will be terminated when the network of MGs reaches a stable state that there is no incentive for each MG to leave the current coalition. However, due to the exhaustive search in the split process, this approach requires a high complexity when dealing with a large number of MG.

¹Active power loss could be one dominant measurement to evaluate the utility function defined in the proposed model. In practice, MGs come in a variety of sizes. Thus, more sophisticated metrics, such as pricing, quality of service and environmental impact, can also be considered from case to case to model a more realistic utility function for real-world MG implementations.

4.4 The Proposed College Admissions Framework

In this section, the college admissions problem is introduced and implemented to solve the power loss minimization problem that is much less computationally demanding than the coalition formation game.

4.4.1 The College Admissions Problem

The Gale-Shapley college admissions problem is a many-to-one extension of the stable marriage problem, which was originally devised to pair up residents with medical schools [51]. It works such that m colleges $\mathcal{C} = \{c_1, \dots, c_m\}$ rank n applicants $\mathcal{A} = \{a_1, \dots, a_n\}$ in the order of preference $\mathcal{R}_c = \{r_{c_1}^n, \dots, r_{c_m}^n\}$, where $r_{c_i}^n$ denotes the i^{th} college's ranking of all n students, by which it is willing to accept them but subject to its quota $q_c = \{q_{c_1}, \dots, q_{c_m}\}$ (this being the maximum number of students that a college can admit). Similarly, each student ranks colleges in order of his or her preference $\mathcal{R}_a = \{r_{a_1}^m, \dots, r_{a_n}^m\}$. For instance, each student proposes to register with his or her most preferred college in turn; hence the method works in a student-optimal manner. The problem is then to allocate students to colleges based on their mutual preferences $\mathcal{R} = \{\mathcal{R}_a, \mathcal{R}_c\}$ and the college's quota q_c . Thus, the college admissions problem can be summarized as $(\mathcal{C}, \mathcal{A}, \mathcal{R}, q_c)$.

Considering the practical market preferences and the varied composition of energy sources and loads in a MG, two forms of the college admissions framework (CAF) are proposed for the energy trading scenario. That is denoted as the buyer-driven CAF and the seller-driven when buyers and sellers take the role of students, respectively.

It is worth noting that the quota q_c for college c is assumed to be fixed in the original problem, while in the energy trading scenario, the quota $q_c = \{q_{c_1}, \dots, q_{c_m}\}$ is a vector of the college MGs' power surplus during time slot t which cannot be pre-determined. Instead q_{c_m} will be decreased when a college MG c_m admits (i.e. sells energy to) a student MG in its coalition and will be increased accordingly when c_m rejects a lower ranked student MG from its coalition. The value that q_{c_m} is decreased and increased is determined by the amount of energy a student MG required. The calculation of the quota differs from the buyer-driven CAF to the seller-driven CAF, as shown in Figure 4.2.

The procedures for the proposed buyer-driven and seller-driven CAF algorithms are shown

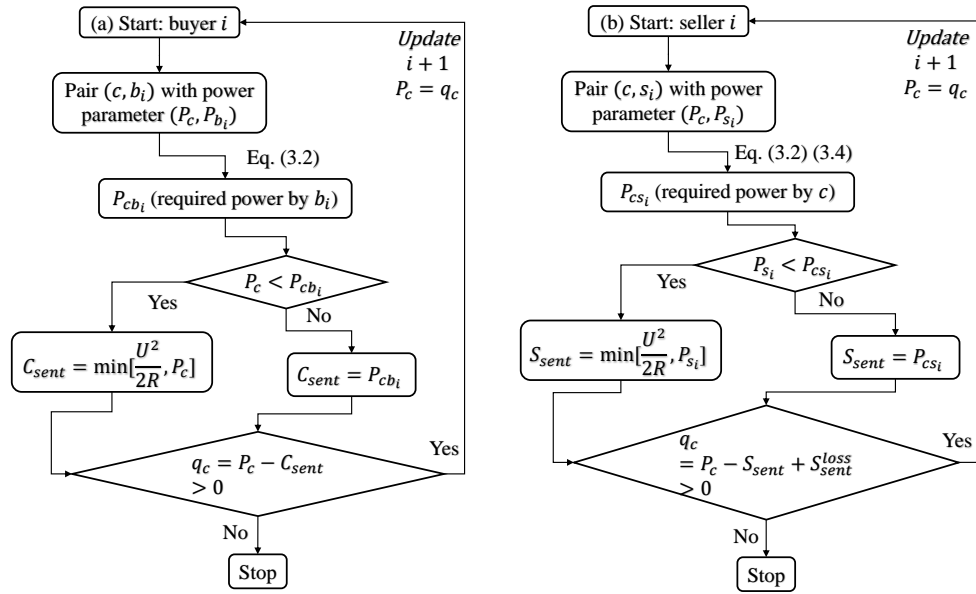


Figure 4.2: The process of q_c calculation in (a) BD-CAF and (b) SD-CAF, where c represents a seller and a buyer, respectively.

next.

4.4.2 The Buyer-driven Model

In the buyer-driven college admissions framework (BD-CAF), buyer MGs apply to seller MGs in turn of preference to form coalitions to reduce their total power losses. A typical coalition consists of one seller and n buyers, such as $\{s_1, b_1, \dots, b_n\}$, where s_1 denotes the seller and b_k is the k^{th} buyer in the order of admission. The BD-CAF procedure is described as follows:

1. Buyer b_i applies to seller s_1 who is b_i 's first choice on its preference list $r_{b_i}^m$, while s_1 with a quota of q_{s_1} (this being the maximum integer number since we only consider to form disjoint coalitions of buyers that s_1 is able to serve and can be calculated depending on s_1 's power surplus P_{s_1} and applicant buyers' power demand P_{b_i}) will only be able to sell a maximum of P_{s_1} power to buyers who rank from the highest to the q_{s_1} -th, or all available buyers if the overall demand is less than P_{s_1} . Thus, a coalition such as $\{s_1, b_1, \dots, b_k\}$ is formed and buyers $\{b_{k+1}, \dots, b_n\}$ are rejected accordingly if $k < n$. The preference list is ordered by the ascending distance to the opposite set that is similar to the negotiation order in Chapter 3 and Section 4.3.2. An MG (e.g. buyer) who has a higher power demand P will be ranked higher than other MGs who are located at the

same distance to the seller. However, a higher ranked buyer will still be rejected if that violates the Pareto Order. It is worth noting that a buyer will not be placed into the seller's coalition if the Pareto Order is violated even if this buyer has a higher ranking on seller j 's preference list.

2. The rejected buyers from the first round apply to their second choice. Similarly, each seller selects the top q_{c_j} MGs from among the new buyers and those who are already in its coalition, seller j updates its coalition and rejects the rest. Quota q_{c_j} is re-calculated whenever a buyer who is ranked higher on its preference list than any of the existing ones attempts to join seller j 's coalition.
3. The process terminates when all buyers are either admitted into a coalition or rejected by all sellers. The latter case indicates that this buyer is better off operating in the grid-connected mode rather than within a coalition with other MGs. Here, a stable matching has been formed.
4. In the power transaction stage, seller MGs are encouraged to sell power to the buyers within their coalitions by the order of admission.

The above process describes one round of the proposed BD-CAF algorithm in steps. The procedure is also illustrated in a flow chart in Figure 4.3 along with the pseudo code in Algorithm 1, where each buyer b_i applies to a place in seller s_j based on their preference list $r_{b_i}^m$ and $r_{s_j}^n$ and s_j 's quota q_{s_j} .

It is worth noting that at any point for a given seller s_j , its quota q_{s_j} is updated every time a higher ranked buyer attempts to join its coalition. Depending on this buyer's power parameters, the lowest ranked buyer in s_j 's coalition can always be rejected. If a buyer is removed from the seller's coalition, there might be a chance for the buyer to be accepted by the seller in the future if the structure of the seller's coalition had been changed, e.g., q_{c_j} had been updated when a buyer who has a less energy demand is accepted and replaced with a buyer who has a higher energy demand, and this seller would have spare energy for this buyer.

4.4.3 The Seller-driven Model

In the seller-driven form (SD-CAF), seller MGs apply to buyer MGs in turn of their preferences. A coalition becomes a group consisting of one buyer with m sellers, such as $\{b_1, s_1, \dots, s_m\}$,

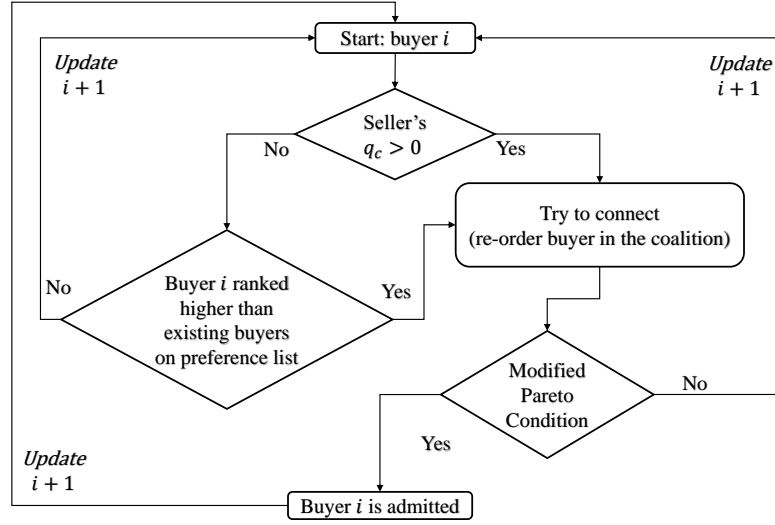


Figure 4.3: One iteration of BD-CAF process

where b_1 is the buyer and s_g is the g^{th} seller in the order of admission. The SD-CAF follows a similar procedure as the one described in Section 4.4.2, except the role of students are switched to sellers. For sellers ($P > 0$), the actual amount of power dispatched to the macro station or to the buyer MGs equals P . While for buyers ($P < 0$), an additional amount of energy is required to compensate the power losses on the cable to meet their total energy demand. In this case, the buyer who acts as a college would always take account of the extra power loss P_{loss}^{extra} to solve the actual amount of power P_{ij} using eq.(3.2) and (3.4) to determine the utility and the quota q_c (as shown in Figure 4.2. (b)). A buyer might decide to accept more sellers in average to meet its energy demand when compared to the BD-CAF case that will lead to different partitions.

4.5 Algorithm Analysis

A key property of college admissions based approach is that the resulting match between the college and the students is stable. This means that each party achieves an optimal utility within the current assignment and no one will unilaterally leave. The quota q_s of college MG (that is a seller in the BD-CAF model) is not pre-determined before the matching process. Although this differs from the original problem, the proposed CAF with varied quota is still stable and converges to a final solution. In this section, by taking an example of the BD-CAF model, the stability and convergence of the CAF is proved. The complexity of the CAF is also analysed

Algorithm 1 One round of the BD-CAF Algorithm for MG cooperation with varied quotas.

```

1: procedure BD-CAF( $\mathcal{H} = \{\{b_i\}, \{s_j\}\}, r_{b_i}^m, r_{s_j}^n, q_{s_j}$ )
2:   while  $\exists b_i$  is willing to form a coalition  $\{b_i, s_j\}$  do
3:     for  $\forall b_i$  do
4:       for  $\forall s_j$  in order of  $r_{b_i}^m$  do
5:         if  $s_j$ 's power surplus  $P_{s_j} > 0$  then
6:           if Pareto Order holds then
7:             update  $q_{s_j}$  and partition  $\mathcal{H}$ 
8:             remove  $b_i$  from  $r_{s_j}^n$ 
9:           else
10:            if  $b_i =$  last unmatched buyer then
11:              update  $r_{b_i}^m, j++$ 
12:               $i++$ , keep  $s_j$  on  $r_{b_i}^m$ 
13:            else
14:              if  $\text{rank}(b_i) > \forall b \in \{b, s_j\} \wedge b_i \neq b$  then
15:                update  $q_{s_j}$ 
16:                add  $b_i$  into  $\{b, s_j\}$ , update  $\mathcal{H}$ 
17:                lowest ranked  $b$  might be removed
18:              else
19:                 $i++$ 
20: end procedure  $\rightarrow$  return  $\mathcal{H}$ 

```

along with the merge-and-split based coalition formation game proposed in Chapter 3.

4.5.1 Stability and Convergence Analysis

The matching from the college admissions problem is stable if:

- A college would not reject any of its current students to admit another new student;
- A student would have no incentive to transfer to any of the other colleges but prefers to stay with the current one.

From the analysis in [56], this also indicates that there is no blocking pair (a, c) existing among all members. That is, a and c prefer to match even though they both have been matched with someone else previously.

Lemma 1. As every time the configuration of MGs changes, Algorithm 1 is re-run. If at time $t = l$ Algorithm 1 runs and terminates, the resulting partition \mathcal{H}_l is Nash stable.

Proof. A partition is Nash stable if each player is better off under the current match and no

one has the incentive to leave [51]. If \mathcal{H}_l is not stable, then there exists at least one pair of a buyer and a seller (b, s) that blocks \mathcal{H}_l where b and s prefer each other to their current partners. This will break the structure of the match \mathcal{H}_l and lead to a different match $\dot{\mathcal{H}}_l$. In fact, such a blocking pair cannot exist. Suppose that b is not admitted by s but prefers s to its current partner s_b . Then, b must have applied to s at some stage and subsequently been rejected in favour of other higher ranked buyer MGs who also prefer s , thus s has no more space to admit b . On the other hand, if s prefers b to its current partner b_s , then b must have applied and been admitted to a higher ranked seller MG before getting a chance to apply to s . In fact, Algorithm 1 would prevent such a mismatch $\dot{\mathcal{H}}_l$ since each round of the negotiations between buyer MGs and seller MGs are constrained by a strict preference relation and are validated by the Pareto Order. Here is one example of a possible ranking matrix:

	s_1	s_2	s_3
b_1	(1, 1)	(2, 1)	(3, 3)
b_2	(3, 2)	(2, 2)	(1, 1)
b_3	(3, 3)	(2, 3)	(1, 2)

The first number of each pair in the rows gives the ranking of sellers (i.e., s_1, s_2, s_3) by the buyers (i.e., b_1, b_2, b_3), the second number of each pair in the columns is the ranking of the buyers by the sellers. Following Algorithm 1, we have the resulting partition $\mathcal{H}_l^* = \{\{s_1, b_1\}, \{s_2, b_3\}, \{s_3, b_2\}\}$. It is easy to verify that \mathcal{H}_l^* is Nash stable. \square

Lemma 2. The proposed BD-CAF in Algorithm 1 with time-varying quota is guaranteed to converge to a final partition $\mathcal{H}_{\text{final}}$.

Proof. From **Lemma 1.**, partitions $\mathcal{H}_1, \dots, \mathcal{H}_{\text{final}}$ resulting from each iteration of the BD-CAF procedure are Nash stable. To prove convergence, two conditions must be met. That is:

1. *The number of all potential partitions h over a set of N members is not increasing indefinitely.*

For 1, it is obvious that if the number of MGs is finite then h is finite and is determined by the Bell number B_N . That counts all partitions of a set of N elements [121].

2. *There are no two states that switch to each other repeatedly.*

For 2, the coalition formation process must have been experienced several transitions before reaching to a final partition $\mathcal{H}_{\text{final}}$, i.e. $\mathcal{H}_1 \rightarrow \mathcal{H}_2 \rightarrow \dots \rightarrow \mathcal{H}_{\text{final}}$. At each

negotiation, an MG i will only transfer from an old partition \mathcal{H}_{old} to a new partition \mathcal{H}_{new} if and only if the Pareto Order is satisfied. In many problems, the college quota q_c is a constant and can be pre-determined, but here q_c varies with the power imbalance P of the MGs over time. However the variation of the quotas will only increase the size of a coalition up to at most one more MG. That is because, every time a higher ranked buyer b_h is willing to join an existing coalition in a partition \mathcal{H}_{old} within which the seller is already connected with a less ranked buyer b_l . Only two possible results will occur:

- (a) If the power imbalance P of the seller MG is still positive after virtually admitting b_h , b_l will be maintained in the coalition hence the coalition size increases by 1.
- (b) If the power imbalance P of the seller becomes negative after virtually admitting b_h , the existing buyer b_l will be replaced by b_h hence the coalition size remains the same.

In either case, the varied quota will not violate the *Pareto Order* and each new partition \mathcal{H}_{new} will not be able to switch back to a previous one \mathcal{H}_{old} .

□

Hence, we have shown that the proposed CAF with varied quota maintains stability and converges to a final solution that is in line with the Gale-Shapley college admissions problem.

4.5.2 Complexity Analysis

For a network consisting of N MGs, the merge-and-split method will calculate the utility at most B_N times. This is because in the split process, the algorithm will need to compute all possible set partitions over N members in the worst case scenario. Thus, the successful searches can be done in time $\mathcal{O}(B_N)$.

In the BD-CAF model, m seller MGs, denoted as $\mathcal{S} = \{s_1, \dots, s_m\}$ and n buyer MGs, denoted as $\mathcal{B} = \{b_1, \dots, b_n\}$ take the role of colleges and students, respectively. The scalar q_s is the quota of a seller $\forall s \in \mathcal{S}$ where $1 \leq q_s \leq n$, and r_s^n, r_b^m is the preference list of s and b for its counterparts. It is worth noting that the length of r_s^n is n and that $m + n = N$. In the worst case scenario, buyers have reverse rankings of the sellers when compared to the rankings of the buyers by the sellers. A buyer, denoted as b , will apply to sellers from the most preferred

to the least but will be rejected accordingly until the last seller admits it. For buyers, the number of unsuccessful searches is $\mathcal{O}(m \times (m - 1) + 1)$. For sellers, the preferred buyer will always apply last. If q_s is big enough to host all buyers (i.e. $q_s = n$), the seller will admit buyers in time $\mathcal{O}(n)$; if q_s is small enough that it can only admit the most preferred buyer (i.e. $q_s = 1$), the seller will admit the first $n - 1$ buyers but reject them accordingly, after at most $(n - 1)^2 + 1$ searches [51] during which only the last but the most preferred buyer will be admitted. In conclusion, the number of search operations for the BD-CAF process is $\mathcal{O}(m \times (m - 1) + 1 + (n - 1)^2 + 1)$, which is bounded above by $\mathcal{O}(N^2)$. This is much lower than the merge-and-split based coalition formation algorithms that are related to the Bell number B_N . Thus, in theory the BD-CAF algorithm is as much as 1159 times faster than the merge-and-split algorithm for a network of 10 MGs. However, we should note that the limitation of the many-to-one matching (CAF based algorithms) is that it misses some combinations of the coalitions found by the many-to-many matching (merge-and-split based algorithms). Through Monte Carlo simulations using the parameters from Table 4.1, the number of utility function calculations is computed by using the merge-and-split algorithm from Chapter 3, denoted as N_{MS} , and the BD-CAF, denoted as N_{BDCAF} , respectively. The ratio that is defined as:

$$\text{ratio} = \frac{N_{MS}}{N_{BDCAF}} \quad (4.5)$$

is further plotted in Figure 4.4. It is shown that BD-CAF is 700 and 18000 times faster than merge-and-split for a network of 10 MGs and 20 MGs, respectively.

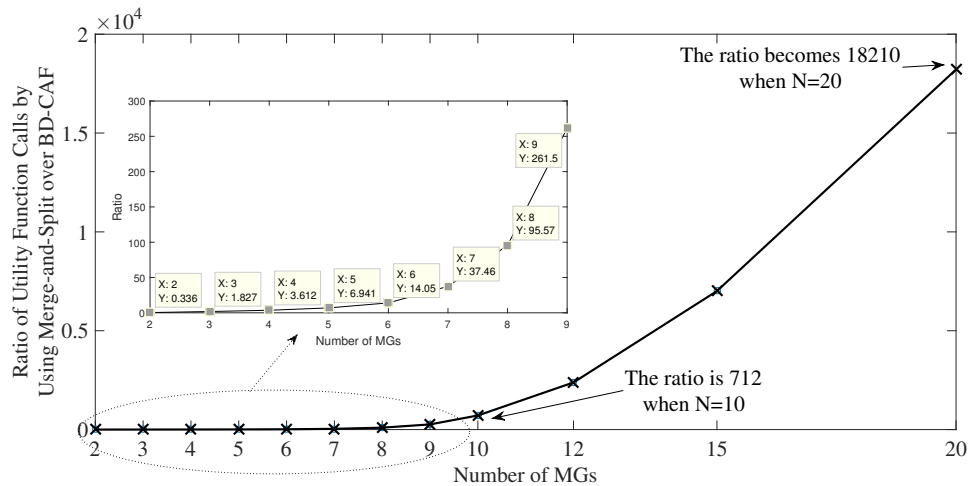


Figure 4.4: Complexity comparison between merge-and-split and BD-CAF in terms of the frequency of utility calculations

4.6 Simulation Results

In this section, 10,000 different scenarios via Monte Carlo simulations are conducted for the coalition formation process using two baseline algorithms (i.e., a non-cooperative model and a merge-and-split coalition game from Chapter 3) and the proposed CAF (i.e., BD-CAF and SD-CAF) among MGs $i \in \{1, \dots, n\}$, where $n = 30$. Consider a distribution network that consists of one macro station and several MGs randomly deployed over an area of $10 \text{ km} \times 10 \text{ km}$. Each MG is allowed to exchange energy with each other and with the MS. The parameters of the system setting are chosen from [12, 67, 92] and are summarized in Table 4.1. A performance comparison among the aforementioned algorithms is shown in the following figures 4.5, 4.6 and 4.7. The utility improvement from each intermediate step is checked to ensure the correctness of the algorithms. In addition, a detailed case study on a 3 MGs network shown in Section 4.7 gives a breakdown of how coalitions are formed and how utilities are improved after forming coalitions. The values of the utility for each participating MG in each intermediate step are further shown in Table 4.2.

Figure 4.5 shows the average power loss per MG when applying the BD-CAF and the SD-CAF from Section 4.4.2 and 4.4.3, compared with the non-cooperative model and the merge-and-split coalition game from Chapter 3. When the number of MGs increases, the power loss per MG when utilizing the coalition formation games yield a significant reduction compared to the non-cooperative model, while the BD-CAF and the SD-CAF yield a similar performance. For a network of 20 MGs, the power loss is reduced by 33% and 27% when using the merge-and-split and the CAF respectively. It is also shown that although the proposed CAF yields a slightly lower power loss reduction i.e. 6% less than the merge-and-split, the computational complexity is much less, as previously shown in Figure 4.4. Brute force method is not considered here since we have already thoroughly compared the power loss between brute force and merge-and-split in Chapter 3. The main purpose of Figure 4.5 is to show the power loss comparison between CAF and merge-and-split, that CAF is only 6% worse than merge-and-split compared to the non-cooperative method. Then, we analysed the computational complexity between CAF and merge-and-split and further discussed the trade-off between power loss reduction and complexity in Section 4.8.

In Figure 4.6, it is observed that the merge-and-split tends to form larger coalitions than the proposed CAF methods. This is because during the college admissions procedure, two colleges will have no chance to form into one coalition. In other words, CAF only allows a many-to-

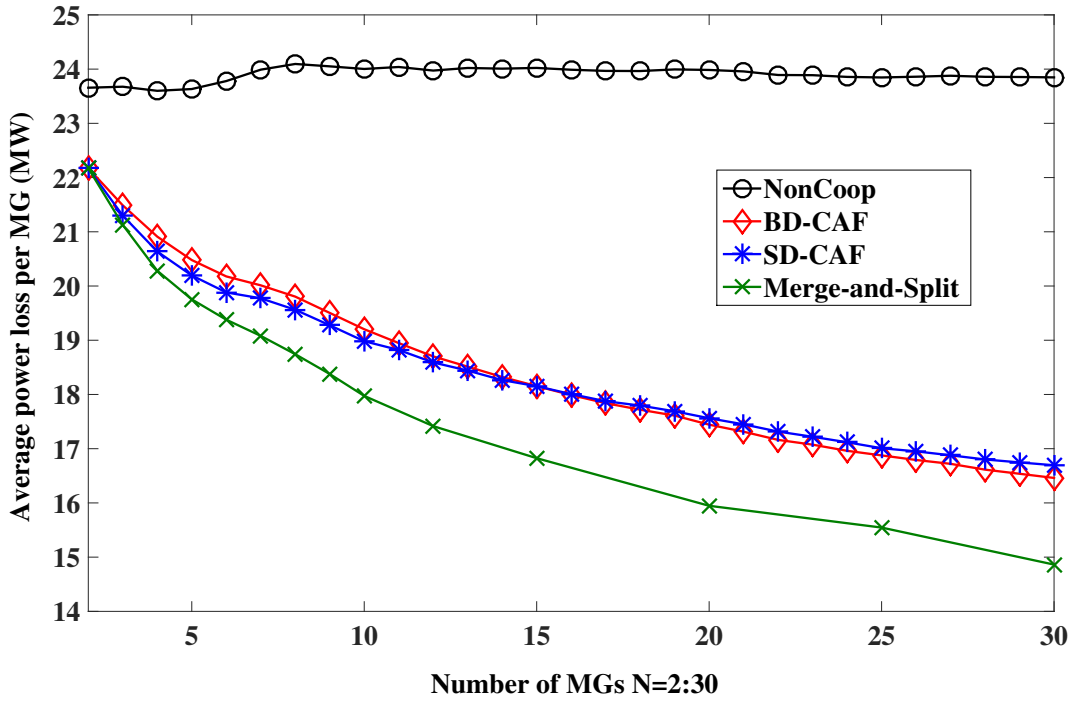


Figure 4.5: Average power loss comparison.

one matching, while the merge-and-split allows a many-to-many matching. In the proposed system, seller MGs and buyer MGs take the role of college in turn, but neither case will lead to a coalition that consists of multiple sellers and multiple buyers. This will cause CAF to miss some coalitions that are formed by the merge-and-split method. Thus, the CAF will yield smaller coalition size. This also explains why the CAF yields less power loss reduction than the merge-and-split as shown in Figure 4.5. This is because smaller coalitions would normally yield less local cooperation that would increase the likelihood that MGs trade energy with the MS and result a higher power loss. As the number of MGs increases from 2 to 20, it is also observed that the average coalition size rises gradually from 1.3 (when $N = 2$ for all three algorithms) to 2.3 (when $N = 20$, for merge-and-split), 2 (when $N = 20$, for SD-CAF), and 1.9 (when $N = 20$, for BD-CAF), respectively. As the combinations of coalitions formed between 2 MGs are the same when $N = 2$, the average coalition size of all three algorithms stays the same. With the number N increasing, this result is in line with the analysis that the average coalition size of merge-and-split is larger than CAF. In addition, the reason why the average coalition size of SD-CAF is larger than BD-CAF is that in SD-CAF, sellers would apply to a preferable buyer who is normally in need of an extra amount of energy to cover the power loss on the cable, hence a buyer would tend to admit more sellers in average than a seller

would do in BD-CAF. However, the variation of power loss as well as the average coalition size are not significant when compared to the variation of the computational complexity for a large number of MGs in the network as shown previously in Figure 4.4, 4.5 and 4.6.

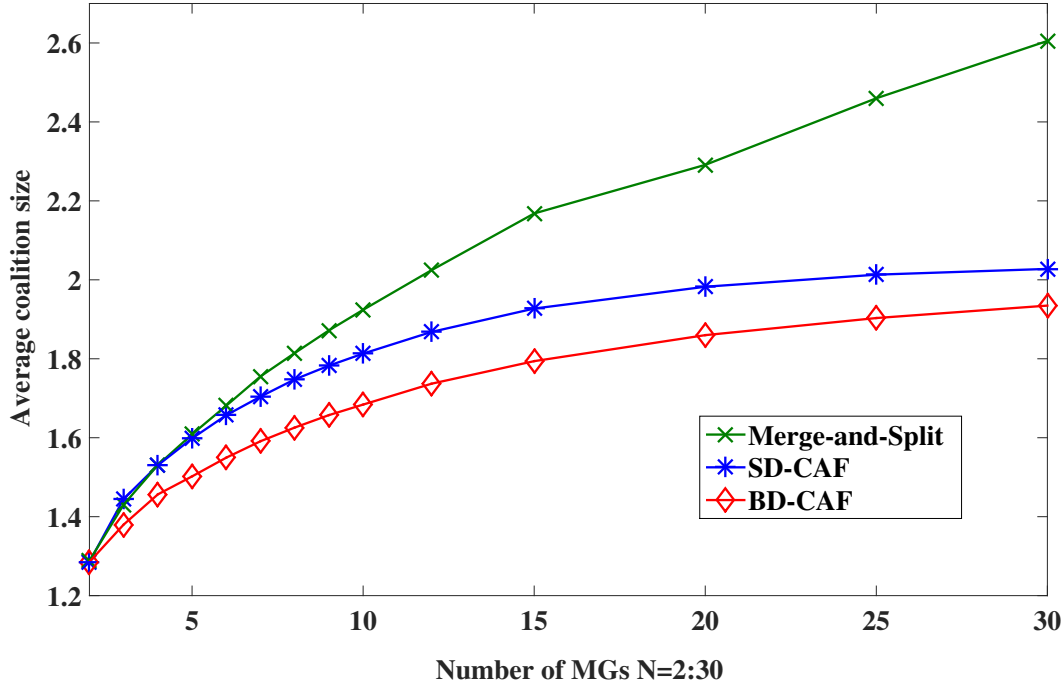


Figure 4.6: Average coalition size comparison

Figure 4.7 further shows the average power loss per buyer for the BD-CAF (denoted as BD/B), and the SD-CAF (denoted as SD/B), and the average power loss per seller for both methods (denoted as BD/S and SD/S), respectively. This is also compared with the average power loss per MG for both methods (denoted as BD/MG and SD/MG). It can be seen that regardless of which methods being used, there is always a higher power loss for buyers than sellers. This is because buyers will always buy an extra amount of power to cover the power loss to meet its actual demand. As the number of MGs increases, it is also interesting to note that sellers yield a better performance in SD-CAF than in BD-CAF (i.e. the SD/S curve is lower than the BD/S curve) and buyers also yield a better performance in BD-CAF than in SD-CAF (i.e. the BD/B curve is lower than the SD/B curve). These results are in line with the theory for the Gale-Shapley college admissions problem [51] that the matching is optimal for the one who proposes first.

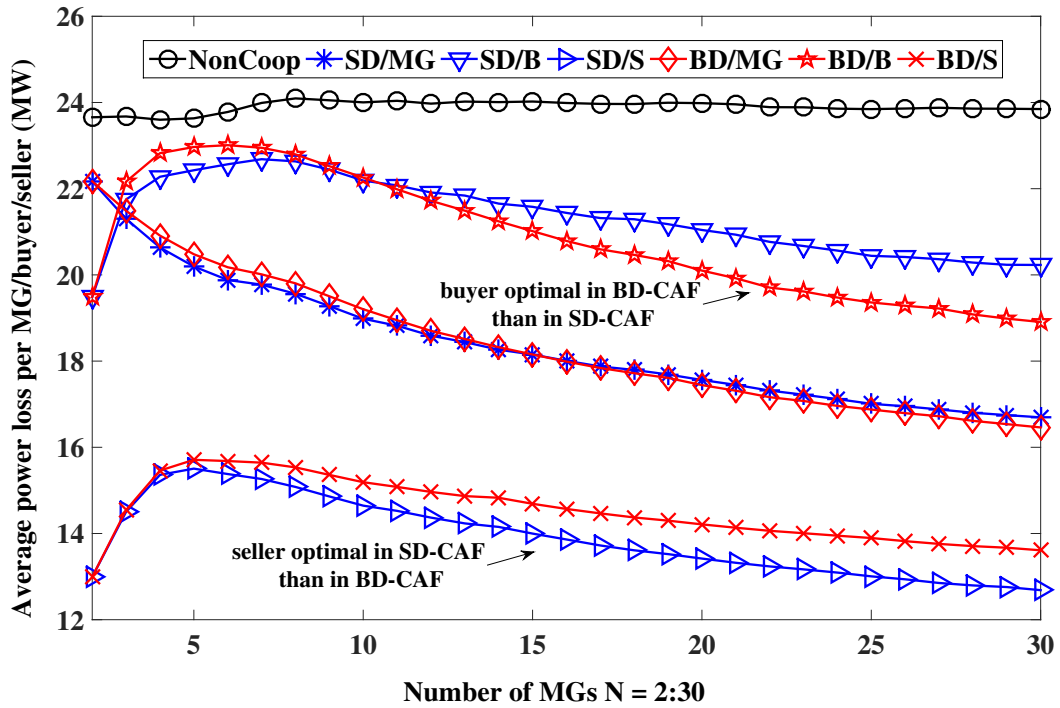


Figure 4.7: Comparison of power loss per buyer, per seller and per MG when using BD-CAF and SD-CAF with the non-cooperative model as the baseline.

4.7 Three MGs Case Study

Further, the proposed BD-CAF algorithm is implemented in a case study for a simple scenario where there is one MS connected to the grid and 3 MGs located equidistant from the MS and to each other. MG 1, 2, and 3 are assumed to be supplied mainly by solar panels, wind turbines and a combination of both generations, respectively.

The real daily load and generation data is used and extracted from [122]. For simplicity, all three MGs are assumed to have an identical composition of load and the same level of mixed load profile. Since the types and penetration of the energy sources differ from MG 1 to MG 3, an hourly power imbalance of each MG in a day is obtained, as shown in Figure 4.8. In addition, the timeslots that MGs have the potential to cooperate when there exists both buyers and sellers at the same time are highlighted in Figure 4.8, that is when $t = 0-7, 17-18, 20-24$ hr. For instance, MG 2 who has a positive power imbalance during the 1st to the 7th hour might want to sell its power surplus to MG 1 and MG 3, who both have negative power imbalance and act as buyers. Other simulation parameters are given in Table 4.1.

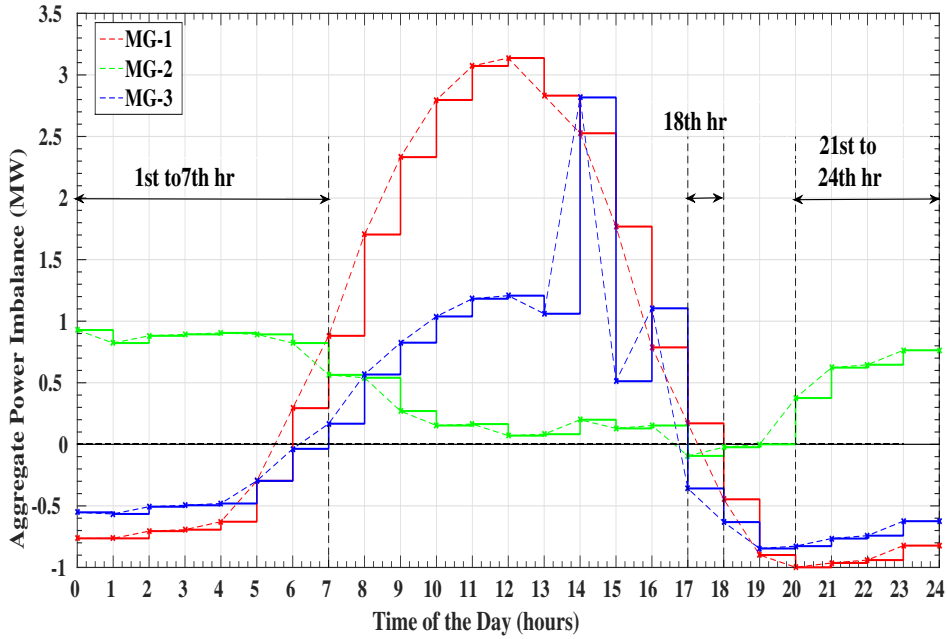


Figure 4.8: Aggregate power imbalance in a day with highlighted cooperation timeslots.

Algorithm 1 is implemented for this model. The utility improvement is compared with a non-cooperative model. The utility improvement of the merge-and-split and of the CAF is comparable when the size of the network N is small, but differs drastically for a larger N in terms of computational complexity as discussed in Section 4.5.2. The cooperation patterns of the final partition are shown in the 2nd column of Table 4.2. The individual utility (payment) of MG i in a coalition \mathcal{H} is calculated following a proportional fairness division scheme as in Chapter 3 eq. (3.6), and is given in the 3rd column in contrast to the payment in the non-cooperative model given in the 4th column. For instance, seller MG 2 and buyer MG 1, MG 3 form a coalition during the 2nd hour, where their payments in terms of power loss are reduced from 2.3, 1.2 and 1.6 GBP when under no cooperation, i.e. $\{\{2^s\}, \{1^b\}, \{3^b\}\}$ to 0.9, 0.5 and 0.7 GBP, respectively, with a 58.5% average saving per MG.

Compared to the non-cooperative model where each MG only trades energy with the MS, coalitions among MG 1, 2, 3 are formed under the BD-CAF model during different periods of the day. In Figure 4.9, it can be observed that the pattern of the coalitions has changed 3 times in the day. During the 1st to the 6th hour, two connections of $2 \rightarrow 1, 2 \rightarrow 3$ are established, the coalition \mathcal{H} can be represented as $\{1, 2, 3\}$; then during the 7th hour, link $2 \rightarrow 1$ is disconnected, i.e. $\mathcal{H} = \{\{1\}, \{2, 3\}\}$; from the 8th hour, link $2 \rightarrow 3$ is disconnected, thus no coalition

Parameter	Values
Simulation Area	10 km X 10 km
Power imbalance P of each MG	$\sim U(-3,3)$ MW
Power Loss Fraction at MS α	2%
Medium Voltage at MS U_o	33 kV
Low Voltage at MG U_l	11 kV
Resistance on the Line R	0.2 Ω /km
Wholesale Price ω_{up}	6 p/kWh
Retail Price ω_{dn}	14 p/kWh
Local Price among MG ω_m	10 p/kWh

* $\sim U(\cdot, \cdot)$ represents a uniform distribution.

Table 4.1: Simulation parameters for Chapter 4

has formed, i.e. $\mathcal{H} = \{\{1\}, \{2\}, \{3\}\}$; in the 18th hour, the connection between 2 and 1 is established again, i.e. $\mathcal{H} = \{\{1, 2\}, \{3\}\}$ but disconnected from the 19th hour, i.e. $\mathcal{H} = \{\{1\}, \{2\}, \{3\}\}$ and reconnected during the 21st to the 24th hour, i.e. $\mathcal{H} = \{\{1, 2\}, \{3\}\}$.

Through cooperation, the peak time ($t = 17-18$ hr) saving per MG is 38.9%, and the off-peak time ($t = 0-7, 20-24$ hr) saving per MG is 50.4% when compared to the non-cooperative model. From Figure 4.9, it is shown that MG 1 buys energy from MG 2 during $t = 0-6, 20-24$ and sells energy to MG 2 during $t = 17-18$. In the rest of the day, MG 1 trades energy with the MS if needed. The cooperation helps MG 1 save 6.3 GBP in the day; similar results can be obtained for MG 2 and MG 3. These effects can be also observed when applying BD-CAF on a network that has more than 3 MGs.

These results can also give insights for deployment of future MGs. For instance, based on the cooperation pattern given by the proposed BD-CAF algorithm, some MGs would consider to deploy physical connections with whom they can get the most benefit, such as the connection between MG 1 and MG 2. It also indicates that there is no need to build connections between those MGs who might have little cooperation opportunities, such as the connection between MG 1 and MG 3 in Figure 4.9. In practice, the scheduling can be achieved from comprehensive simulation using historical data across the area on a day-ahead basis.

Time Index t	Coalition Formed	Coop-payment (GBP)	NonCoop-payment (GBP)	Average Saving per MG
1	$\{\{2^s, 1^b, 3^b\}\}$	$\{\{0.9, 0.5, 0.7\}\}$	$\{\{2.3, \{1.2, \{1.6\}\}\}$	58.5%
2	$\{\{2^s, 1^b, 3^b\}\}$	$\{\{1.1, 0.5, 0.8\}\}$	$\{\{2.3, \{1.0, \{1.7\}\}\}$	51.7%
3	$\{\{2^s, 1^b, 3^b\}\}$	$\{\{0.8, 0.4, 0.6\}\}$	$\{\{2.1, \{1.1, \{1.5\}\}\}$	61.9%
4	$\{\{2^s, 1^b, 3^b\}\}$	$\{\{0.7, 0.4, 0.5\}\}$	$\{\{2.1, \{1.1, \{1.5\}\}\}$	65.7%
5	$\{\{2^s, 1^b, 3^b\}\}$	$\{\{0.5, 0.3, 0.4\}\}$	$\{\{1.9, \{1.1, \{1.4\}\}\}$	72.6%
6	$\{\{2^s, 1^b, 3^b\}\}$	$\{\{0.2, 0.2, 0.2\}\}$	$\{\{0.9, \{1.1, \{0.9\}\}\}$	79.1%
7	$\{\{1^s, \{2^s, 3^b\}\}\}$	$\{\{0.4, \{0.9, 0.1\}\}\}$	$\{\{0.4, \{1.0, \{0.1\}\}\}$	10.0%
18	$\{\{1^s, 2^b, \{3^b\}\}\}$	$\{\{0.1, 0.1, \{1.0\}\}\}$	$\{\{0.2, \{0.3, \{1.0\}\}\}$	38.9%
21	$\{\{2^s, 1^b, \{3^b\}\}\}$	$\{\{1.8, 0.3, \{2.5\}\}\}$	$\{\{3.0, \{0.5, \{2.5\}\}\}$	26.7%
22	$\{\{2^s, 1^b, \{3^b\}\}\}$	$\{\{1.2, 0.3, \{2.3\}\}\}$	$\{\{2.9, \{0.8, \{2.3\}\}\}$	40.4%
23	$\{\{2^s, 1^b, \{3^b\}\}\}$	$\{\{1.1, 0.3, \{2.2\}\}\}$	$\{\{2.8, \{0.8, \{2.2\}\}\}$	41.1%
24	$\{\{2^s, 1^b, \{3^b\}\}\}$	$\{\{0.7, 0.3, \{1.8\}\}\}$	$\{\{2.4, \{1.0, \{1.8\}\}\}$	46.9%

* 1^b represents that MG-1 is a buyer, likewise 2^s represents that MG-2 is a seller.

Table 4.2: Monetary saving before and after coalition formation

4.8 Summary

A fast, computationally efficient algorithm to minimize the power loss cost of energy trading among distributed MGs is proposed in this chapter. The power loss minimization problem is first formulated as coalition formation game then transferred to a college admissions game with variable quotas. The proposed College Admissions Framework (CAF) is proved to be able to converge to a stable solution. In addition, it is much less complex than the state-of-the-art coalition game based on merge-and-split.

Through computer-based Monte Carlo simulations, the performance comparison of the proposed CAF with two baseline algorithms (the merge-and-split and the non-cooperative model)

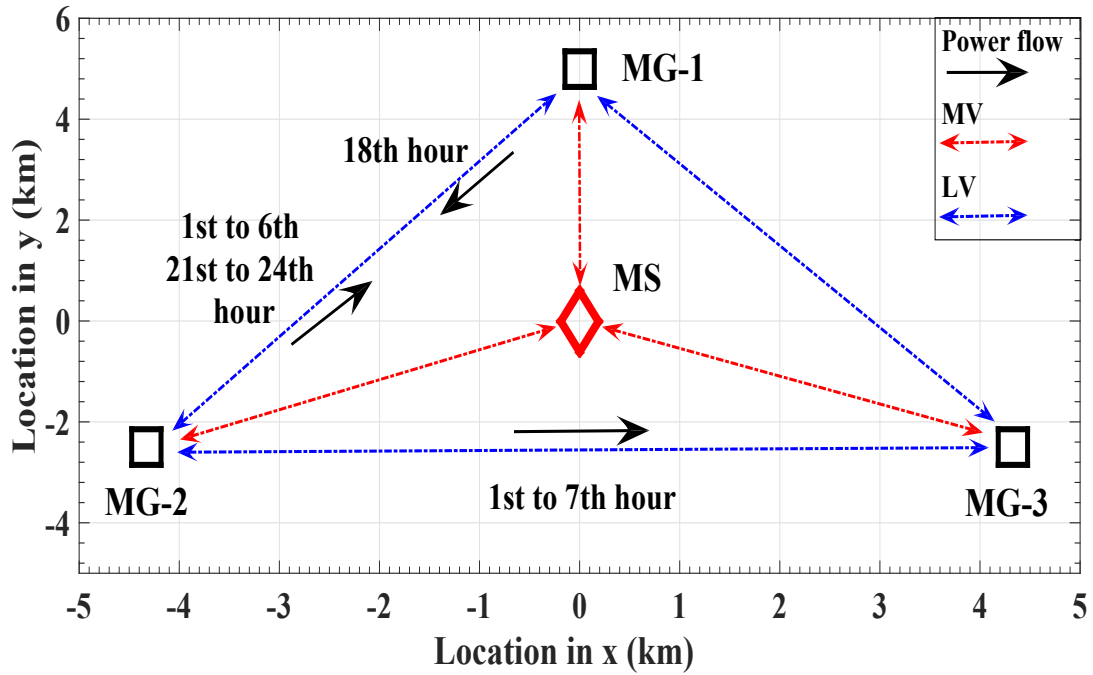


Figure 4.9: Four states of cooperation among the MGs and MS in a day, where MV = medium voltage 33 kV line and LV = low voltage 11 kV line, other simulation parameters following Table 4.1 and Figure 4.8.

is discussed in terms of power loss, coalition size and computational complexity. The proposed CAF methods outperform the non-cooperative model in terms of power loss reduction by 27%, whereas the merge-and-split outperforms the non-cooperative model by 33% for a network of 20 MGs. Although CAF is only 6% worse than the merge-and-split in terms of power loss reduction, it is 18000 times faster than the merge-and-split in terms of computational complexity. For a larger network, this trade-off becomes significant due to the simplicity and tractability for the proposed CAF. The performance of the proposed CAF algorithms is further analysed based on real-world data in a case study, where the average monetary saving per MG is 49.5% when compared to the non-cooperative model.

In the next chapter, we study a more specific problem that a MG-like charging station needs to decide how to schedule the arriving EVs optimally under the uncertain on-site solar energy.

Chapter 5

EVs Charging Using Renewable Energy

In this chapter, an EV charging station is specifically modelled as an MG that consists of controllable load, i.e., EVs, on-site solar panels and battery storage. The aim is to match as many as EV charging requirements with the uncertain solar energy generation so that the utility of the charging station is improved. This is analogous to that of pairing MGs in Chapter 3 and Chapter 4 so as to minimize power losses. Since the station usually has a limited charging capacity due to its physical constraints, it cannot accommodate all the arriving EVs. Thus, a decision has to be made by the charging station whether a new arriving car can be admitted and then be scheduled for charging. This not only depends on the charging station's physical constraints but also depends on how certain the charging station is towards its energy supply. In this chapter, a more specific problem that a MG-like charging station needs to decide how to optimally schedule the arriving EVs under uncertain renewable energy is studied. We propose a stochastic solar generation model, a performance index to measure the charging stations utility and design a two-stage scheduling mechanism to solve this utility maximization problem.

5.1 Introduction

EV technology has attracted a growing interest from the public in recent years. It is expected to have more electric cars on the road, according to a draft report [35] by the UK government that Britain is to ban all new petrol and diesel cars from 2040. EVs, as an alternative to the traditional internal combustion engine vehicles, are widely perceived as a green solution to improve energy efficiency and reduce carbon emissions [8]. Typically, EVs have high energy requirements with high charging rates, hence their rapid growth under the notion of a smarter grid can place a considerable amount of stress on the existing power grid without effective scheduling mechanisms. On the other hand, with appropriate scheduling, EVs that work as mobile storage devices have shown useful properties in terms of load balancing through charging and discharging their batteries.

There are some existing works investigating solutions to EV charging scheduling that can help to balance the load and avoid overload on the main power grid, such as in [123–126]. These works mainly consider the case that the energy for charging EVs are drawn from the main power grid and focus on a deterministic setting that the scheduling problem can be solved using Mixed Integer Linear Programming (MILP) or various congestion management approaches [127]. However, if the charging energy for an EV is entirely drawn from coal-fired power plants, the CO₂ produced is generally more than for an alternative fuel-driven vehicle [11]. The environmental benefits of introducing EV in the first place will not be appealing. It might be of interest to consider the integration of renewable energy in coordination with EV charging scheduling.

Renewable energy generation normally varies with time and is difficult to predict precisely within a certain period. This brings challenge and difficulty in the integration of renewable energy for charging EVs. Suppose that EVs are charged at a MG-like charging station that is equipped with on-site solar panels as well as local energy storage. It is important to estimate the available capacity at the station, since this will affect the quality of the charging service. Although integrating renewable energy for EVs charging has been researched from several aspects, most of these work has failed to address the necessity of an effective admission control prior to EVs' arrival where both the charging station's capacity and EVs' charging requirements are evaluated. Hence the work proposed in this chapter aims to fill the gap in using renewable energy effectively to charge EVs.

In this chapter, a commercial charging station powered by on-site solar panels and a local energy storage unit that can provide a charging service in the daytime is considered. By adopting the proposed scheduling mechanism, the charging station can achieve a higher revenue than buying the energy from the main power grid with more flexibility. Specifically, a stochastic solar energy generation model is proposed by introducing a multiplier k for the solar energy prediction that accounts for the effect of prediction error. The prediction error can be seen as the difference between an observed true value and its forecast based on other observations such as historical data. Then, a composite power metric index, called the Figure of Merit (FoM), is developed to measure the charging station's performance by taking account of EV users' charging requirements. A penalty factor is also taken account to measure the trade-off between turning away new arrivals and missing their charging deadlines if admitted. The problem is formulated to maximize the FoM by deciding which arriving EVs to admit based on the uncertain solar

energy supply and individual EV user's charging requirements. Since the objective function of the formulated optimization problem is non-linear and consists of parameters that will only be known precisely in the future, it is difficult to solve using traditional optimization algorithms. Thus, a priority-based two-stage admission and scheduling mechanism is proposed to find the optimal value of parameter k from the solar energy model that maximizes the charging station's FoM .

Based on our work previously presented in [15], the parameter k is further optimized over the time domain. The impact of introducing a local energy storage unit on the charging station's FoM is also investigated. The main contributions of this chapter can be summarized as follows.

- A multiplier k is introduced to account for the effect of the prediction error of solar energy generation.
- A power metric, the Figure of Merit (FoM), is developed to measure the charging station's performance.
- A priority-based two-stage admission control and scheduling mechanism is proposed to solve the FoM maximization problem.
- Further, methods to optimize k as a function of time of day, i.e. as the function $k(t)$, is discussed.
- The impact of integrating a local energy storage unit is evaluated in terms of storage capacity and starting state.

The remainder of this chapter is organized as follows. Section 5.2 reviews the recent literature in charging EVs. Section 5.3 presents the system description and the mathematical models for EVs arrival, solar energy generation and the charging station's FoM , followed by the formulation of the optimization problem. In Section 5.4, a two-stage framework is proposed for the charging station to achieve an optimal FoM with on-site solar energy and storage unit. Section 5.5 illustrates the numerical evaluations of the proposed mechanism. Finally, the summary of key findings of this chapter is given in Section 5.6.

5.2 Literature Review

In this section, recent works on EV charging scheduling is reviewed for three aspects: charging location, energy sources and discharging, that are also related to the work proposed in this chapter.

5.2.1 Charging Location

In recent years, there are a growing number of research on EVs charging scheduling. EVs can receive charging service at various locations, such as at home (usually during night time from evening to the next morning) or at public charging stations (usually during day time from morning to the evening). There are also some research about navigating EVs to an optimal location for the charging service.

En-route. Since the limited capacity of EV's battery, en-route charging stations will allow EV drivers to extend their range. However, the charging outlet and EV's battery both have a rating limit, a full charge usually takes a long time. In addition, if a large number of on-the-move EVs are intending to charge their batteries at the same charging station, it will cause the station to be overloaded,. This will also affect EV drivers' travel plans, due to the long waiting time. To address this problem, the work in [128] proposed a charging station selection scheme to minimize EV drivers' travel duration. The proposed approach considered the anticipated charging reservations such as arrival time, the expected charging time, parking durations, as well as a dynamic reservation updating system to tackle the uncertainty of EVs' mobility due to traffic jams on the road. Further, the work in [129] established an efficient publish and subscribe based communication framework to enable the selection of the charging stations for on-the-move EVs. The proposed communication framework not only shows a low communication cost but can also reduce EVs' waiting time and increase the number of EV arrivals. A novel navigation system proposed in [130] took account of EV drivers' intentions on the charging station selection. By using these intentions, the system can accurately predict congestions at charging stations and suggest the most efficient route for EV drivers.

On-site. After the successful selection of an optimal charging location, such as a public charging station or at EV drivers' garage, an efficient scheduling mechanism is also essential to meet individual EV's requirement, to achieve a maximal revenue for the charging station as well as to coordinate with other residential demand to reduce the impact on the distribution network.

Uncontrolled and random EV charging can cause increased power loss, voltage fluctuation and overload to the distribution network. References [69, 114, 126, 131–135] have proposed solutions to deal with multiple domestic EV charging activities in distribution systems. A coordinated charging scheme is proposed in [131] to minimize the power loss and to maximize the power factor of the main power grid. Both quadratic and dynamic techniques are used to solve the stochastic programming problem for household loads forecasting. A real-time load management control scheme is developed in [132] to support the coordination of EV charging in a low voltage residential network. By incorporating dynamic market energy prices and EV drivers' preferred time zones, the generation cost can be reduced. The work in [135] proposed a cooperative protocol for EVs to facilitate coordinated handover at the charging station who is blocked and occupied by fully charged EVs and is not able to serve other vehicles. The authors have shown that coordinated handover can improve the charging station's utilization and provide sufficient resources for EV drivers.

Scheduling management at a charging station is also studied, such as work in [9, 10, 39, 123–125, 136–140]. A battery replacement strategy is proposed in [39] to increase the efficiency of chargers and minimize EV drivers' waiting time at charging stations. By integrating renewable energy and energy storage devices, a multi-stage stochastic optimization model is formulated to minimize the power consumption cost. The work in [139] targets the day-time charging scenario for EVs at commercial building parking-lots. A two-stage approximate dynamic programming framework is proposed to determine the optimal charging strategies by using both short-term and long-term forecast for the electricity price. The work in [140] proposed a two-stage optimal economic operation framework at a MG-like EV parking lot with on-site solar panels and energy storage. Based on the day-ahead electricity price, a stochastic approach is presented to estimate the uncertainty of the solar energy generation; then a real-time operation is conducted based on a model-predictive-control based strategy for the EV charging.

However, there is still a lack of attention on how to exploit the on-site renewable energy at one charging station that considers both the station and EV drivers' utility. In this work, we specifically model the charging station as an MG that consists of a controllable EV charging load, on-site solar panels and energy storage units. The aim is to match as many EV charging requirements as possible with the available solar energy, as well as to optimize both the charging station's utility and EV drivers' satisfaction level.

5.2.2 Energy Sources

Widespread usage of EVs will cause a considerable amount of energy demand to the power grid if the charging energy is entirely drawn from that source. In order to cope with this issue, there are some works focusing on the integration of renewable energy for EV charging.

Renewable Energy Integration. Although EV charging scheduling involving renewable energy is now being researched such as the work in [9, 10, 70, 133, 134, 138, 141], they fail to address the necessity of introducing an effective admission control scheme prior to the real-time scheduling. Rather, these works assume the charging station has the capacity to charge all arrivals. Although prior work in [61] has addressed the admission issue prior to the charging scheduling, it neglected the case of how to use renewable energy sources when only a forecast of the expected energy is available.

On the other side, many papers have focused on the benefits to either the EVs or the charging station, but not both simultaneously. References [123, 124, 130] have mainly focused on EV users' perspectives. In [123], the EV users are incentivized to report their charging requirements to the charging station truthfully, thus the quality of charging service is guaranteed. Other work in [39, 133, 136, 142] has mainly focused on optimizing the system's cost or utility, but they did not pay much attention to the EV users' satisfaction level. Some papers have considered a deterministic energy availability setting in a charging scenario such as in [9, 133, 143], but their approaches cannot cope well with the uncertainty of renewable energy prediction.

5.2.3 Discharging

On the other hand, an EV who has a higher battery state might have the incentive to sell its excess energy to the power grid during peak time and charge its battery during the off-peak time. By leveraging the charging and discharging of the battery, EVs that switch between energy buyers and sellers will not only be economically profitable but will also contribute to balance the overload on the power grid.

Vehicle to Grid Service. When EVs are plugged into the power grid, they can be seen as a large distributed battery network and are used to regulate the supply and the demand in the power grid. Since the mobility of EVs is very high in reality, their behaviours are dynamic and difficult to predict. In addition, an individual EV cannot provide the minimum power capacity that the power grid requires. It is of interest to consider the effects of groups of EVs in the

power grid. By forming coalitions of EVs [71], the aggregate energy from a group of EVs can provide sufficient required capacity to the grid. On the other hand, pricing signals can be used to schedule, guide and coordinate EV charging [137, 140, 144]. A pricing model as an incentive can encourage more EVs to participate to form coalitions from selling their energy to the grid. There should also be a coalition server in each coalition working as the aggregator [145]. The aggregator is then to manage local EVs with the grid operators through adequate communications.

Another question might be how to divide the fairness among a coalition of EVs since the EV model from [145] requires an aggregator to process the communication signals, sign a contract with the grid operator, and pass information (e.g. real-time prices) to the individual EV. Different structures of a coalition might lead to a distinct overall payoff as well as the individual payoff of each EV. It is also of interest to extend the vehicle-to-grid service to vehicle-to-vehicle and vehicle-to-roadside interactions [24]. In the management of EVs charging and discharging, Particle Swarm Optimization (PSO) [136] is used to intelligently allocate energy to a large fleet of EVs. The proposed algorithm is robust to uncertainty and is capable of making decisions in real-time with limited communication bandwidth to work seamlessly with existing facilities.

In this chapter, we aim to fill the gap in using renewable energy effectively to charge EVs by introducing a realistic stochastic solar generation model and an effective admission control mechanism, and consider both the charging station's utility and EV users' satisfaction level.

5.3 System Model

A commercial-level charging station is considered, such as a shopping mall, that is equipped with on-site solar panels and energy storage units. The charging station is supposed to have M charging points installed and provide the charging service in the daytime, as shown in Figure 5.1.

5.3.1 EV Arrival Model

Suppose that EVs arrive at the charging station following a Poisson distribution with an average arrival rate λ . The average arrival rate λ is normally assumed as a constant variable in many papers, such as [61, 141, 146]. However, this may lead to inaccurate models in practice since

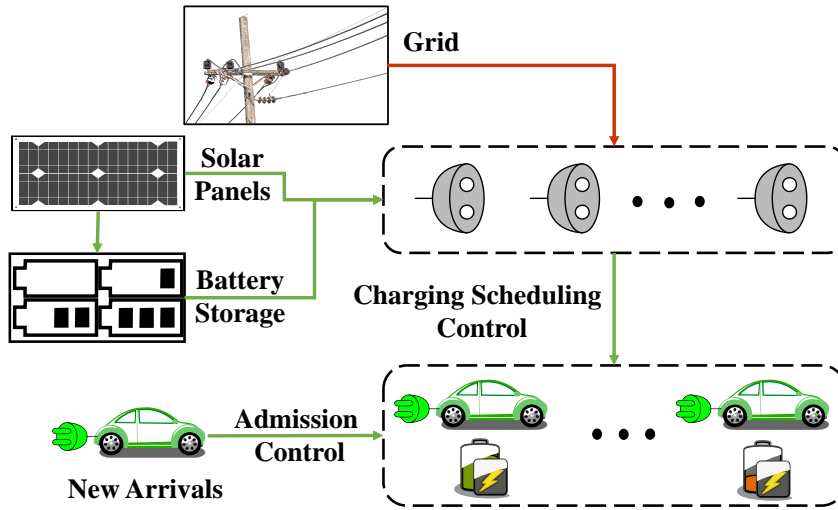


Figure 5.1: System model.

the arrival of vehicles is semi-periodic in nature, i.e. λ is higher during peak time than off-peak time. Hence, the arrival rate can be also modelled as a time-dependent variable $\lambda(t)$ for a potential higher accuracy, such as work in [68, 147]. For simplicity, we assume a stationary average arrival rate λ of EVs in this work. The expected number of EV arrivals per timeslot, N_{ar} , can be denoted as $N_{ar} \sim \text{Poiss}(\lambda)$. A comparison of the Poisson probability density function (PDF) with parameter $\lambda = 5, 10, 12$ is shown in Figure 5.2.

EV i arrives with a charging task:

$$(E_i, t_i^a, t_i^d, a_i^m), \quad (5.1)$$

where E_i is the charging energy requirement [kWh], t_i^a is the arrival time, a_i^m is the maximum charging rate [kW], the deadline urgency t_i^d is being the maximum number of timeslots within which EV i requires to be charged. Hence, the active charging interval for EV i is $[t_i^a, t_i^a + t_i^d]$. The energy level of EV i 's battery can be increased by $\Delta_i(t) = \tau a_i(t)$ within each timeslot, where τ is the duration of one timeslot which is assumed to be 10 minutes in this chapter. The variable $a_i(t)$ is the actual charging rate with $a_i(t) \in [0, a_i^m], \forall t$ and can be assumed as a constant for each timeslot. The remaining energy requirement for EV i at t can be written as:

$$R_i(t) = E_i - \sum_{x=1}^t \Delta_i(x). \quad (5.2)$$

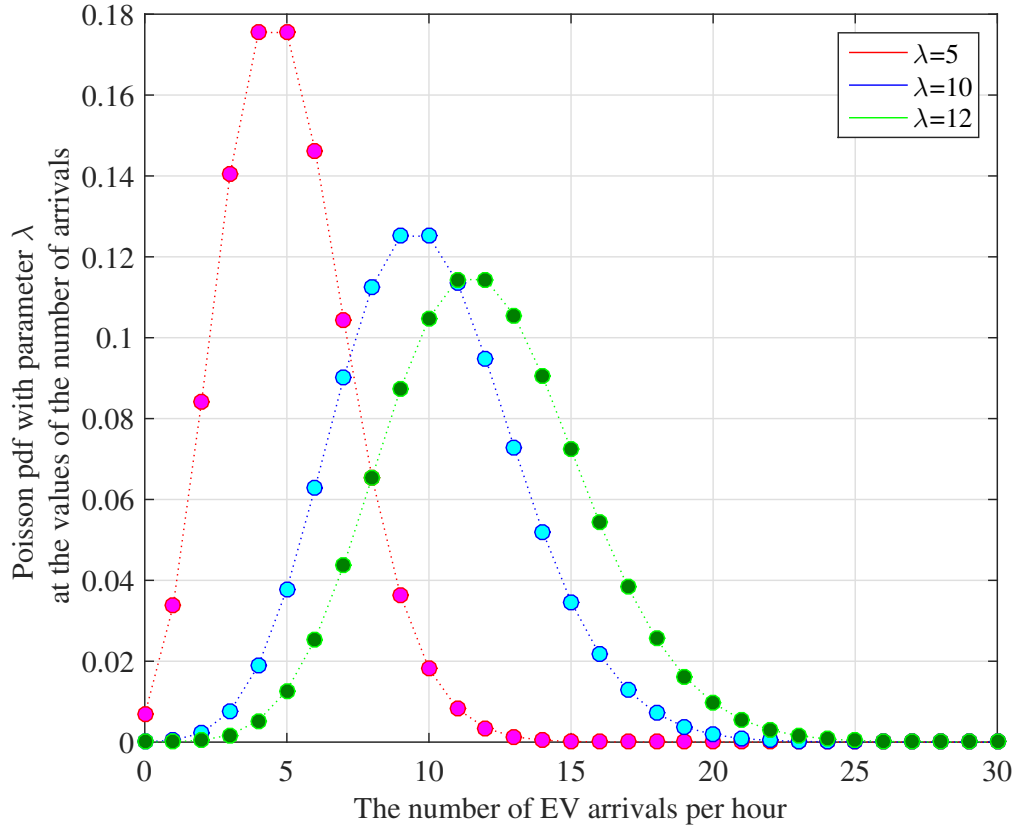


Figure 5.2: A comparison of the Poisson probability density function (PDF) with parameter $\lambda = 5, 10, 12$.

EVs can be put in different priority orders based on their battery states and the remaining charging times. A priority factor is further defined to capture this relation as:

$$\omega_i(t) = \frac{t_i^a + t_i^d - t}{R_i(t)}. \quad (5.3)$$

EV i is more patient if it has a longer deadline with a lower energy requirement. The lower $\omega_i(t)$ is, the more urgent it is for EV i to be charged, so a higher charging rate $a_i(t)$ is preferred. This relation can be further captured to reflect to EV users' satisfaction level as:

$$SAT_i(t) \sim \frac{1}{\omega_i(t)(a_i^m - a_i(t))^2}. \quad (5.4)$$

For an EV to have a higher satisfaction level, a higher $SAT_i(t)$ is preferred. This principle is also accounted for in the design of the admission and scheduling mechanism, that EVs are

admitted by the order of their priority factor $\omega_i(t)$ and are allocated highest possible charging rates $a_i(t)$ in turn. In addition, the squared term $(a_i^m - a_i(t))^2$ would be able to reflect that a lower rate $a_i(t)$ is penalized more than that the absolute term $|a_i^m - a_i(t)|$ does and a higher rate $a_i(t)$ is favoured more than that the absolute term does. Thus, the satisfaction level is better justified than using the absolute term. If we intend to quantify the satisfaction level $SAT_i(t)$ in the future work, a squared objective function is also differentiable and has many other nicer mathematical properties.

5.3.2 Energy Supply Model

The MG-like charging station considered in this chapter is shown in Figure 5.1. The energy used to charge EVs can be bought from the grid with a price p_g , and is assumed to be sufficient to meet all charging requirements unless all charging spots are used, as in work [61]. Alternatively, the energy can be generated from the on-site solar panels with a lower maintenance fee p_s and stored in the storage unit and used for later. At each considered timeslot, the storage can be charged from the solar panels or discharged to serve the EVs. We also assume that the initial installation costs of solar panels and energy storage are reimbursed, and are excluded from the scope of this work.

Solar Generation. Energy generated from the deployed solar panels is time-varying and limited, denoted as $S(t)$. In general, the cost of the solar panels usually includes the product installation fee for a lifetime of 20 years, the operation and maintenance cost, which can be accounted for 9.81 cents/100 m^2 PV for 30 minutes. The size of PV panels can vary from 50 to 3000 m^2 with a general assumption of 1kW power input with 20% efficiency per unit solar panel, more details can be found in [148]. Three examples of solar generation sample traces with low, medium and high generation profiles are plotted in Figure 5.3.

Based on historical data and weather forecast, $S(t)$ can be predicted, though the prediction is not always accurate. An effective scheduling mechanism should be able to adapt to this prediction uncertainty and be able to estimate the total capacity of the solar energy generation within a period, since the actual energy values cannot be predicted precisely. The prediction uncertainty can be assumed as independent and identically distributed Gaussian samples with standard deviation σ and mean zero, denoted as $e(t) \sim \mathcal{N}(0, \sigma)$, since the correlations can be removed by applying various techniques from time series analysis. Thus, the actual solar

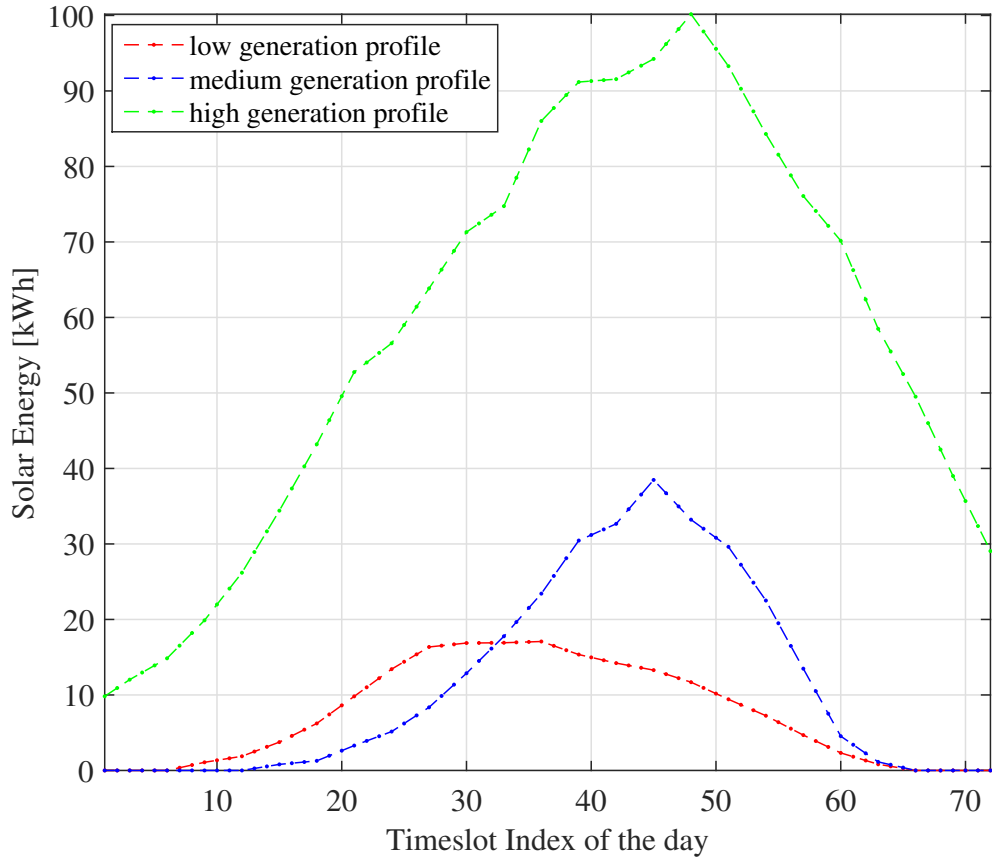


Figure 5.3: Examples of actual solar generation sample traces with low, medium and high generation profiles, extracted from [4].

energy generation $S(t)$ can be represented as

$$S(t) = \hat{S}(t) + e(t), \quad (5.5)$$

where the prediction profile of the solar energy generation $\hat{S}(t)$ and its standard deviation σ are extracted and estimated from the national grid database [4].

A prediction interval gives a range within which we expect the future observations to lie. The system should not be too optimistic as that will lead to over admission of EVs and the system will miss many charging deadlines. Conversely, it should not be pessimistic which will lead to charging less cars than the system will allow and losing revenue. Hence a multiplier k is introduced to capture the effect of prediction error $e(t)$. The future solar energy observation

$S(t)$ in eq. (5.5) is expected to lie within a prediction interval:

$$[\hat{S}(t) - k\sigma, \hat{S}(t) + k\sigma], \quad k \in \mathbb{R}, \quad (5.6)$$

with a specified probability $P_r(k)$ that depends on k . For instance,

1. if $k = 0$, $S(t) = \hat{S}(t)$;
2. if $k = 1$, $S(t)$ has a probability of 0.68 (according to the 3σ rule, where the value of 0.68 is connected with σ deviation in a Gaussian distribution) to lie within $[\hat{S}(t) - \hat{\sigma}, \hat{S}(t) + \hat{\sigma}]$.

Let us denote the lower bound of the prediction interval as:

$$S_{lb}(t, k) = \hat{S}(t) + k\sigma, \quad k \in \mathbb{R}, \quad (5.7)$$

where $S(t)$ has a specific probability to lie above $S_{lb}(t, k)$. For instance,

1. if $k = -1$, $S(t) > \hat{S}(t) - \sigma$ with probability 0.84 ($= 1 - \frac{1-0.68}{2}$);
2. if $k = 1$, $S(t) > \hat{S}(t) + \sigma$ with probability 0.16 ($= \frac{1-0.68}{2}$).

Storage. A local energy storage unit can be introduced to hedge against the uncertainty of the random variables such as the solar energy generation and EVs' charging requirements. By providing sufficient flexibility, storage can help increase the station's *FoM*. During a certain timeslot t , the excess solar energy after charging EVs can be stored for later use. However, introducing energy storage will also introduce an extra cost to the charging station. An operational cost p_b of the storage is yielded per unit energy charged or discharged, that is every time when the energy state of the storage $B(t)$ changes. The cost p_b can be assumed to be proportional to the storage capacity B . In this work, we aim to exploit the appropriate capacity of the storage to fulfil this task as an energy buffer. Thus, we assume the storage is controlled by the charging station which decides when to charge or discharge the storage unit in order to maximize the *FoM*.

Therefore, we aim to find the optimal value of k to make the future solar generation observation neither too conservative (if k is approaching a negative value) nor too optimistic (if k is approaching a positive value), so that the charging station can achieve an optimal performance.

Thus, a power metric is needed to better measure its performance. To this end, a composite index is developed in Section 5.3.3 to measure the charging station's performance.

5.3.3 The Figure of Merit (FoM)

The revenue of the charging station is related to providing charging service to the admitted EVs. If an admitted EV is not charged as promised, the charging station will pay a penalty. This fits into a scenario where a trade-off exists between the admission rate and the successful service rate. Hence only evaluating the admission rate is not a fair measure of the system performance. A composite performance index is further defined to capture this trade-off to better measure the charging station's utility, called the Figure of Merit (FoM):

$$FoM = U \cdot \frac{N_{ad} - \gamma N_{ms}}{N_{ar}}. \quad (5.8)$$

The terms in this equation are defined as follows:

1) U : is the utilization of the energy supply and defined as the ratio of energy usage of the day. Depends on the capacity of the energy storage, there will possibly be some solar energy wasted and some left in the storage unit. Without loss of generality, U can be written as:

$$U(k) = 1 - \frac{\sum_{t=1}^T S_r(t, k) + E_b(k)}{\sum_{t=1}^T S(t)}, \quad (5.9)$$

where S_r is the cumulative excess solar energy, E_b is the amount of energy left in the storage at the end of the day at 6pm, S_{tot} is the total solar energy generation.

2) γ : is the penalty factor and can be defined as:

$$\gamma = \frac{\gamma_{ms}}{\gamma_{pd}}, \quad (5.10)$$

where γ_{ms} represents the penalty weight placed on missing charging deadlines and γ_{pd} represents the penalty weight placed on rejecting cars. Considering turning away arriving EVs will affect the charging station's reputation in the long run but it is not as significant as failing to deliver the promised charging service by the desired deadline, thus it is reasonable to assume that $\gamma > 1$. The penalty factor γ can be seen as a normalized coefficient to reflect the effect of how much more severe it is to miss charging deadlines than to decline cars on admission. For instance, setting $\gamma = 3$ means that the penalty of missing charging deadlines is 3 times larger

than rejecting new arrivals.

3) N_{ad}, N_{ms}, N_{ar} : represent the number of admitted EVs, the number of EVs who miss their charging deadlines, and the number of new arrivals, respectively.

Depending on the value of parameter k from the solar energy prediction model, the values of S_r and N_{ad} vary in the admission process. Hence, S_r and N_{ad} are not only functions of time t but also functions of parameter k . Further, eq. (5.8) can be written as

$$\begin{aligned} FoM(k) &= U(k) \cdot \left(1 - \gamma \frac{N_{ms}}{N_{ad}(k)}\right) \cdot \frac{N_{ad}(k)}{N_{ar}} \\ &= U(k) \cdot (1 - \gamma R_s(k)) \cdot (1 - P_d(k)), \end{aligned} \quad (5.11)$$

where R_s is the ratio of missing charging deadlines and P_d is the probability of declining cars upon arrival.

The proposed composite performance index FoM is able to reflect the benefit for both the charging station's utility and EVs' satisfaction. By the definition of FoM in Eq. (5.8), some factors are considered to reflect the station's performance, such as the utilization of the energy supply U , the penalty factor γ , the number of EVs being admitted N_{ad} and the number of EVs missing their charging deadlines N_{ms} . However, the values of U , N_{ad} and N_{ms} are determined by taking account of EV owners' satisfaction level defined in Eq. (5.4). The objective for EV i is to maximize its satisfaction subject to its priority factor $\omega_i(t)$ and its allocated charging rate $a_i(t)$.

5.3.4 Optimization Problem Formulation

In the proposed system, if solar generation and EVs' charging tasks are known, the optimization problem can be solved using mixed integer programming. However, the charging station does not know precisely how much solar energy will be generated from the solar panels in the future, and needs to make decisions under uncertainty. The objective of the charging station is to maximize its Figure of Merit (FoM) by finding the optimal value of parameter k . That is to maximize the utilization of the energy supply and its admission rate but to minimize the rate of missing charging deadlines as in eq. (5.11). The value of FoM can be further calculated by determining P_d based on the estimated solar generation at the admission stage (Section 5.4.1), R_s based on the real-time solar generation and S_r, E_b based on the allocated charging rate $a_i(t)$

at the scheduling stage (Section 5.4.2). Therefore, the optimization problem can be formulated as follows.

$$\begin{aligned}
 & \underset{k}{\text{maximize}} && FoM(t, k) \\
 & \text{subject to} && a_i(t) \in [0, a_i^m] && \triangleright \text{Charging rate constraint} \\
 & && \sum_{i \in \mathcal{N}_c(t, k)} a_i(t) \leq S(t) + B(t) && \triangleright \text{Demand-supply constraint} \\
 & && |\mathcal{N}_c(t, k)| \leq M && \triangleright \text{Number of chargers constraint} \\
 & && \mathcal{N}_c(t, k) \subseteq \mathcal{N}(t, k) && \triangleright \text{Charging set is a subset of admission set}
 \end{aligned} \tag{5.12}$$

where $\mathcal{N}_c(t, k)$ is the charging set, $|\cdot|$ represents the number of elements in a set, $\mathcal{N}(t, k)$ is the admission set. The proposed model has an inherent two-stage decision process, since the objective function FoM is determined by decisions made in both stages. In the first admission stage (Section 5.4.1), we use a stochastic model to represent PV generation to decide the number of admissions N_{ad} . In the second scheduling stage (Section 5.4.2), we use the currently available data to decide the number of missing charging deadlines N_{ms} and the utilization of the energy supply U . Thus, this is a coupled un-separated stochastic optimization problem. Since the expression of the objective function FoM is non-differentiable, traditional optimization methods such as Lagrange and Dual decomposition are not able to solve such a problem. Furthermore, the optimal decision made at a certain timeslot requires the full knowledge of future information, such as future solar energy generation, which is hard to acquire in practice. A Markov Decision Process (MDP) approach could yield better performance. However, we have not evaluated this approach in the paper as the number of states required to adequately capture the dynamics of the system (such as the number of cars charging, battery states, charging deadlines, etc.) would be very large. This would make the MDP very complex to process. Our objective is to use a single parameter k to adjust the stochastic estimate of solar energy to maximize the FoM . Therefore, we design a heuristic two-stage mechanism to tackle this complicated problem based on current available information to achieve the highest utility FoM at each timeslot, as discussed in the next section.

5.4 Two-stage Admission and Scheduling Mechanism

In order to solve the optimization problem in eq. (5.12), a priority-based two-stage admission and scheduling mechanism is proposed and described in this section.

5.4.1 Admission Control Algorithm (ACA)

Suppose that EV i arrives at the station with a charging task $(E_i, t_i^a, t_i^d, a_i^m)$ at time t . For the charging station, the available solar supply at t is known while the future solar generation is only available as an estimate $\hat{S}(t)$. Along with the energy state $B(t)$ in the storage at t , the admission control is to decide which new arrivals to admit, given that there are $\mathcal{N}_{ar}(t)$ new arrivals during t , where $i \in \mathcal{N}_{ar}(t)$. Among those, only EVs in set $\mathcal{N}_{ad}(t, k)$ are admitted, while the rest are declined and might be diverted to nearby available charging stations.

An admission window is first defined as in Definition 1.

Definition 1. An Admission Window is the maximum remaining time before the deadlines of both the existing and the arriving EVs at t , within which the admission decision to EV $i \in \mathcal{N}_{ar}$ is made. It can be written as

$$A_w(t) = \max\{t_i^a + t_i^d - t, t_j^d\}, i \in \mathcal{N}_{ex}(t, k), j \in \mathcal{N}_{ar}(t), \quad (5.13)$$

where $\mathcal{N}_{ex}(t, k)$ is the set of previously admitted EVs that are still in the charging station waiting for service at t .

Definition 2. The Admission Rule: A new arrival, $i \in \mathcal{N}_{ar}$, is virtually being scheduled from the current time t to the admission window $A_w(t)$. If its virtual finishing time t_i^f is earlier than its deadline $(t_i^a + t_i^d)$, then EV i is admitted.

Along with $\mathcal{N}_{ex}(t, k)$, the set of cars in the system (being the updated admission set) can be expressed as $\mathcal{N}(t, k) = \{\mathcal{N}_{ex}(t, k), \mathcal{N}_{ad}(t, k)\}$, where $\mathcal{N}_{ad}(t, k) \subseteq \mathcal{N}_{ar}(t)$. The procedure of the admission control algorithm is further shown in Algorithm 2. Every time Algorithm 2 is executed, the admission set $\mathcal{N}(t, k)$ is updated.

As discussed in Section 5.3.2, we know that if the charging station is too conservative towards the prediction of solar generation, i.e., the lower bound $S_{lb}(t, k)$ is lower than the actual solar generation $S(t)$, this is the case that parameter k has a negative value. The admission control

Algorithm 2 Admission Control Algorithm (ACA).

```

1: Input:  $(E_i, t_i^a, t_i^d, a_i^m), t, \mathcal{N}_{ex}(t, k), B(t), S_{lb}$ .
2: Output:  $\mathcal{N}(t, k)$ .
3: procedure ACA( $(E_i, t_i^a, t_i^d, a_i^m), t, \mathcal{N}_{ex}, B(t), S_{lb}$ )
4:   Define  $j \in \{\{i, \forall i \in \mathcal{N}_{ar}(t)\}, \mathcal{N}_{ex}(t, k)\}$ .
5:   Compute  $A_w(t)$  from eq. (5.13).
6:   for  $T = t$  to  $A_w(t)$  do
7:     Compute priority  $\omega_j(T)$  from eq. (5.3).
8:     Rank  $\omega_j(T)$  in ascending order as  $\omega_j^a(T)$ .
9:      $\omega_j^a(T) \leftarrow$  top  $M$  elements from  $\omega_j^a(T)$ .
10:    for  $j$  in the order of  $\omega_j^a(T)$  do
11:       $\Delta_j^1(T) = \min\{\tau a_j^m, R_j(T), S_{lb}(T, k)\}$ .
12:      ▷ Update  $R_j(T)$  using eq. (5.2).
13:       $\Delta_j^2(T) = \min\{\tau a_j^m - \Delta_j^1(T), R_j(T), B(t)\}$ .
14:      ▷ Update  $R_j(T)$  using eq. (5.2).
15:       $\Delta_j(T) = \Delta_j^1(T) + \Delta_j^2(T)$ .
16:      Virtually allocate  $\Delta_j(T)$  to  $j$ .
17:      if  $R_j(T) = 0$  then
18:         $t_j^f = T$ ;
19:      Admit  $i$  into set  $\mathcal{N}_{ad}(t, k)$  if  $t_i^f \leq t_i^a + t_i^d$ .
20: Output  $\rightarrow \mathcal{N}(t, k) = \{\mathcal{N}_{ex}(t, k), \mathcal{N}_{ad}(t, k)\}$ .
    
```

would admit fewer EVs than its actual capacity, hence the charging station will lose revenue. If the charging station is too optimistic in its prediction, the admission control would admit more EVs than its actual capacity, hence some admitted cars will not be able to meet their charging deadlines and the charging station will pay a penalty to those cars' owners. In order to compute the Figure of Merit (*FoM*, defined in Section 5.3.3) of the charging station, $\mathcal{N}_c(t, k)$ (being the set of cars being charged at t)¹ needs to be further determined by using the Charging Scheduling Algorithm (CSA) as shown in the next section.

5.4.2 Charging Scheduling Algorithm (CSA)

In Section 5.4.1, all the admitted EVs, i.e., $i \in \mathcal{N}(t, k)$, should be scheduled for charging at this stage. According to the admitted EV's priority order $\omega_i(t)$, the available solar energy $S(t)$, the number of available chargers $m \leq M$, the charging rate limit $a_i(t) \leq a_i^m$ and the available energy in the local storage $B(t)$, the charging station needs to further decide which EVs from the admission set to charge for the current timeslot. This procedure is shown in Algorithm 3.

¹Among all members in set $\mathcal{N}(t, k)$, only EV i where $i \in \mathcal{N}_c(t, k)$ can be charged with $\mathcal{N}_c(t, k) \subseteq \mathcal{N}(t, k)$.

Algorithm 3 Charging Scheduling Algorithm (CSA).

```

1: Input:  $\mathcal{N}(t, k), t, S(t), B(t)$ .
2: Output:  $\mathcal{N}_c(t, k), S_r, E_b$ .
3: procedure CSA( $\mathcal{N}(t, k), t, S(t), B(t)$ )
4:   Define  $i \in \mathcal{N}(t, k)$ .
5:   Compute priority  $\omega_i(t)$  from eq. (5.3).
6:   Rank  $\omega_i(t)$  in ascending order as  $\omega_i^a(t)$ .
7:    $\omega_i^a(t) \leftarrow$  top  $M$  elements from  $\omega_i^a(t)$ .
8:   for  $i$  in the order of  $\omega_i^a(t)$  do
9:      $\Delta_i^1(t) = \min\{\tau a_i^m, R_i(t), S(t)\}$ .
10:                                      $\triangleright$  Update  $R_i(t), S(t)$  using eq. (5.2).
11:      $\Delta_i^2(t) = \min\{\tau a_i^m - \Delta_i^1(t), R_i(t), B(t)\}$ .
12:                                      $\triangleright$  Update  $R_i(t), B(t)$  using eq. (5.2).
13:      $\Delta_i(t) = \Delta_i^1(t) + \Delta_i^2(t)$ .
14:     Allocate  $\Delta_i(t)$  to  $i$ .
15:      $B(t) = B(t) + \min\{B - B(t), S(t)\}$ .
16:                                      $\triangleright$  Update  $S(t)$ .
17:                                      $\triangleright$   $S_r \leftarrow S(t)$ .
18: Output  $\rightarrow \mathcal{N}_c(t, k), S_r$ , and  $S_{tot}$ .

```

The charging rate $a_i(t)$ is allocated as shown in lines 8-14 of Algorithm 3 based on the real-time solar generation and the energy in the storage. Then, the charging set $\mathcal{N}_c(t, k)$, the cumulative excess solar energy S_r and the total actual solar generation S are computed and determined accordingly from Algorithm 3.

In the next section, we use numerical evaluations to show how the proposed two-stage admission Control algorithm (ACA) and the charging scheduling algorithm (CSA) are implemented to solve the Figure of Merit (FoM) maximization problem formulated in eq. (5.12) under different energy supply scenarios.

5.5 Numerical Evaluations

A MG-like charging station using various energy sources to charge the arriving EVs is discussed. This section shows how the proposed two-stage admission and scheduling mechanism affects the charging station's Figure of Merit and the optimal value of parameter k . Since our main focus is to investigate the impact of the uncertain solar generation on the charging station's performance, we assume typical stochastic distributions for other variables. Specifically, EV arrivals are assumed to follow a Poisson distribution; EV charging requirements and their dead-

line urgencies are assumed to follow uniform distribution. By gradually increasing the system's complexity, several scenarios are evaluated numerically by using Monte Carlo simulations.

5.5.1 Energy from the Grid

In this section, the energy supply is assumed to draw from the power grid and is sufficient to meet all the charging requirements. A First in, First out (FIFO) scheme is implemented as the benchmark to the proposed priority-based admission (AD) scheme. The performance of AD and FIFO is compared in terms of rejection probability, successful service rate, delay times, and the number of EVs in the system, as shown in Figure 5.4. The simulation parameters follow Table 5.1 with EV's arrival rate λ from 0.5 to 4 per timeslot.

Parameter	Values
No. of chargers M	5
Charger's capacity	50 [kW]
Charging station's opening time	6am-6pm
Total timeslots in a day T	72
EV arrival rate λ	[0.5, 1, 1.5, 2]
EV battery capacity	$\sim U(25, 40)$ [kWh]
EV charging energy requirement E_i	$\sim U(8.3, 13.3)$ [kWh]
EV maximum charging rate a_i^m	$\sim U(30, 50)$ [kW]
EV deadline urgency t_i^d	$\sim U(1, 15)$ [timeslots]
Shorter and longer deadlines	$\sim U(1, 7), U(1, 30)$ [timeslots]
Penalty factor γ	[1, 3, 6]
Estimated standard deviation of solar prediction error $\hat{\sigma}$	13 [kWh]
Cost of buying energy from the grid p_g	15 [p/kWh]
Maintenance cost of solar panels p_s	5 [p/kWh]
Operational cost of the storage p_b	10 [p/kWh]

* $\sim U(\cdot, \cdot)$ represents a uniform distribution.

Table 5.1: Simulation parameters for Chapter 5

Further, the Figure of Merit (FoM) is calculated ² following eq. (5.8) when using AD and FIFO, respectively, based on the results from Figure 5.4 (a) and (b). If the penalty factor is set to be $\gamma = 3$, the charging station outperforms up to 13 times in terms of FoM under AD (where $FoM = 0.9416$) than FIFO (where $FoM = 0.0711$) when $\lambda = 2.5$. This result is in line with Figure 5.4 (c) and (d), where the delay times and the number of cars in the system increase significantly under the FIFO scheme when the arrival rate λ increases from 2.5. This

²Note that the utilization $U = 1$ in this case.

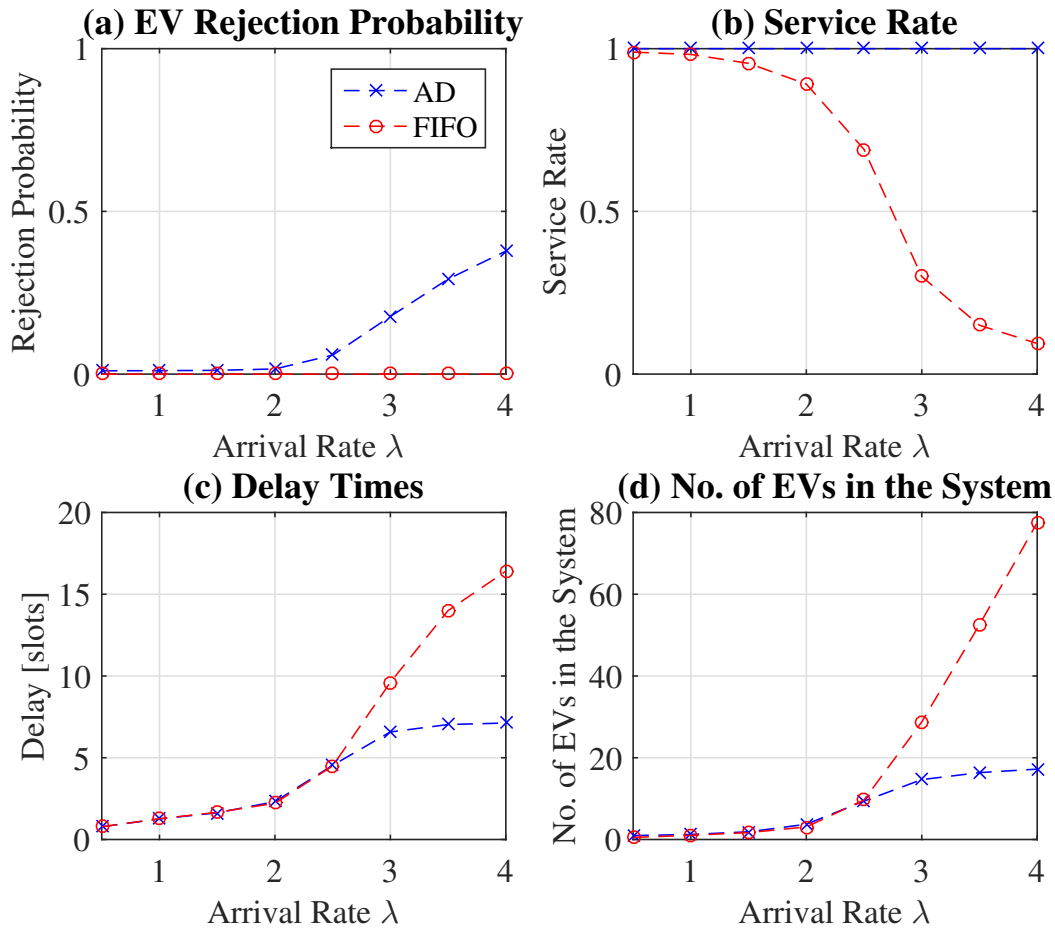


Figure 5.4: Performance comparison between Admission Control and FIFO in terms of (a) Rejection probability (b) Service rate (c) Average delay per EV per timeslot (d) Average number of EVs in the system per timeslot.

is because the charging station's capacity is limited due to the physical constraints (such as the total number of chargers, each charger's capacity and individual EV's maximum charging rate), even though the energy supply from the grid is sufficient. Thus, introducing an effective admission and scheduling scheme is important for the charging station to gain revenue.

In the next section, we increase the complexity of the system by replacing the energy supply from the power grid with the energy from the on-site solar panels.

5.5.2 Energy from the Solar Panels

This is the case where the charging station uses solar energy to charge EVs. Suppose that we know how much energy is generated precisely from the solar panels, that is the true value $S(t)$

equals the prediction $\hat{S}(t)$ in eq. (5.5). The solar energy prediction profile used is shown in Figure 5.5 (a). It can be observed in Figure 5.5 (b) that EVs' rejection probability is massively influenced by the availability of solar energy when compared to using the energy from the power grid.

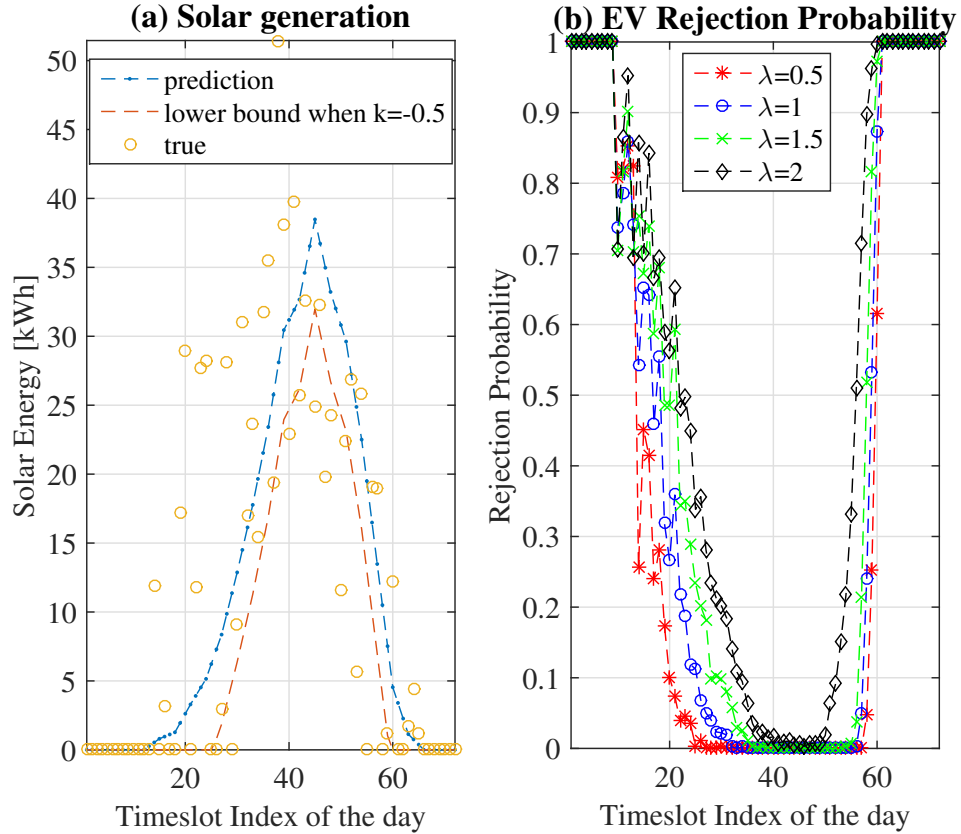


Figure 5.5: EVs rejection probability over various arrival rate λ in (b) when using solar energy in (a).

While in practice, the prediction is not always equal to the true value as discussed in Section 5.3.2. The prediction profile of the solar generation $\hat{S}(t)$ and the standard deviation of the prediction error σ are extracted and estimated from the national grid database [4]. If $k = -0.5$, the relation of the solar prediction profile, the true values and the defined lower bound of the prediction (eq. (5.5), (5.6), (5.7)) is shown in Figure 5.5 (a). Next, the formulated FoM maximization problem is solved by finding the best value of k .

1) Optimize k : Parameter k is first optimized as a constant value. The objective is to find the best choice of k that maximizes the value of FoM , subject to the energy constraints and the

solar prediction uncertainty. A Monte Carlo simulation for 500 runs is conducted following the parameters listed in Table 5.1.

The value of FoM is computed when EVs arriving from 0.5 to 2 per timeslot, and is shown in Figure 5.6. It can be observed that the optimal value of k reduces (meaning that the charging station is being more conservative towards the solar prediction) with a heavier penalty factor and a higher arrival rate. This can also be seen in Table 5.2, where four scenarios are simulated with $\lambda = 1, 1.5$ and $\gamma = 3, 6$ over 1000 different scenarios via Monte Carlo simulations. Among the average 72 arrivals (when $\lambda = 1$), the average number of cars being accepted decreases from 38 to 35 with γ increasing from 3 to 6; the results are similar when $\lambda = 1.5$. In addition, we notice that the average number of cars not meeting their charging deadlines decreases from 1 to 0.5 and from 1.6 to 1 when $\lambda = 1$ and $\lambda = 1.5$, respectively, when the penalty γ increases from 3 to 6. The optimal value of k under various arrival rate λ and penalty factor γ is further summarized in Table 5.3.

λ	γ	k^*	U	N_{ar}	N_{ad}	N_{ms}
1	3	-0.1	0.6	72	38	1
1	6	-0.3	0.6	72	35	0.5
1.5	3	-0.3	0.7	108	51	1.6
1.5	6	-0.4	0.7	108	48	1

* U : ratio of solar energy usage, N_{ar} : average number of arrivals, N_{ad} : average number of admitted EVs, N_{ms} : average number of EVs missing their deadlines.

Table 5.2: Numbers for admission and scheduling process

$\lambda \backslash \gamma$	1	3	6
1	0	-0.1	-0.3
1.5	0	-0.3	-0.4
2	-0.2	-0.5	-0.7

Table 5.3: Optimal value of k for solar only case.

Shorter and Longer Deadline Urgencies. The impact on the optimal value of k and FoM is further investigated if the arriving EVs have shorter (e.g., 7 timeslots being half of the baseline of 15 timeslots) and longer (e.g., 30 timeslots) deadline urgencies. Simulation results show the comparison in terms of FoM for $t_d = 7, 15, 30$ in Figure 5.7.

First, a normalized degree of variation of a vector \mathbf{a} is defined to better measure the changes in

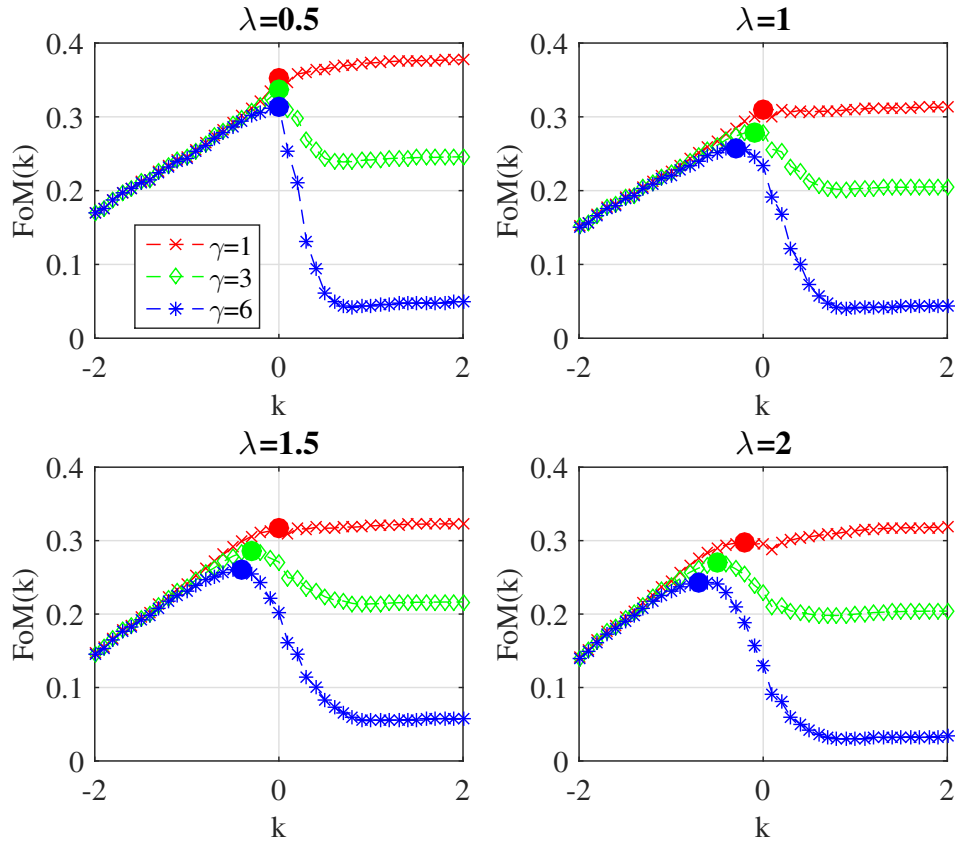


Figure 5.6: Rejection probability when using the energy from the solar panels.

values of k and FoM as:

$$D(a^*) = \frac{\Delta a^*}{\max(\mathbf{a}) - \min(\mathbf{a})}, \quad (5.14)$$

where a^* is the value of interest.

It is shown that the optimal value of k is reduced (being more conservative) by 2.5% under the shorter deadline scenario; and is increased (being less conservative) by 2.5% under the longer deadline scenario. However, when compared to the corresponding changes in FoM^* (being 49.3% and 44.6%, respectively), these variations in k are small enough to be neglected. This indicates that the deadline urgency t_d will not significantly affect the optimal value of k , thus the proposed scheme could work well for EVs with various deadline urgencies. In addition, longer deadline urgency means that the charging station has more available time to successfully schedule more EVs. Hence, it is also observed that the value of FoM is higher.

Stronger Uncertainty (2σ). This section shows how the proposed scheme could work well for

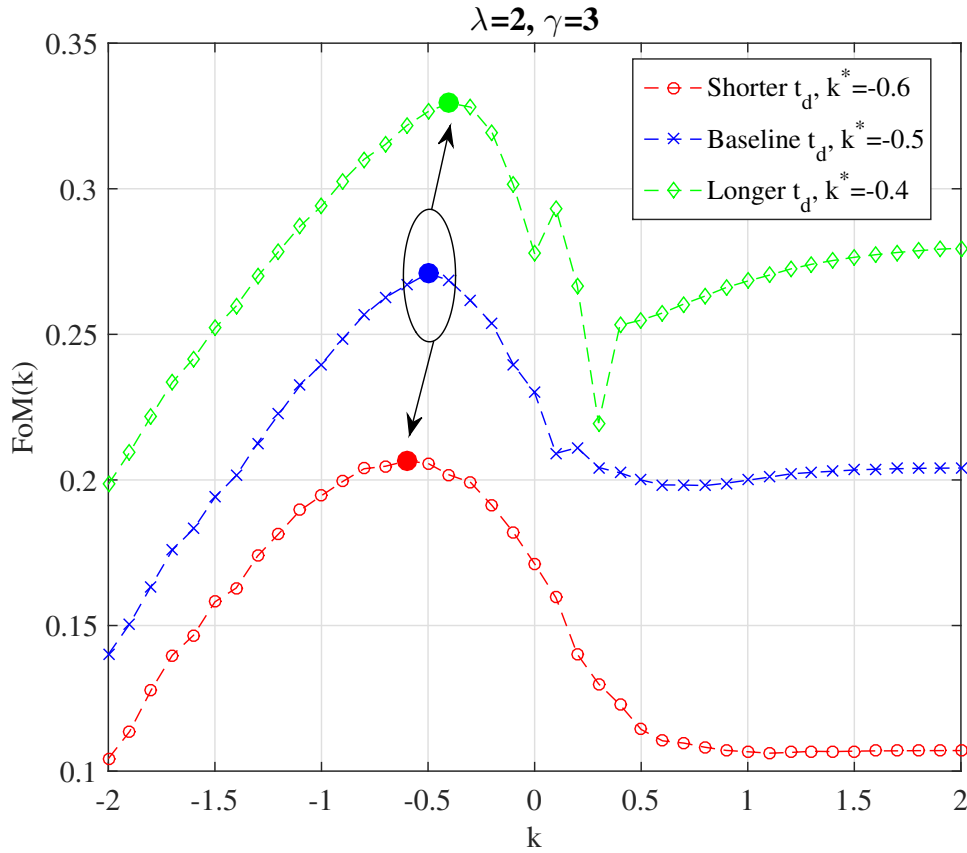


Figure 5.7: Figure of Merit (FoM) with shorter and longer deadline urgencies.

systems with stronger uncertainty. In one-step ahead forecasting, it is known that the standard deviation of the forecast distribution is almost the same as the standard deviation of the residuals. Hence, the standard deviation of the solar prediction error σ can be estimated from the prediction profile \hat{S} . If a less accurate forecasting method is being used, it is expected that the standard deviation of the residuals is higher, hence the system is with stronger uncertainty. We conduct simulations with parameters following Table 5.1, but replace the standard deviation with $\sigma_s = 2\sigma$ to find the optimal value of k that maximizes FoM . The comparison to σ in terms of FoM is shown in Figure 5.8. It can be observed that a lower arrival rate ($\lambda = 1.5$) yields a higher FoM . This is because more arrivals will lead to more EVs being rejected due to the charging station's limited capacity. Since a higher penalty is paid in total, the FoM is lower. It is also seen that when the uncertainty is stronger (2σ), having an overly conservative prediction ($k < -1.3$) will lead to no EVs being accepted at all. In addition, it is shown that the optimal value of k increases by 2.5% when $\lambda = 1.5$ and by 5% when $\lambda = 2$, thus a stronger

uncertainty will require the charging station to make a less conservative prediction. However, when compared to the corresponding changes in FoM (being 58.6% and 80.1%, respectively), these variations in k are small enough to be ignored. This indicates that a stronger uncertainty (2σ) will not significantly affect the optimal value of k . Thus, the proposed scheme could work well for systems with a stronger uncertainty.

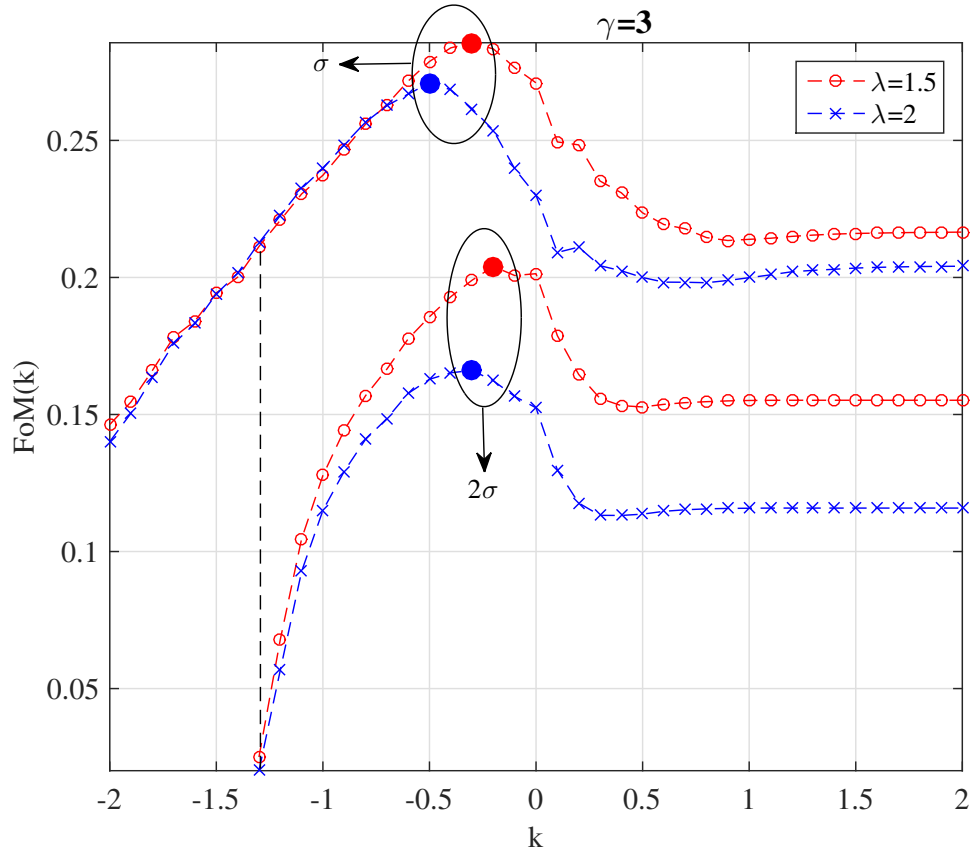


Figure 5.8: Performance comparison when the system has a stronger uncertainty.

2) Optimize $k(t)$: In the previous section, k is assumed as a constant. Intuitively, the charging station should be more certain about the solar prediction as the time approaching to the end of the day. Hence, it is expected that parameter k varies over time. We take the case that $\lambda = 1.5, \gamma = 3$ as an example. From Table 5.3, it is known that the optimal value of k as a constant variable is -0.3. We assume that k is a linear function of time t , and can be written in the following form as

$$k(t) = k^* + m_r \cdot t, \quad (5.15)$$

where m_r is the gradient and is a constant. Re-arrange eq. (5.15) as

$$k(t) = -0.3 + \frac{k_r + 0.3}{72}t, \quad k_r \in [k_{min}, k_{max}], \quad (5.16)$$

where $k_{min} = -3, k_{max} = 3$, according to the 3σ rule. The objective is then transformed to find which one from this set of lines in $k(t)$ can make $FoM(k(t))$ achieve its maximum value. The value of FoM when k_r is from -3 to 3 is computed and shown in Figure 5.9. It can be observed that FoM reaches its optimal value 0.3014 when $k_r = 0.4$. From eq. (5.16), the optimal $k(t)$ can be written as

$$k(t) = -0.3 + 0.00972t, \quad (5.17)$$

where FoM is improved by 5.5% when compared to the case that k has a constant value in Section 5.5.2. This comparison is also shown in Figure 5.9.

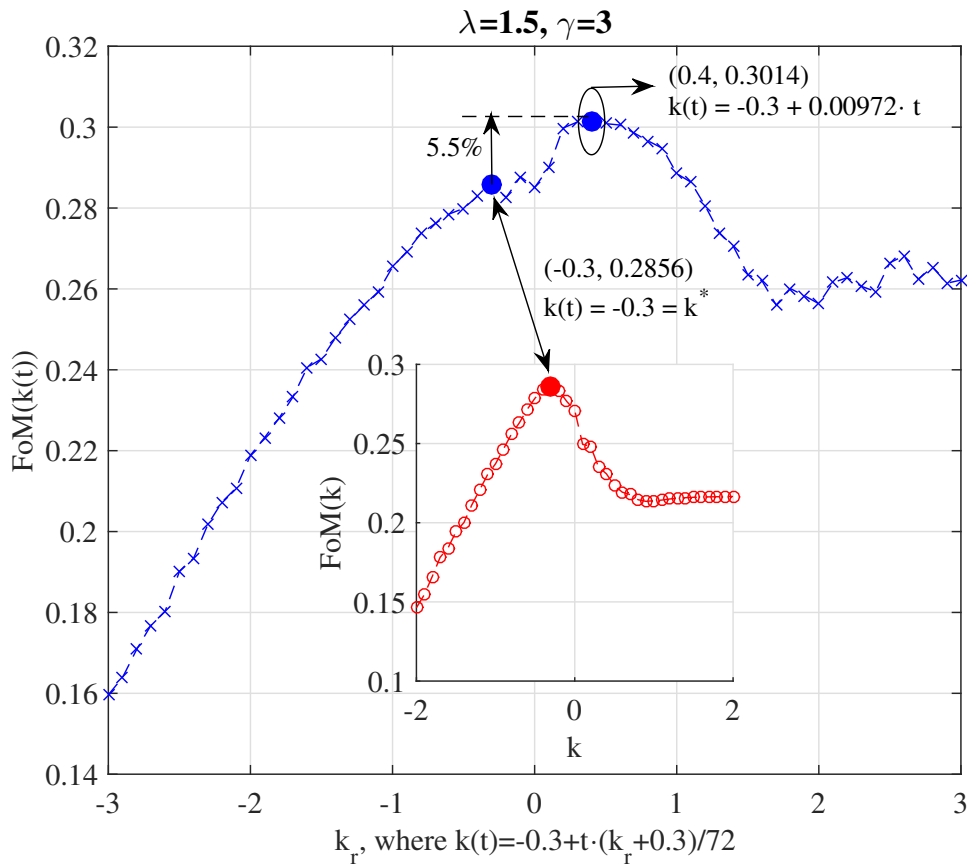


Figure 5.9: Figure of Merit (FoM) when multiplier k is a function of time t .

In addition, the set of lines in $k(t)$ is demonstrated in Figure 5.10. It can be seen that the optimal line $k^*(t)$ is increasing over time, meaning that the charging station is making a less conservative prediction of the solar generation. This is because with less time left till the end of the day, the impact of paying penalties on the value of the FoM is becoming less significant. This is in line with the result in Figure 5.9, which FoM outperforms by 5.5% when adopting $k^*(t)$ than k^* .

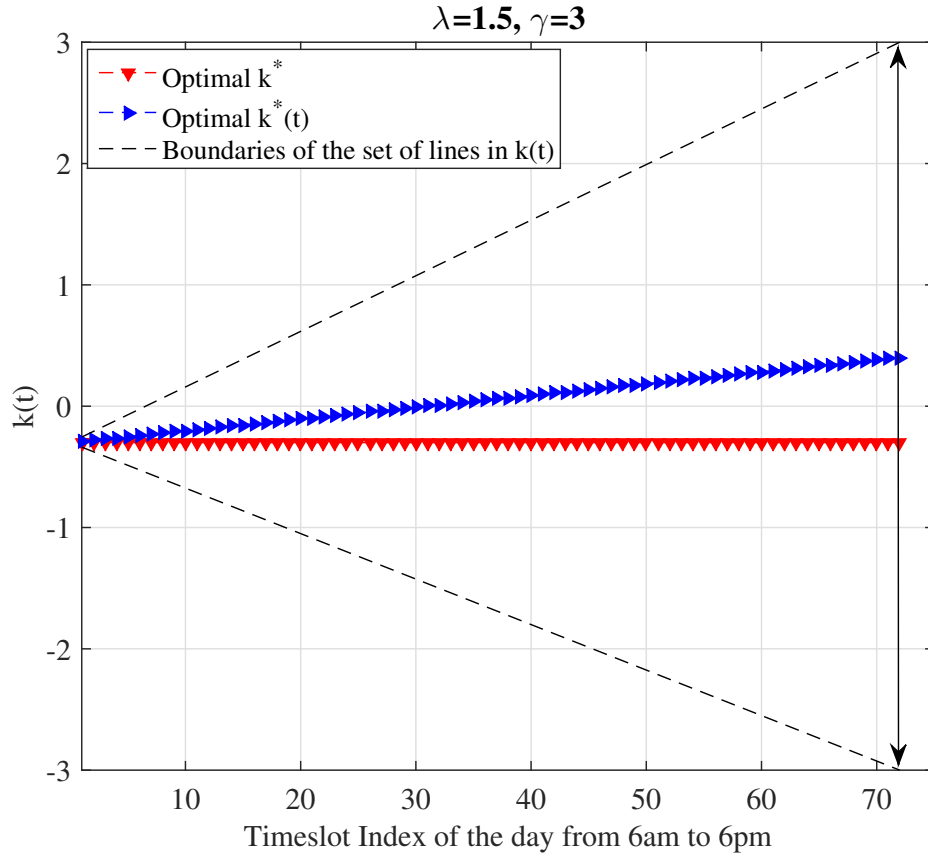


Figure 5.10: The set of lines in $k(t)$ with the highlighted optimal $k^*(t)$ and the optimal k^* .

5.5.3 Energy from the Storage

A high rejection rate of the arriving cars will cause a reputation loss to the station over time. Introducing a local storage unit can not only reduce the fluctuation of solar prediction uncertainty but can also increase EVs' admission rate by leveraging the stored energy for charging. In this section, We show the impact of the storage capacity and its starting state on system's performance in terms of FoM . A low storage capacity is similar to using the energy from the

solar panels while a high storage capacity might be similar in terms of reliability to using the energy from the power grid.

1) Sufficient Storage Capacity: Suppose that the storage has a sufficient capacity to accommodate all excess solar energy. First, 500 different scenarios via Monte Carlo simulations are conducted to compute the optimal value of k as a constant, as shown in Table 5.4.

$\lambda \backslash \gamma$	1	3	6
1	0	-0.1	-0.3
1.5	-0.1	-0.3	-0.4
2	-0.3	-0.7	-0.8

Table 5.4: Optimal value of k for solar with storage.

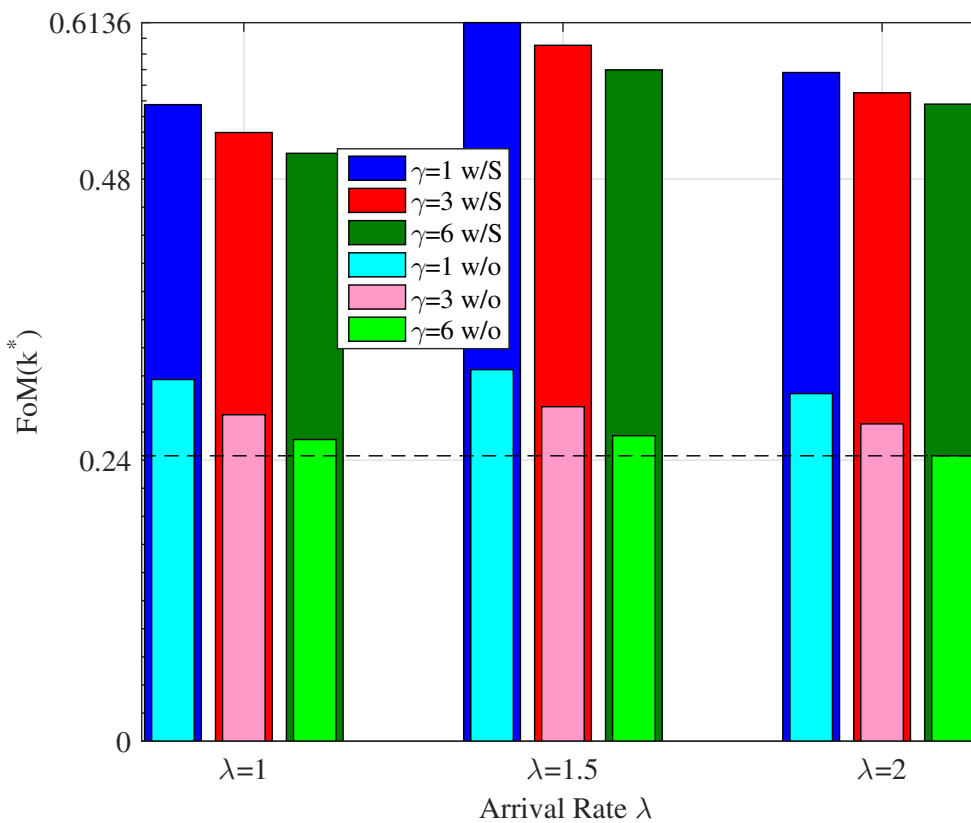


Figure 5.11: Comparison of FoM with (w/S) and without (w/o) storage facility under optimal k values from Table 5.4 and Table 5.3.

The comparison of FoM under the optimal k values is further shown when with (Table 5.4)

and without (Table 5.3) a storage unit in Figure 5.11.

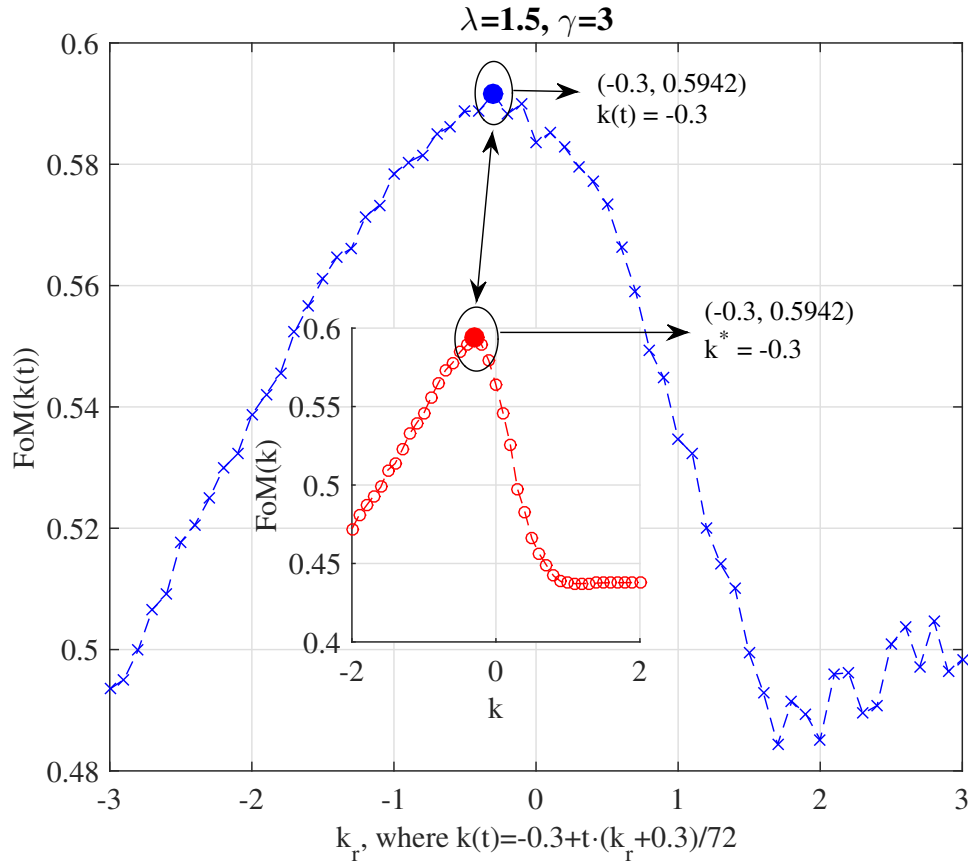


Figure 5.12: Figure of Merit (FoM) when multiplier k is a function of time t with sufficient storage capacity.

We still take the case that $\lambda = 1.5, \gamma = 3$ as an example. Following the steps in Section 5.5.2, the k constant can be optimized over time t . The corresponding FoM is computed as shown in Figure 5.12, where the optimal value of FoM and k coincide with the constant case, i.e. $k^*(t) = k^* = -0.3$. This is because sufficient storage capacity is able to balance the intermittent and time-varying solar energy generation. Next, the impact of the storage capacity and its starting state on the charging station's performance is discussed.

2) Insufficient Storage Capacity: First, we define the storage capacity as B [kWh]. Through 500 Monte Carlo simulations when a sufficient storage is assumed, the average storage capacity limit is $X = 257$ kWh. Thus, it is reasonable to assume the full storage capacity as $B = X$. In this section, we investigate the performance of the system when the charging station imple-

ments a smaller storage: $1/4$, $1/2$ and $3/4$ of B . We still take the case that $\lambda = 1.5, \gamma = 3$ as an example. Following the steps in Section 5.5.2, the optimal value of FoM is computed as shown in Figure 5.13. When the storage has a small capacity ($B/4$), the optimal value of k coincides with the case when there is no storage installed, as in eq. (5.17). As the capacity increases ($B/2, 3B/4, B$), the optimal value of k remains as a constant -0.3 as shown in Figure 5.12. From Figure 5.13, it can be seen that the performance gain in terms of FoM when compared to a zero storage case is 43%, 69%, 90%, 96% for a storage with a size of $B/4, B/2, 3B/4, B$ respectively. If the operational cost of the energy storage is proportional to its capacity, implementing energy storage with capacity $B/4$ with a FoM gain of 43% is the most economically beneficial. If the aim is to be able to store more excess solar energy, implementing three storage units with capacity of $B/4$ each can not only achieve a FoM gain of 129% but can also save $1/4$ of the cost compared to implementing a full capacity storage system.

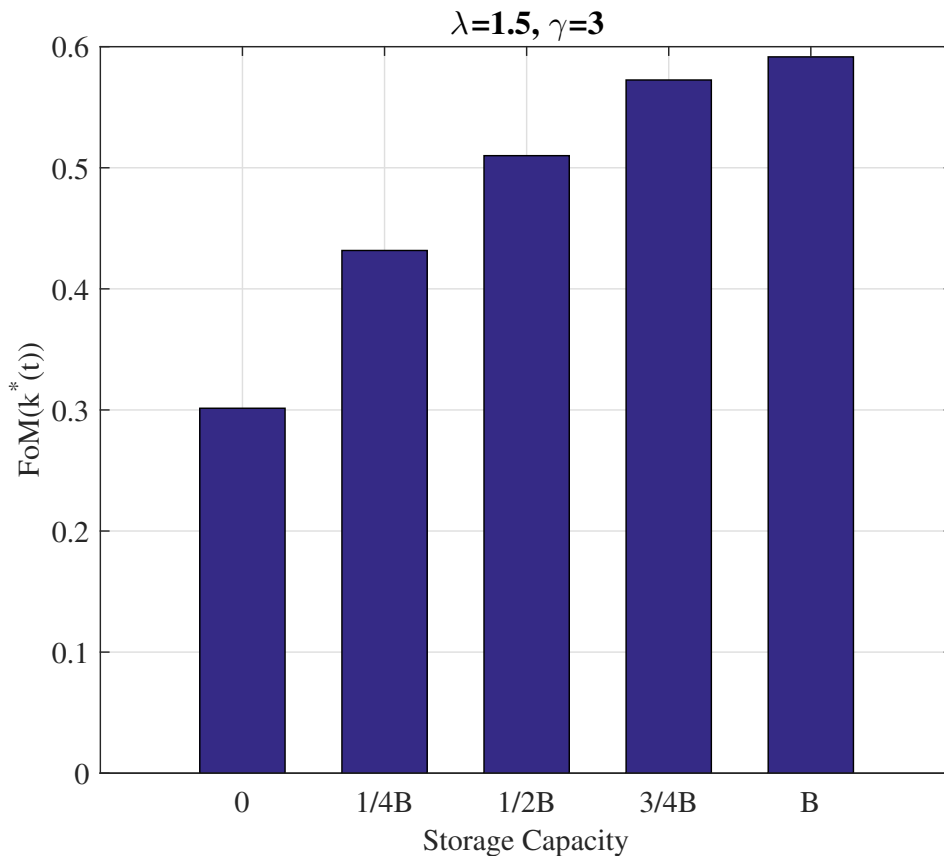


Figure 5.13: Figure of Merit (FoM) with various storage capacity under their corresponding optimal value of $k(t)$.

3) Starting State of Storage: In the previous discussions in Section 5.5.3, it is assumed that the storage starts empty at 6am. Here, it is further investigated how the starting state of the storage affects the system, so does the proposed scheme. Suppose that the storage capacity is 193 kWh, which accounts for three $B/4$ storage units. We still take the case that $\lambda = 1.5, \gamma = 3$ as an example. Following the steps in Section 5.5.2, the optimal value of k remains as a constant -0.3 when the storage starts empty, $1/4$ full, $1/2$ full, and $3/4$ full, while the optimal value of FoM increases from 0.5725 to 0.6123, 0.6488 and 0.6869, respectively, as shown in Figure 5.14. Further, the amount of energy in the storage with a different initial state is demonstrated in Figure 5.15. It is straightforward to see that the more energy to start with in the storage, the more EVs the charging station is able to charge in the beginning of the day (when solar energy is low). Hence, the value of FoM is increasing with the storage's starting state, but the optimal value of k stays the same as -0.3 . This indicates that the starting state of the storage will not affect the optimal value of k . Thus, the proposed scheme could work well regardless the storage's starting state.

5.5.4 Discussion of the cost of various energy sources

In this section, we discuss the cost paid by the station for the energy supply in order to meet EVs' charging requirements when use the energy from the grid, on-site solar panels and storage units, respectively. We assume that the connection to the grid is uninterrupted and the energy drawn from the grid is sufficient to meet all charging requirements, but that it is more expensive than the other two in Table 5.1. Let p_g denote the cost of buying per unit energy from the grid, p_b denote the operational cost of the storage that is yielded per unit energy charged or discharged, and p_s denote the maintenance cost of solar panels per unit energy output.

We show the comparison of the cost paid by the station to cover various energy sources over 500 different scenarios via Monte Carlo simulations in Figure 5.16. Following the simulation parameters in Table 5.1, EVs' arrival rate λ is assumed to vary from 0.5 to 2 per timeslot and the penalty factor is set as $\gamma = 3$. The financial cost paid by the station in one day is calculated under optimal operation in these three cases. If the energy is bought from the grid, following the steps in Section 5.5.1, EVs are admitted based on their priority orders. If the energy is drawn from solar panels and storage units, following the steps in Section 5.5.2, the optimal value of $k(t)$ to maximize FoM is first computed, then used to calculate the corresponding cost when the station operates under these optimal points (i.e., at the maximal FoM). It can be

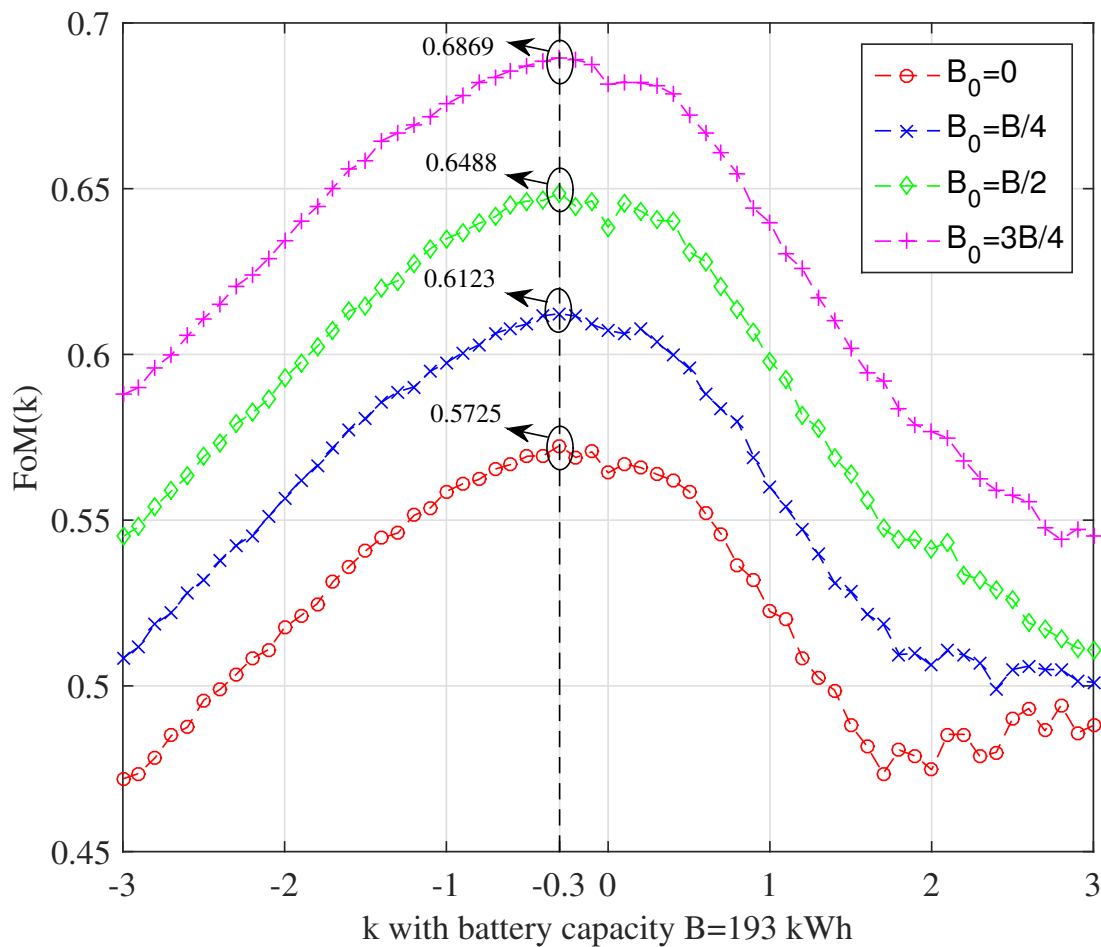


Figure 5.14: The FoM comparison when the storage starts empty, 1/4 full, 1/2 full, and 3/4 full with the battery capacity $B = 193$ kWh.

seen from Figure 5.16 that energy from the grid is the most expensive source with energy from the solar panels being the cheapest option. Implementing storage units can hedge against the uncertainty of the station and increase its performance in terms of FoM , but it will bring extra cost as shown in Figure 5.16 where the blue curve lies above the green curve.

5.6 Summary

In this chapter, an EV charging admission and scheduling problem at a MG-like charging station is studied. The charging station needs to decide which arriving EVs to admit and scheduled accordingly due to its limited capacity to achieve an optimal utility. To this end, a multiplier k to account for the effect of solar energy prediction uncertainty is first introduced. Then, a

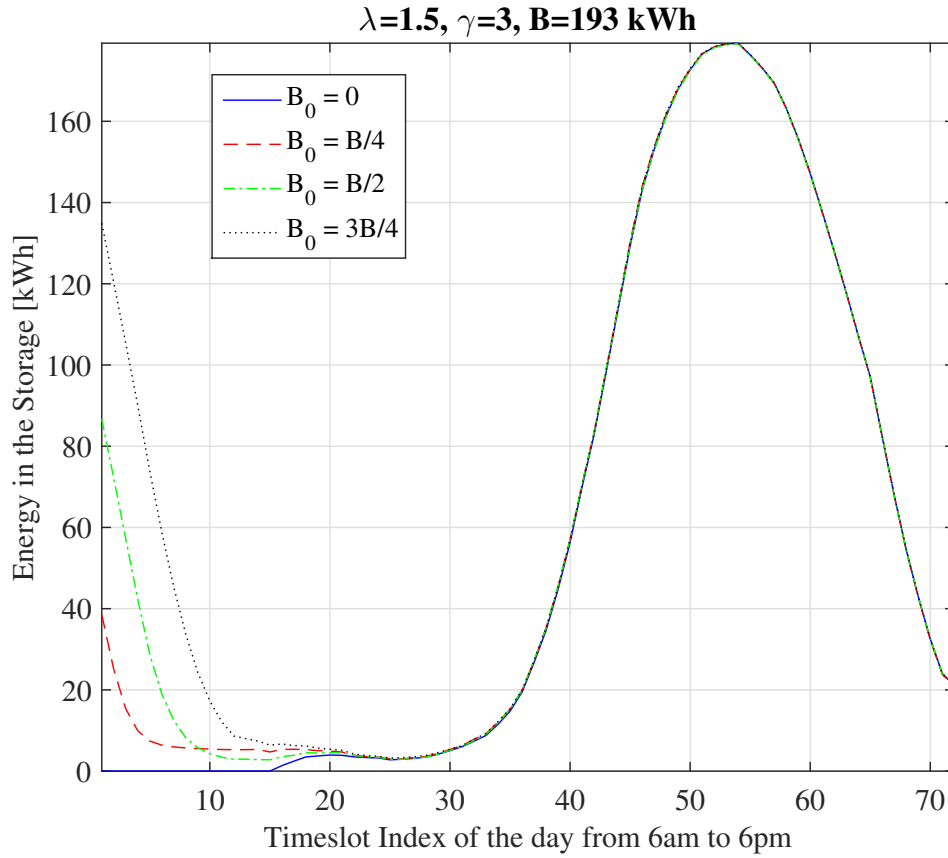


Figure 5.15: Energy in the storage with various starting states for a $3B/4$ size storage.

composite power metric called the Figure of Merit (FoM) is defined to measure the charging station's performance. Thus, the problem is formulated as FoM maximization. A two-stage admission and scheduling mechanism is thereafter proposed to solve the optimization problem.

The parameter k from the stochastic solar energy generation model is first optimized as a constant (where FoM has a 29.5% gain compared to when k is not optimized (i.e., $k = 0$) for $\lambda = 1.5, \gamma = 6$) then as a function of time (where FoM has a 5.5% gain compared to when k is optimized but as a constant (i.e., $k = -0.3$) for $\lambda = 1.5, \lambda = 3$) by finding the maximum value of FoM under various energy supply scenarios. Through Monte Carlo simulations, the solution to the FoM optimization problem is shown. In addition, the impact of some of the key factors (such as shorter and longer deadline urgencies, stronger uncertainty of the prediction error, the storage capacity and its starting state) on the charging station's performance is discussed in terms of FoM and the corresponding optimal value of k .

In the next chapter, conclusions of the studies in this thesis is given, along with some sugges-

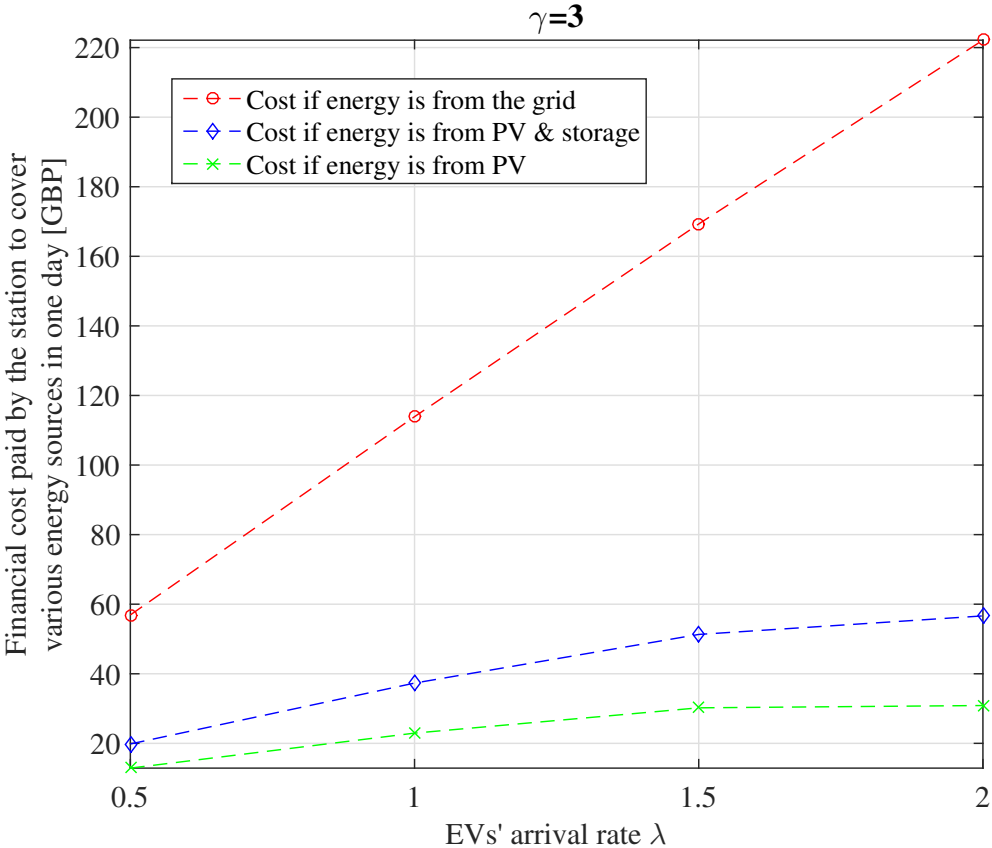


Figure 5.16: Financial cost paid by the station to cover various energy sources in one day.

tions for future work directions.

Chapter 6

Conclusions and Future Work

This thesis has contributed to the design of decision-making techniques for energy management in the smart grid with emphasis on energy efficiency and uncertainty analysis. In this concluding chapter, Section 6.1 summarizes the key contributions of the thesis. Section 6.2 outlines some limitations of this work and suggestions for future work.

6.1 Conclusions

This thesis presented the applications of decision-making approaches for energy management in microgrid energy trading scenario and electric vehicles charging scheduling. To demonstrate the achievable performance, we focused on a simple configuration that the randomly distributed microgrids considered in the coalition formation process are able to transfer power to each other and the microgrid-like charging station is equipped with on-site solar panels and energy storage units providing service during daylight hours. The key contributions of this thesis are summarized as follows.

6.1.1 Coalition Formation for Energy Trading among Distributed Microgrids

The uncertainty of renewable energy generation and consumers' behaviour brings difficulty in matching the demand with the supply within the microgrid during a certain period. Instead, there is a need for buyer microgrids and seller microgrids to trade energy with the main power grid. However, the power loss among nearby microgrids due to the power transfer is more likely less than that between the microgrids and the main power grid.

To alleviate this power loss and enhance energy efficiency, a cooperative game theoretic framework is proposed to study the energy trading problem among seller and buyer microgrids, where microgrids can make distributed decisions whether to form a coalition with others. The merge-and-split based coalition formation game shows a high computational complexity for a large

network. Three alternative approaches to this method are proposed to support microgrid collaboration more efficiently. From Monte Carlo simulations, the results have shown that game theory based methods yield a better performance in terms of smaller power loss and larger coalition size (with the modified algorithms showing a better overall performance) than a non-cooperative game. Although the merge-and-split based coalition formation games can yield significant power loss reduction, the growth of the computational complexity follows a factorial order with the number of microgrids due to the brute-force search of all partitions of a set of microgrids in the split process.

Thus, an efficient framework is further established for the power loss minimization problem as a college admissions game with variable energy quotas, whose computational complexity only grows at a quadratic rate with the number of microgrids. The college admissions based algorithm becomes a good candidate for a network with a large number of distributed microgrids. Through Monte Carlo simulations, the proposed framework shows comparable power loss reduction to the merge-and-split based algorithms, but runs 700 and 18000 times faster for a network of 10 microgrids and 20 microgrids.

6.1.2 Priority-based Energy Scheduling Mechanism for Electric Vehicles Charging

To provide an efficient charging service to future electric vehicles, it is important for the charging station to estimate its available capacity. As the charging station usually has a fixed number of chargers and a limited charging capacity, it cannot accommodate all the arriving vehicles. Thus, a decision must be made by the charging station whether a new arriving vehicle can be admitted and then be scheduled for charging. This not only depends on the charging station's physical constraints but also depends on how certain the charging station is towards its energy supply.

The problem of EV charging using various energy sources (such as energy from the main power grid, on-site solar photovoltaic panels, and local energy storage devices) is studied along with their impacts on the charging station's performance. Unlike the energy from the main power grid, energy from the on-site solar panels varies with time and cannot be predicted precisely. To this end, a multiplier k is introduced to measure the effect of solar prediction uncertainty and a composite performance index, called the Figure of Merit, is developed to capture the charging station's utility. It considers the EV users charging requirements as well as the penalty

for turning away new arrivals and missing charging deadlines. The aim is then to maximize the Figure of Merit by deciding which arriving EV to admit, considering the uncertain solar energy supply and EV users requirements. If this information is known, the optimization problem can be solved by using mixed integer programming. However, the charging station does not know precisely how much solar energy will be generated from the solar panels in the future, and needs to make decisions under uncertainty. Thus, a two-stage priority-based admission and scheduling mechanism is further proposed to find the optimal trade-off between accepting EVs and missing charging deadlines by determining the best value of k under various energy supply scenarios.

Through numerical evaluations, the solution to the optimization problem is shown with the multiplier k being optimized as a constant variable and a function of time, respectively. The impact of some of the key factors such as shorter and longer deadline urgencies, stronger uncertainty of the prediction error, the storage capacity and its initial state on the charging stations performance is also discussed.

6.2 Future Work

Following the investigations of the two smart grid applications: microgrid energy trading and electric vehicles charging scheduling, there are several future research directions can be extended. Some suggestions are summarized as follows.

6.2.1 Microgrid Energy Trading

A possible direction to the current work is to include complex power electronics constraints such as include reactive power control service to regulate the voltage at the point of common coupling of each microgrid, as well as to consider the irrationality of consumers' behaviour. This requires a more realistic energy system modelling and improved mechanism that is able to better incentivise consumers' participation in the decision-making process under systems' dynamics and uncertainty.

6.2.2 Electric Vehicles Charging Scheduling

The uncertainty of solar energy generation prediction is modelled by introducing a parameter k based on the 3σ rule in the current work. This simple but realistic stochastic model can also be applied to other applications involving renewable energy. The utility function and the system can be further modelled by a more detailed model of the system dynamics and the weather forecast uncertainty. This motivates improved approaches to be developed for stochastic planning and operational models.

References

- [1] R. Wallace, *Power Systems Engineering 5*. University of Edinburgh, Edinburgh, United Kingdom, 2015.
- [2] “Frequency Response Services on UK National Grid.” <http://www2.nationalgrid.com/uk/services/balancing-services/frequency-response/> [Online; accessed 27-Jul-2017].
- [3] Z. Han, D. Niyato, W. Saad, T. Basar, and A. Hjørungnes, *Game Theory in Wireless and Communication Networks*. Cambridge University Press, 2011.
- [4] “National Grid Data Explorer.” <http://www2.nationalgrid.com/UK/Industry-information/Electricity-transmission-operational-data/Data-Explorer/> [Online; accessed 16-Nov-2017].
- [5] “NIST Framework and Roadmap for Smart Grid Interoperability Standards, Release 3.0,” Sept. 2014. <http://dx.doi.org/10.6028/NIST.SP.1108r3> [Online; accessed 16-Nov-2017].
- [6] “Microgrids At Berkeley Lab.” <https://building-microgrid.lbl.gov/about-microgrids> [Online; accessed 16-Nov-2017].
- [7] “U.S. Department of Energy - How Microgrids Work.” <https://energy.gov/articles/how-microgrids-work> [Online; accessed 16-Nov-2017].
- [8] S. F. Tie and C. W. Tan, “A Review of Energy Sources and Energy Management System in Electric Vehicles,” *Renewable and Sustainable Energy Reviews*, vol. 20, pp. 82 – 102, April 2013.
- [9] T. Zhang, W. Chen, Z. Han, and Z. Cao, “Charging Scheduling of Electric Vehicles With Local Renewable Energy Under Uncertain Electric Vehicle Arrival and Grid Power Price,” *IEEE Transactions on Vehicular Technology*, vol. 63, pp. 2600–2612, July 2014.
- [10] W. Wei, F. Liu, and S. Mei, “Charging Strategies of EV Aggregator Under Renewable Generation and Congestion: A Normalized Nash Equilibrium Approach,” *IEEE Transactions on Smart Grid*, vol. 7, pp. 1630–1641, May 2016.
- [11] N. Masuch, J. Keiser, M. Ltzenberger, and S. Albayrak, “Wind Power-Aware Vehicle-to-Grid Algorithms for Sustainable EV Energy Management Systems,” in *IEEE International Electric Vehicle Conference (IEVC)*, pp. 1–7, March 2012.
- [12] Y. Wang and J. S. Thompson, “Utilizing Coalition Games to Optimize Micro-grid Distribution Networks,” in *Proc. 15th Annual PostGraduate Symposium on the Convergence of Telecommunications, Networking and Broadcasting*, pp. 289–294, June 2014.

- [13] Y. Wang and J. S. Thompson, "A College Admissions Framework for Distributed Microgrids Cooperation in Smart Grid," in *IEEE International Energy Conference (ENERGYCON)*, pp. 1–6, April 2016.
- [14] Y. Wang and J. S. Thompson, "CAF: A College Admissions Framework for Distributed Microgrids in a Case Study," in *IEEE International Conference on Smart Grid and Clean Energy Technologies (ICSGCE)*, pp. 113–118, October 2016.
- [15] Y. Wang and J. S. Thompson, "Admission and Scheduling Mechanism for Electric Vehicle Charging with Renewable Energy," in *IEEE International Conference on Communications Workshops (ICC Workshops)*, pp. 1304–1309, May 2017.
- [16] Y. Wang and J. S. Thompson, "Two-Stage Admission and Scheduling Mechanism for Electric Vehicle Charging." submitted to *IEEE Transactions on Smart Grid* under 2nd round revision, August 2017.
- [17] H. E. Farag, M. M. A. Abdelaziz, and E. F. El-Saadany, "Voltage and Reactive Power Impacts on Successful Operation of Islanded Microgrids," *IEEE Transactions on Power Systems*, vol. 28, pp. 1716–1727, May 2013.
- [18] Y. Wang, W. Saad, A. I. Sarwat, and C. S. Hong, "Reactive Power Compensation Game under Prospect-Theoretic Framing Effects," *IEEE Transactions on Smart Grid*, January 2017.
- [19] Y. Wang, *Behavioral Game Theory for Smart Grid Energy Management*. PhD thesis, University of Miami, Coral Gables, Florida, United States, 2015. http://scholarlyrepository.miami.edu/oa_dissertations/1377/ [Online; accessed 16-Nov-2017].
- [20] F. Tomaevi, K. Baranai, and M. Delimar, "Reactive Power Optimization Based on Load Profile Partitioning," in *IEEE International Energy Conference (ENERGYCON)*, pp. 627–632, May 2014.
- [21] "PowerWorld Solutions." <https://www.powerworld.com/> [Online; accessed 16-Nov-2017].
- [22] R. D. Zimmerman, C. E. Murillo-Sanchez, and R. J. Thomas, "MATPOWER: Steady-State Operations, Planning, and Analysis Tools for Power Systems Research and Education," *IEEE Transactions on Power Systems*, vol. 26, pp. 12–19, February 2011.
- [23] "MATLAB and Simulink." <https://uk.mathworks.com/discovery/power-system-simulation-and-optimization.html> [Online; accessed 16-Nov-2017].
- [24] E. Hossain, Z. Han, and H. V. Poor, *Smart Grid Communications and Networking*. Cambridge University Press, 2012.
- [25] "IET The Institution of Engineering and Technology - Smart Grids." <http://www.theiet.org/policy/key-topics/smart-grid/> [Online; accessed 16-Nov-2017].

-
- [26] G. Liu, Y. Xu, and K. Tomsovic, "Bidding Strategy for Microgrid in Day-Ahead Market Based on Hybrid Stochastic/Robust Optimization," *IEEE Transactions on Smart Grid*, vol. 7, pp. 227–237, January 2016.
- [27] C. M. Colson and M. H. Nehrir, "Comprehensive Real-Time Microgrid Power Management and Control With Distributed Agents," *IEEE Transactions on Smart Grid*, vol. 4, pp. 617–627, March 2013.
- [28] T. Morstyn, B. Hredzak, and V. G. Agelidis, "Control Strategies for Microgrids with Distributed Energy Storage Systems: An Overview," *IEEE Transactions on Smart Grid*, December 2016.
- [29] T. Logenthiran, D. Srinivasan, and T. Z. Shun, "Demand Side Management in Smart Grid Using Heuristic Optimization," *IEEE Transactions on Smart Grid*, vol. 3, pp. 1244–1252, September 2012.
- [30] K. P. Detroja, "Optimal Autonomous Microgrid Operation: A holistic View," *Applied Energy*, vol. 173, pp. 320 – 330, July 2016.
- [31] N. Ruiz, I. Cobelo, and J. Oyarzabal, "A Direct Load Control Model for Virtual Power Plant Management," *IEEE Transactions on Power Systems*, vol. 24, pp. 959–966, May 2009.
- [32] A. Y. Saber and G. K. Venayagamoorthy, "Resource Scheduling Under Uncertainty in a Smart Grid With Renewables and Plug-in Vehicles," *IEEE Systems Journal*, vol. 6, pp. 103–109, March 2012.
- [33] Y. Levron, J. M. Guerrero, and Y. Beck, "Optimal Power Flow in Microgrids With Energy Storage," *IEEE Transactions on Power Systems*, vol. 28, pp. 3226–3234, August 2013.
- [34] "How the Smart Grid Enables Utilities to Integrate Electric Vehicles," techreport, Silver spring networks, June 2010. <https://grist.files.wordpress.com/2011/10/silverspring-whitepaper-electricvehicles.pdf> [Online; accessed 16-Nov-2017].
- [35] "New Diesel and Petrol Vehicles to be Banned from 2040 in UK," July 2017. <http://www.bbc.co.uk/news/uk-40723581> [Online; accessed 16-Nov-2017].
- [36] L. Dickerman and J. Harrison, "A New Car, a New Grid," *IEEE Power and Energy Magazine*, vol. 8, pp. 55–61, March 2010.
- [37] Q. Wang, X. Liu, J. Du, and F. Kong, "Smart Charging for Electric Vehicles: A Survey From the Algorithmic Perspective," *IEEE Communications Surveys Tutorials*, vol. 18, pp. 1500–1517, Second Quarter 2016.
- [38] W. Tushar, C. Yuen, S. Huang, D. B. Smith, and H. V. Poor, "Cost Minimization of Charging Stations With Photovoltaics: An Approach With EV Classification," *IEEE Transactions on Intelligent Transportation Systems*, vol. 17, pp. 156–169, January 2016.

- [39] Q. Dong, D. Niyato, P. Wang, and Z. Han, "The PHEV Charging Scheduling and Power Supply Optimization for Charging Stations," *IEEE Transactions on Vehicular Technology*, vol. 65, pp. 566–580, February 2016.
- [40] K. Morrow, D. Karner, and J. Francfort, "Plug-in Hybrid Electric Vehicle Charging Infrastructure Review," [online], Idaho National Laboratory, Idaho Falls, Idaho, United States, 2008. <https://avt.inl.gov/sites/default/files/pdf/phev/phevInfrastructureReport08.pdf> [Online; accessed 16-Nov-2017].
- [41] "SolarCity Electric Vehicle Charging Station." <http://www.solarcity.com/> [Online; accessed 16-Nov-2017].
- [42] "Urban Green Energy and GE Energy Industrial Solutions Unveil the Sanya Skypump, an Electric-Vehicle Charging Station Equipped with Wind and Solar Power," 2012. <http://www.geindustrial.com/gsearch/SANYA%2BSKYPUMP> [Online; accessed 16-Nov-2017].
- [43] Z. Rezvani, J. Jansson, and J. Bodin, "Advances in Consumer Electric Vehicle Adoption Research: A Review and Research Agenda," *Transportation Research Part D: Transport and Environment*, vol. 34, pp. 122 – 136, January 2015.
- [44] Y. Wang, W. Saad, Z. Han, H. V. Poor, and T. Basar, "A Game-Theoretic Approach to Energy Trading in the Smart Grid," *IEEE Transactions on Smart Grid*, vol. 5, pp. 1439–1450, May 2014.
- [45] T. Cui, Y. Wang, S. Yue, S. Nazarian, and M. Pedram, "A Game-Theoretic Price Determination Algorithm for Utility Companies Serving a Community in Smart Grid," in *IEEE PES Innovative Smart Grid Technologies Conference (ISGT)*, pp. 1–6, February 2013.
- [46] W. Saad, Z. Han, H. V. Poor, and T. Basar, "Game-Theoretic Methods for the Smart Grid: An Overview of Microgrid Systems, Demand-Side Management, and Smart Grid Communications," *IEEE Signal Processing Magazine*, vol. 29, pp. 86–105, September 2012.
- [47] J. Drechsel, *Selected Topics in Cooperative Game Theory in Cooperative Lot Sizing Games in Supply Chains*. Lecture Notes in Economics and Mathematical Systems, Springer, 2010.
- [48] R. B. Myerson, *Game Theory: Analysis of Conflict*. Harvard University Press, 1997.
- [49] W. Saad, Z. Han, M. Debbah, A. Hjørungnes, and T. Basar, "Coalitional Game Theory for Communication Networks," *IEEE Signal Processing Magazine*, vol. 26, pp. 77–97, September 2009.
- [50] R. A. V. Ramirez, *Low Complexity Radio Resource Management for Energy Efficient Wireless Networks*. PhD thesis, University of Edinburgh, Edinburgh, United Kingdom, 2014. <https://www.era.lib.ed.ac.uk/handle/1842/9691> [Online; accessed 16-Nov-2017].
- [51] D. Gale and L. S. Shapley, "College Admissions and the Stability of Marriage," *American Mathematical Monthly*, vol. 69, no. 1, pp. 9–15, 1962.

- [52] D. Gale and M. Sotomayor, “Some Remarks on the Stable Matching Problem,” *Discrete Applied Mathematics*, vol. 11, no. 3, pp. 223 – 232, 1985.
- [53] L. Chang, A. Jaros, E. Lett, and M. Lucas, “College Admissions and the Stability of Marriage,” [online], Duke University, Durham, North Carolina, United States, 2012. https://sites.duke.edu/econ206_01_s2011/files/2012/05/52Gale-Shapley-presentation_II_Coase.pdf.pdf [Online; accessed 16-Nov-2017].
- [54] J. Alcalde and A. Romero-Medina, “Sequential Decisions in the College Admissions Problem,” *Economics Letters*, vol. 86, pp. 153–158, February 2005.
- [55] T. Kavitha, K. Mehlhorn, D. Michail, and K. E. Paluch, “Strongly Stable Matchings in Time $O(Nm)$ and Extension to the Hospitals-residents Problem,” *ACM Transactions on Algorithms*, vol. 3, May 2007.
- [56] K. Iwama and S. Miyazaki, “A Survey of the Stable Marriage Problem and Its Variants,” *International Conference on Informatics Research for Development of Knowledge Society Infrastructure*, pp. 131–136, 2008.
- [57] P. Bir, T. Fleiner, R. W. Irving, and D. F. Manlove, “The College Admissions Problem with Lower and Common Quotas,” *Theoretical Computer Science*, vol. 411, no. 3436, pp. 3136 – 3153, 2010.
- [58] J. W. Kathrine and A. Raj, “Packet Scheduling Algorithms in Different Wireless Networks A Survey,” *International Journal of Engineering Research and Technology*, vol. 1, October 2012.
- [59] H. Yu, S. Ruepp, and M. S. Berger, “Enhanced First-In-First-Out-Based Round-Robin Multicast Scheduling Algorithm for Input-Queued Switches,” *IET Communications*, vol. 5, pp. 1163–1171, May 2011.
- [60] X. Zhang and L. N. Bhuyan, “Deficit round-robin scheduling for input-queued switches,” *IEEE Journal on Selected Areas in Communications*, vol. 21, pp. 584–594, May 2003.
- [61] Z. Wei, J. He, M. Xing, and L. Cai, “Utility Maximization for Electric Vehicle Charging with Admission Control and Scheduling,” in *IEEE International Conference on Communications (ICC)*, pp. 661–666, June 2015.
- [62] S.-H. Oh and S.-M. Yang, “A Modified Least-Laxity-First Scheduling Algorithm for Real-Time Tasks,” in *Proc. 5th International Conference on Real-Time Computing Systems and Applications*, pp. 31–36, October 1998.
- [63] A. Subramanian, M. J. Garcia, D. S. Callaway, K. Poolla, and P. Varaiya, “Real-Time Scheduling of Distributed Resources,” *IEEE Transactions on Smart Grid*, vol. 4, pp. 2122–2130, December 2013.
- [64] S. Galli, A. Scaglione, and Z. Wang, “For the Grid and Through the Grid: The Role of Power Line Communications in the Smart Grid,” *Proceedings of the IEEE*, vol. 99, pp. 998–1027, June 2011.

- [65] Y. Yan, Y. Qian, H. Sharif, and D. Tipper, "A Survey on Smart Grid Communication Infrastructures: Motivations, Requirements and Challenges," *IEEE Communications Surveys Tutorials*, vol. 15, pp. 5–20, First Quarter 2013.
- [66] X. Fang, S. Misra, G. Xue, and D. Yang, "Smart Grid - The New and Improved Power Grid: A Survey," *IEEE Communications Surveys Tutorials*, vol. 14, pp. 944–980, Fourth Quarter 2012.
- [67] W. Saad, Z. Han, and H. V. Poor, "Coalitional Game Theory for Cooperative Micro-Grid Distribution Networks," in *IEEE International Conference Communications Workshops (ICC Workshops)*, pp. 1–5, June 2011.
- [68] H. Liang, A. K. Tamang, W. Zhuang, and X. S. Shen, "Stochastic Information Management in Smart Grid," *IEEE Communications Surveys Tutorials*, vol. 16, pp. 1746–1770, Third Quarter 2014.
- [69] S. Shao, M. Pipattanasomporn, and S. Rahman, "Grid Integration of Electric Vehicles and Demand Response With Customer Choice," *IEEE Transactions on Smart Grid*, vol. 3, pp. 543–550, March 2012.
- [70] L. Zhu, F. R. Yu, B. Ning, and T. Tang, "Optimal Charging Control for Electric Vehicles in Smart Microgrids with Renewable Energy Sources," in *IEEE 75th Vehicular Technology Conference (VTC Spring)*, pp. 1–5, May 2012.
- [71] S. Kamboj, K. S. Decker, K. Trnka, N. Pearre, C. Kern, and W. Kempton, "Exploring the Formation of Electric Vehicle Coalitions for Vehicle-To-Grid Power Regulation," *AAMAS workshop on Agent Technologies for Energy Systems*, May 2010.
- [72] B. Djokic, M. Miyakawa, S. Sekiguchi, I. Semba, and I. Stojmenovic, "A Fast Iterative Algorithm for Generating Set Partitions," *Computer Journal*, vol. 32, pp. 281–282, June 1989.
- [73] D. E. Olivares, A. Mehrizi-Sani, A. H. Etemadi, C. A. Caizares, R. Iravani, M. Kazerani, A. H. Hajimiragha, O. Gomis-Bellmunt, M. Saadifard, R. Palma-Behnke, G. A. Jimnez-Estvez, and N. D. Hatziargyriou, "Trends in Microgrid Control," *IEEE Transactions on Smart Grid*, vol. 5, pp. 1905–1919, July 2014.
- [74] W. Su, J. Wang, and J. Roh, "Stochastic Energy Scheduling in Microgrids With Intermittent Renewable Energy Resources," *IEEE Transactions on Smart Grid*, vol. 5, pp. 1876–1883, July 2014.
- [75] A. L. Dimeas and N. D. Hatziargyriou, "Operation of a Multiagent System for Microgrid Control," *IEEE Transactions on Power Systems*, vol. 20, pp. 1447–1455, August 2005.
- [76] V. C. Gungor, D. Sahin, T. Kocak, S. Ergut, C. Buccella, C. Cecati, and G. P. Hancke, "A Survey on Smart Grid Potential Applications and Communication Requirements," *IEEE Transactions on Industrial Informatics*, vol. 9, pp. 28–42, February 2013.
- [77] Z. Fan, P. Kulkarni, S. Gormus, C. Efthymiou, G. Kalogridis, M. Sooriyabandara, Z. Zhu, S. Lambotharan, and W. H. Chin, "Smart Grid Communications: Overview of Research Challenges, Solutions, and Standardization Activities," *IEEE Communications Surveys Tutorials*, vol. 15, pp. 21–38, First Quarter 2013.

- [78] C. H. Lo and N. Ansari, "The Progressive Smart Grid System from Both Power and Communications Aspects," *IEEE Communications Surveys Tutorials*, vol. 14, pp. 799–821, Third Quarter 2012.
- [79] I. Ali and S. Hussain, "Communication Design for Energy Management Automation in Microgrid," *IEEE Transactions on Smart Grid*, September 2017.
- [80] D. Kumar, F. Zare, and A. Ghosh, "DC Microgrid Technology: System Architectures, AC Grid Interfaces, Grounding Schemes, Power Quality, Communication Networks, Applications and Standardizations Aspects," *IEEE Access*, vol. 5, June 2017.
- [81] W. Meng, X. Wang, and S. Liu, "Distributed Load Sharing of an Inverter-Based Microgrid with Reduced Communication," *IEEE Transactions on Smart Grid*, July 2017.
- [82] Y. Xu, "Latency and Bandwidth Analysis of LTE for a Smart Grid," Master's thesis, KTH Royal Institute of Technology, Stockholm, Sweden, 2011. <http://kth.diva-portal.org/smash/get/diva2:565509/FULLTEXT01.pdf> [Online; accessed 12-Aug-2014].
- [83] Z. M. Fadlullah, M. M. Fouda, N. Kato, A. Takeuchi, N. Iwasaki, and Y. Nozaki, "Toward Intelligent Machine-to-Machine Communications in Smart Grid," *IEEE Communications Magazine*, vol. 49, pp. 60–65, April 2011.
- [84] V. C. Gungor, B. Lu, and G. P. Hancke, "Opportunities and Challenges of Wireless Sensor Networks in Smart Grid," *IEEE Transactions on Industrial Electronics*, vol. 57, pp. 3557–3564, October 2010.
- [85] P. Wang, H. Hou, X. He, C. Wang, T. Xu, and Y. Li, "Survey on Application of Wireless Sensor Network in Smart grid," *Procedia Computer Science*, vol. 52, pp. 1212 – 1217, 2015.
- [86] Y. Xu and W. Liu, "Novel Multiagent Based Load Restoration Algorithm for Microgrids," *IEEE Transactions on Smart Grid*, vol. 2, pp. 152–161, March 2011.
- [87] C. M. Colson and M. H. Nehrir, "Algorithms for Distributed Decision-Making for Multi-Agent Microgrid Power Management," in *IEEE Power and Energy Society General Meeting*, pp. 1–8, July 2011.
- [88] G. E. Asimakopoulou, A. L. Dimeas, and N. D. Hatziargyriou, "Leader-Follower Strategies for Energy Management of Multi-Microgrids," *IEEE Transactions on Smart Grid*, vol. 4, pp. 1909–1916, December 2013.
- [89] W. Y. Chiu, H. Sun, and H. V. Poor, "Energy Imbalance Management Using a Robust Pricing Scheme," *IEEE Transactions on Smart Grid*, vol. 4, pp. 896–904, June 2013.
- [90] G. B. Giannakis, V. Kekatos, N. Gatsis, S. J. Kim, H. Zhu, and B. F. Wollenberg, "Monitoring and Optimization for Power Grids: A Signal Processing Perspective," *IEEE Signal Processing Magazine*, vol. 30, pp. 107–128, September 2013.
- [91] J. Matamoros, D. Gregoratti, and M. Dohler, "Microgrids Energy Trading in Islanding Mode," in *IEEE International Conference on Smart Grid Communications (SmartGridComm)*, pp. 49–54, November 2012.

- [92] C. Wei, Z. M. Fadlullah, N. Kato, and A. Takeuchi, "GT-CFS: A Game Theoretic Coalition Formulation Strategy for Reducing Power Loss in Micro Grids," *IEEE Transactions on Parallel and Distributed Systems*, vol. 25, pp. 2307–2317, September 2014.
- [93] C. Wei, Z. M. Fadlullah, N. Kato, and I. Stojmenovic, "On Optimally Reducing Power Loss in Micro-grids With Power Storage Devices," *IEEE Journal on Selected Areas in Communications*, vol. 32, pp. 1361–1370, July 2014.
- [94] I. Atzeni, L. G. Ordez, G. Scutari, D. P. Palomar, and J. R. Fonollosa, "Noncooperative and Cooperative Optimization of Distributed Energy Generation and Storage in the Demand-Side of the Smart Grid," *IEEE Transactions on Signal Processing*, vol. 61, pp. 2454–2472, May 2013.
- [95] E. Hammad, A. Farraj, and D. Kundur, "Cooperative Microgrid Networks for Remote and Rural Areas," in *IEEE 28th Canadian Conference on Electrical and Computer Engineering (CCECE)*, pp. 1572–1477, May 2015.
- [96] W. Lee, L. Xiang, R. Schober, and V. W. S. Wong, "Direct Electricity Trading in Smart Grid: A Coalitional Game Analysis," *IEEE Journal on Selected Areas in Communications*, vol. 32, pp. 1398–1411, July 2014.
- [97] W. Tushar, C. Yuen, D. B. Smith, and H. V. Poor, "Price Discrimination for Energy Trading in Smart Grid: A Game Theoretic Approach," *IEEE Transactions on Smart Grid*, vol. 8, pp. 1790–1801, July 2016.
- [98] Monika, D. Srinivasan, and T. Reindl, "Real-Time Display of Data from a Smart Grid on Geographical Map Using a GIS Tool and its Role in Optimization of Game Theory," in *IEEE Innovative Smart Grid Technologies - Asia (ISGT ASIA)*, pp. 1–6, November 2015.
- [99] W. Saad, A. L. Glass, N. B. Mandayam, and H. V. Poor, "Toward a Consumer-Centric Grid: A Behavioral Perspective," *Proceedings of the IEEE*, vol. 104, pp. 865–882, April 2016.
- [100] Y. Wang and W. Saad, "On the Role of Utility Framing in Smart Grid Energy Storage Management," in *IEEE International Conference on Communication Workshops (ICC Workshops)*, pp. 1946–1951, June 2015.
- [101] K. R. Apt and A. Witzel, "A Generic Approach to Coalition Formation," *International Game Theory Review*, vol. 11, no. 03, pp. 347–367, 2009.
- [102] J. V. Neumann and O. Morgenstern, *Theory of Games and Economic Behavior*. Princeton University Press, 1944.
- [103] K. Sungwook, "An Adaptive Smart Grid Management Scheme Based on the Coopetition Game Model," *ETRI Journal*, vol. 36, pp. 80–88, February 2014.
- [104] W. Saad, Z. Han, T. Basar, A. Hjørungnes, and J. B. Song, "Hedonic Coalition Formation Games for Secondary Base Station Cooperation in Cognitive Radio Networks," in *IEEE Wireless Communications and Networking Conference (WCNC)*, pp. 1–6, April 2010.

-
- [105] J. Alcalde and A. Romero-Medina, “Simple Mechanisms to Implement the Core of College Admissions Problems,” *Games and Economic Behavior*, vol. 31, no. 2, pp. 294–302, 2000.
- [106] J. Alcalde and A. Romero-Medina, “Coalition Formation and Stability,” *Social Choice and Welfare*, vol. 27, pp. 365–375, 2006.
- [107] A. Abdulkadiroglu, “College Admissions with Affirmative Action,” *International Journal of Game Theory*, vol. 33, pp. 535–549, 2005.
- [108] F. Kojima, “Finding All Stable Matchings with Couples,” *Journal of Dynamics and Games*, vol. 2, no. 3/4, pp. 321–330, 2015.
- [109] K. C. Ágoston, P. Biró, and I. McBride, “Integer Programming Methods for Special College Admissions Problems,” *Journal of Combinatorial Optimization*, vol. 32, pp. 1371–1399, November 2016.
- [110] W. Saad, Z. Han, R. Zheng, M. Debbah, and H. V. Poor, “A College Admissions Game for Uplink User Association in Wireless Small Cell Networks,” in *IEEE INFOCOM 2014 - IEEE Conference on Computer Communications*, pp. 1096–1104, April 2014.
- [111] R. A. V. Ramrez, E. Altman, J. S. Thompson, and R. V. M. Ramos, “A Stable Marriage Framework for Distributed Virtual MIMO Coalition Formation,” in *IEEE 24th Annual International Symposium on Personal, Indoor, and Mobile Radio Communications (PIMRC)*, pp. 2707–2712, September 2013.
- [112] B. Holfeld and E. Jorswieck, “On Stable Many-to-Many Matching for Distributed Medium Access with Reuse of Spectral Resources,” in *Proc. 20th International ITG Workshop on Smart Antennas (WSA)*, pp. 1–8, March 2016.
- [113] S. Chen, N. B. Shroff, and P. Sinha, “Energy Trading in the Smart Grid: From End-User’s Perspective,” in *Asilomar Conference on Signals, Systems and Computers*, pp. 327–331, November 2013.
- [114] B. G. Kim, S. Ren, M. van der Schaar, and J. W. Lee, “Bidirectional Energy Trading and Residential Load Scheduling with Electric Vehicles in the Smart Grid,” *IEEE Journal on Selected Areas in Communications*, vol. 31, pp. 1219–1234, July 2013.
- [115] S. Nykamp, M. G. C. Bosman, A. Molderink, J. L. Hurink, and G. J. M. Smit, “Value of Storage in Distribution Grids: Competition or Cooperation of Stakeholders,” *IEEE Transactions on Smart Grid*, vol. 4, pp. 1361–1370, September 2013.
- [116] S. Kahrobaee, R. A. Rajabzadeh, L. K. Soh, and S. Asgarpoor, “A Multiagent Modeling and Investigation of Smart Homes With Power Generation, Storage, and Trading Features,” *IEEE Transactions on Smart Grid*, vol. 4, pp. 659–668, June 2013.
- [117] P. G. D. Silva, D. Ili, and S. Karnouskos, “The Impact of Smart Grid Prosumer Grouping on Forecasting Accuracy and Its Benefits for Local Electricity Market Trading,” *IEEE Transactions on Smart Grid*, vol. 5, pp. 402–410, January 2014.

- [118] D. Zhu and G. Hug, “Decomposed Stochastic Model Predictive Control for Optimal Dispatch of Storage and Generation,” *IEEE Transactions on Smart Grid*, vol. 5, pp. 2044–2053, July 2014.
- [119] J. Lee, J. Guo, J. K. Choi, and M. Zukerman, “Distributed Energy Trading in Microgrids: A Game-Theoretic Model and Its Equilibrium Analysis,” *IEEE Transactions on Industrial Electronics*, vol. 62, pp. 3524–3533, June 2015.
- [120] D. Gregoratti and J. Matamoros, “Distributed Energy Trading: The Multiple-Microgrid Case,” *IEEE Transactions on Industrial Electronics*, vol. 62, pp. 2551–2559, April 2015.
- [121] E. T. Bell, “Exponential Numbers,” *American Mathematical Monthly*, vol. 41, pp. 411–419, 1934.
- [122] I. H. Gil, *Integrated Assessment of Quality of Supply in Future Electricity Networks*. PhD thesis, The University of Edinburgh, Edinburgh, United Kingdom, 2014. <https://www.era.lib.ed.ac.uk/handle/1842/9641> [Online; accessed 16-Nov-2017].
- [123] S. Stein, E. Gerding, V. Robu, and N. R. Jennings, “A Model-Based Online Mechanism with Pre-Commitment and its Applications to Electric Vehicle Charging,” in *Proc. International Conference on Autonomous Agents and Multiagent Systems (AAMAS)*, pp. 669–676, June 2012.
- [124] P. Ströhle, E. H. Gerding, M. D. W. Mathijs, S. Stein, and V. Robu, “Online Mechanism Design for Scheduling Non-Preemptive Jobs under Uncertain Supply and Demand,” in *Proc. International Conference on Autonomous Agents and Multi-agent Systems (AAMAS)*, pp. 437–444, May 2014.
- [125] W. Tang, S. Bi, and Y. J. Zhang, “Online Coordinated Charging Decision Algorithm for Electric Vehicle without Future Information,” *IEEE Transactions on Smart Grid*, vol. 5, pp. 2810–2824, November 2014.
- [126] N. Chen, C. W. Tan, and T. Q. S. Quek, “Electric Vehicle Charging in Smart Grid: Optimality and Valley-Filling Algorithms,” *IEEE Journal of Selected Topics in Signal Processing*, vol. 8, pp. 1073–1083, December 2014.
- [127] H. Guillou, D. L. Ha, V. D. Cung, and M. Jacomino, “Power Allocation Problem in Charging Electric Vehicles with Photovoltaic Production,” in *Proc. International Conference on Supply Chain Management and Information Systems (SCMIS)*, pp. 1–6, October 2010.
- [128] Y. Cao, T. Wang, O. Kaiwartya, G. Min, N. Ahmad, and A. H. Abdullah, “An EV Charging Management System Concerning Drivers’ Trip Duration and Mobility Uncertainty,” *IEEE Transactions on Systems, Man, and Cybernetics: Systems*, December 2017.
- [129] Y. Cao, O. Kaiwartya, R. Wang, T. Jiang, Y. Cao, N. Aslam, and G. Sexton, “Toward Efficient, Scalable, and Coordinated On-the-Move EV Charging Management,” *IEEE Wireless Communications*, vol. 24, pp. 66–73, April 2017.

-
- [130] M. D. W. Mathijs, E. Gerding, S. Stein, V. Robu, and N. R. Jennings, "Intention-Aware Routing to Minimise Delays at Electric Vehicle Charging Station," in *Proc. International Joint Conference on Artificial Intelligence (IJCAI)*, pp. 83–89, January 2013.
- [131] K. Clement-Nyns, E. Haesen, and J. Driesen, "The Impact of Charging Plug-In Hybrid Electric Vehicles on a Residential Distribution Grid," *IEEE Transactions on Power Systems*, vol. 25, pp. 371–380, February 2010.
- [132] S. Deilami, A. S. Masoum, P. S. Moses, and M. A. S. Masoum, "Real-Time Coordination of Plug-In Electric Vehicle Charging in Smart Grids to Minimize Power Losses and Improve Voltage Profile," *IEEE Transactions on Smart Grid*, vol. 2, pp. 456–467, September 2011.
- [133] C. Jin, X. Sheng, and P. Ghosh, "Optimized Electric Vehicle Charging with Intermittent Renewable Energy Sources," *IEEE Journal of Selected Topics in Signal Processing*, vol. 8, pp. 1063–1072, December 2014.
- [134] Q. Huang, Q. S. Jia, Z. Qiu, X. Guan, and G. Deconinck, "Matching EV Charging Load With Uncertain Wind: A Simulation-Based Policy Improvement Approach," *IEEE Transactions on Smart Grid*, vol. 6, pp. 1425–1433, May 2015.
- [135] D. Schrmann, J. Timpner, and L. Wolf, "Cooperative Charging in Residential Areas," *IEEE Transactions on Intelligent Transportation Systems*, vol. 18, pp. 834–846, April 2017.
- [136] W. Su and M. Y. Chow, "Performance Evaluation of a PHEV Parking Station Using Particle Swarm Optimization," in *IEEE Power and Energy Society General Meeting*, pp. 1–6, July 2011.
- [137] Y. Guo, J. Xiong, S. Xu, and W. Su, "Two-Stage Economic Operation of Microgrid-Like Electric Vehicle Parking Deck," *IEEE Transactions on Smart Grid*, vol. 7, pp. 1703–1712, May 2016.
- [138] R. Wang, P. Wang, and G. Xiao, "Two-Stage Mechanism for Massive Electric Vehicle Charging Involving Renewable Energy," *IEEE Transactions on Vehicular Technology*, vol. 65, pp. 4159–4171, June 2016.
- [139] L. Zhang and Y. Li, "Optimal Management for Parking-Lot Electric Vehicle Charging by Two-Stage Approximate Dynamic Programming," *IEEE Transactions on Smart Grid*, vol. 8, pp. 1722–1730, July 2017.
- [140] C. Luo, Y. F. Huang, and V. Gupta, "Stochastic Dynamic Pricing for EV Charging Stations with Renewables Integration and Energy Storage," *IEEE Transactions on Smart Grid*, April 2017.
- [141] I. S. Bayram, G. Michailidis, M. Devetsikiotis, and F. Granelli, "Electric Power Allocation in a Network of Fast Charging Stations," *IEEE Journal on Selected Areas in Communications*, vol. 31, pp. 1235–1246, July 2013.
- [142] S. Bahrami and M. Parniani, "Game Theoretic Based Charging Strategy for Plug-in Hybrid Electric Vehicles," *IEEE Transactions on Smart Grid*, vol. 5, pp. 2368–2375, September 2014.

- [143] D. Dolgov and E. Durfee, “Stationary Deterministic Policies for Constrained MDPs with Multiple Rewards, Costs, and Discount Factors,” in *Proc. International Joint Conference on Artificial Intelligence (IJCAI)*, pp. 1326–1331, July 2005.
- [144] S. Martinenas, A. B. Pedersen, M. Marinelli, P. B. Andersen, and C. Trholt, “Electric Vehicle Smart Charging Using Dynamic Price Signal,” in *IEEE International Electric Vehicle Conference (IEVC)*, pp. 1–6, December 2014.
- [145] C. Wu, H. Mohsenian-Rad, and J. Huang, “Vehicle-to-Aggregator Interaction Game,” *IEEE Transactions on Smart Grid*, vol. 3, pp. 434–442, March 2012.
- [146] H. Qin and W. Zhang, “Charging Scheduling with Minimal Waiting in a Network of Electric Vehicles and Charging Stations,” in *Proc. of 8th ACM International Workshop on Vehicular Inter-networking*, pp. 51–60, September 2011.
- [147] M. Alizadeh, A. Scaglione, and Z. Wang, “On the Impact of Smart Grid Metering Infrastructure on Load Forecasting,” in *Proc. 48th Annual Allerton Conference on Communication, Control, and Computing*, pp. 1628–1636, September 2010.
- [148] P. P. Singh and S. Singh, “Realistic Generation Cost of Solar Photovoltaic Electricity,” *Renewable Energy*, vol. 35, pp. 563–569, March 2010.